

# Threshold and Flavour Effects in the Renormalization Group Equations of the MSSM II: Dimensionful couplings

Andrew D. Box\* and Xerxes Tata†

*Dept. of Physics and Astronomy,*

*University of Hawaii,*

*Honolulu, HI 96822, U.S.A.*

## Abstract

We re-examine the one-loop renormalization group equations (RGEs) for the dimensionful parameters of the minimal supersymmetric Standard Model with broken supersymmetry, allowing for arbitrary flavour structure of the soft SUSY breaking (SSB) parameters. We include threshold effects by evaluating the  $\beta$ -functions in a sequence of (non-supersymmetric) effective theories with heavy particles decoupled at the scale of their mass. We present the most general form for high scale SSB parameters that obtains if we assume that the supersymmetry breaking mechanism does not introduce new inter-generational couplings. This form, possibly amended to allow additional sources of flavour-violation, serves as a boundary condition for solving the RGEs for the dimensionful MSSM parameters. We then present illustrative examples of numerical solutions to the RGEs. We find that in a SUSY GUT with the scale of SUSY scalars split from that of gauginos and higgsinos, the gaugino mass unification condition may be violated by  $\mathcal{O}(10\%)$ . As another illustration, we show that in mSUGRA, the rate for the flavour-violating  $\tilde{t}_1 \rightarrow c\tilde{Z}_1$  decay obtained using the complete RGE solution is smaller than that obtained using the commonly-used “single-step” integration of the RGEs by a factor 10-25, and so may qualitatively change expectations for topologies from top-squark pair production at colliders. Together with the RGEs for dimensionless couplings presented in a companion paper, the RGEs in Appendix B of this paper form a complete set of one-loop MSSM RGEs that include threshold and flavour-effects necessary for two-loop accuracy.

PACS numbers: 11.30.Pb, 11.10.Hi, 14.80.Ly

---

\*Electronic address: [abox@phys.hawaii.edu](mailto:abox@phys.hawaii.edu)

†Electronic address: [tata@phys.hawaii.edu](mailto:tata@phys.hawaii.edu)

## I. INTRODUCTION

Renormalization group equations (RGEs) have played a vital role for the extraction of phenomenological predictions of theories where the physics is specified at a scale much higher than the energy scale directly relevant for phenomenology [1]. A very familiar example of this is the prediction of the weak mixing angle  $\theta_W$  in grand unified theories (GUTs), widely regarded as one of the important successes of the idea of grand unification in the context of supersymmetry (SUSY) [2]. RGE methods have become ubiquitous for many studies of physics beyond the Standard Model (SM), where relationships between various model parameters, *renormalized at some very high scale*, are specified by the new physics.

Of interest to us here are supersymmetric models of particle physics [3–7] where supersymmetry fixes the dimensionless couplings of superpartners in terms of the corresponding gauge and Yukawa couplings of SM particles. Model-dependence arises via the potentially very large number of undetermined dimensionful soft SUSY breaking (SSB) parameters that reflects our ignorance about how supersymmetry is broken [8]. In practice, one resorts to models with underlying assumptions that fix all the SSB masses and couplings, renormalized at a high scale, in terms of a handful of parameters [9–12]. These high scale parameters have, of course, to be evolved to the low scale relevant for phenomenology in order to sum the large logarithms that may otherwise invalidate any (fixed-order) perturbative calculation [13].

This paper is a follow-up of an earlier paper, hereafter referred to as Paper I [14], where we used the seminal papers of Machacek and Vaughn [15] to obtain the one-loop RGEs for the dimensionless couplings of the Minimal Supersymmetric Standard Model (MSSM), carefully including threshold effects [16, 17] that are essential to include for true two-loop precision. Here, we extend the existing literature, and present the one-loop RGEs for the dimensionful (in general, complex) parameters including both flavour-mixing effects and threshold corrections. As discussed in Ref. [14], these RGEs can then be augmented by the two-loop terms of the MSSM RGEs [18–21], without the need to include threshold corrections to these for the required precision. Just as in Paper I, where we found that SUSY breaking threshold effects cause the gaugino-fermion-sfermion [higgsino-fermion-sfermion] couplings to evolve differently from the corresponding gauge [Yukawa] couplings, resulting in an enlarged system of RGEs for the dimensionless couplings, we will see that as we decouple heavy super-partners

and Higgs bosons, a similar situation obtains for the RGEs of dimensionful parameters. For instance, the super-potential higgsino mass  $\mu$  evolves differently from  $\tilde{\mu}$ , that enters via the corresponding Higgs boson mass squared parameter,  $|\tilde{\mu}|^2$ . Also, at scales below the masses of the heavier particles in the Higgs boson sector, where just the SM Higgs boson,  $h$ , and the associated would-be-Goldstone bosons that complete the scalar doublet (see Paper I) remain in the theory, we will see that only certain combinations of model parameters can be evolved in the corresponding low energy theory. These complications, to our knowledge, have not been included in previous studies.

We use the RGEs for the dimensionful parameters of a general field theory with real spin-zero fields and two-component spinor fields given in Ref. [22] to derive our results. In Sec. II we first re-cast the results of Ref. [22] in a form suitable for use by phenomenologists more used to the formalism with four-component spinors coupled to complex scalar fields and, of course, also gauge fields. As explained in Paper I, this re-casting does much of the work needed for the derivation of the MSSM RGEs. We discuss particle decoupling in Sec. III and describe our derivation of the RGEs in Sec. IV. In Sec. V, we numerically analyse the solutions of (some of) the RGEs and discuss squark flavour mixing. We apply our results to obtain the rate for the flavour-violating decay of the lighter  $t$ -squark,  $\tilde{t}_1 \rightarrow c\tilde{Z}_1$  in Sec. VI. We conclude in Sec. VII with general remarks and a summary of our results. The set of RGEs that we obtain are listed in Appendix B.

## II. FORMALISM

Luo, Wang and Xiao [22], that we use as the starting point, write the Lagrangian density for a general field theory as,

$$\begin{aligned}
\mathcal{L}_{(2)} = & i\psi_p^\dagger \sigma^\mu D_\mu \psi_p + \frac{1}{2} D_\mu \phi_a D^\mu \phi_a - \frac{1}{4} F_{\mu\nu A} F_A^{\mu\nu} \\
& - \frac{1}{2} \left[ (\mathbf{m}_f)_{pq} \psi_p^T \zeta \psi_q + \text{h.c.} \right] - \frac{1}{2!} \mathbf{m}_{ab}^2 \phi_a \phi_b \\
& - \left( \frac{1}{2} \mathbf{Y}_{pq}^a \psi_p^T \zeta \psi_q \phi_a + \text{h.c.} \right) - \frac{1}{3!} \mathbf{h}_{abc} \phi_a \phi_b \phi_c - \frac{1}{4!} \boldsymbol{\lambda}_{abcd} \phi_a \phi_b \phi_c \phi_d,
\end{aligned} \tag{1}$$

where the matrix  $\zeta = i\sigma_2$  is introduced to make the spinor bilinear Lorentz invariant. The gauge interactions for the real fields  $\phi_a$  and two-component spinors  $\psi_p$  are contained in the corresponding covariant derivatives, the matrices  $\mathbf{m}_f$  and  $\mathbf{Y}^a$  are symmetric (but not

Hermitian), while the entries of the scalar mass matrix  $\mathbf{m}^2$  as well as of the trilinear and quartic scalar couplings  $\mathbf{h}$  and  $\boldsymbol{\lambda}$  are symmetric in all their indices as well as real.

The Lagrangian density can also be written in terms of complex scalar fields  $\Phi_a$  and four-component Dirac and Majorana spinor fields as [14],

$$\begin{aligned}
\mathcal{L}_{(4)} = & \frac{i}{2} \bar{\Psi}_j \gamma^\mu D_\mu \Psi_j + (D_\mu \Phi_a)^\dagger (D^\mu \Phi_a) - \frac{1}{4} F_{\mu\nu A} F_A^{\mu\nu} \\
& - \frac{1}{2} \left[ (\mathbf{m}_X)_{jk} \bar{\Psi}_{Mj} \Psi_{Mk} + i (\mathbf{m}'_X)_{jk} \bar{\Psi}_{Mj} \gamma_5 \Psi_{Mk} \right] + \left[ \frac{1}{2!} \mathbf{B}_{ab} \Phi_a \Phi_b + \text{h.c.} \right] - \mathbf{m}_{ab}^2 \Phi_a^\dagger \Phi_b \\
& - \left[ (\mathbf{U}_a^1)_{jk} \bar{\Psi}_{Dj} P_L \Psi_{Dk} \Phi_a + (\mathbf{U}_a^2)_{jk} \bar{\Psi}_{Dj} P_L \Psi_{Dk} \Phi_a^\dagger \right. \\
& \quad + (\mathbf{V}_a)_{jk} \bar{\Psi}_{Dj} P_L \Psi_{Mk} \Phi_a + (\mathbf{W}_a)_{jk} \bar{\Psi}_{Mj} P_L \Psi_{Dk} \Phi_a^\dagger \\
& \quad \left. + \frac{1}{2} (\mathbf{X}_a^1)_{jk} \bar{\Psi}_{Mj} P_L \Psi_{Mk} \Phi_a + \frac{1}{2} (\mathbf{X}_a^2)_{jk} \bar{\Psi}_{Mj} P_L \Psi_{Mk} \Phi_a^\dagger + \text{h.c.} \right] \\
& + \left[ \frac{1}{2!} \Phi_a^\dagger \mathbf{H}_{abc} \Phi_b \Phi_c + \text{h.c.} \right] - \frac{1}{2!} \frac{1}{2!} \boldsymbol{\Lambda}_{abcd} \Phi_a^\dagger \Phi_b^\dagger \Phi_c \Phi_d - \left[ \frac{1}{3!} \boldsymbol{\Lambda}'_{abcd} \Phi_a^\dagger \Phi_b \Phi_c \Phi_d + \text{h.c.} \right].
\end{aligned} \tag{2}$$

The Yukawa coupling matrices  $\mathbf{U}_a^{1,2}$  that couple Dirac spinor fields to complex scalars, and the matrices  $\mathbf{V}_a$  and  $\mathbf{W}_a$  that couple these scalar fields to one Majorana and one Dirac field, have no particular symmetry (or Hermiticity) properties under interchange of the fermion field indices  $j$  and  $k$ . These indices label the fermion field type (quark, lepton, gaugino, higgsino) and also carry information of flavour and other quantum numbers (*e.g.* weak isospin and colour). On the other hand, the matrices  $\mathbf{X}_a^{1,2}$  that couple scalars to two Majorana fields are symmetric under  $j \leftrightarrow k$  because of the symmetry properties [4] of the Majorana spinor bilinears that appear in (2). The scalar mass squared matrix  $\mathbf{m}^2$  — notice that we have used a different font in (2) to differentiate this mass term for complex scalar fields from the corresponding one for real scalars coupled to two-component spinors in (1) — is Hermitian in the scalar field indices,  $a, b$ , while the matrix  $\mathbf{B}$  is symmetric. The  $CP$  even and odd Majorana fermion mass matrices [4]  $\mathbf{m}_X$  and  $\mathbf{m}'_X$  are both Hermitian and symmetric. The trilinear and quartic scalar couplings  $\boldsymbol{\Lambda}$ ,  $\boldsymbol{\Lambda}'$  and  $\mathbf{H}$  are symmetric under interchanges  $a \leftrightarrow b$  and/or  $c \leftrightarrow d$  for  $\boldsymbol{\Lambda}$ , under interchanges of  $b, c, d$  for  $\boldsymbol{\Lambda}'$ , and finally under  $b \leftrightarrow c$  for  $\mathbf{H}$ . As noted in Paper I, while (2) is not the most general form for the Lagrangian density, it suffices for the derivation of the RGEs of the MSSM with  $R$ -parity conservation.

The evolution of the fermion mass parameters in (1) is determined by the  $\beta$ -function [22],

$$(4\pi)^2 \beta_{\mathbf{m}_f} \Big|_{1\text{-loop}} = \frac{1}{2} [\mathbf{Y}_2^T(F) \mathbf{m}_f + \mathbf{m}_f \mathbf{Y}_2(F)] + 2 \mathbf{Y}^b \mathbf{m}_f^\dagger \mathbf{Y}^b + \frac{1}{2} \mathbf{Y}^b \text{Tr} \left\{ \mathbf{Y}^{b\dagger} \mathbf{m}_f + \mathbf{m}_f^\dagger \mathbf{Y}^b \right\} - 3g^2 \{ \mathbf{C}_2(F), \mathbf{m}_f \} . \quad (3)$$

Here,  $\mathbf{C}_2(F) = \mathbf{t}^A \mathbf{t}^A$  is the quadratic Casimir operator for the fermions, and  $\mathbf{Y}_2(F) = \mathbf{Y}^{b\dagger} \mathbf{Y}^b$ . Notice that we have altered  $\mathbf{Y}_2^\dagger(F)$  (recall  $\mathbf{Y}_2(F)$  is a Hermitian matrix) that appears in the first term of the corresponding equation in Ref. [22] to  $\mathbf{Y}_2^T(F)$ . This ensures that the  $\beta$ -function for  $\mathbf{m}_f$  has the same symmetry property as  $\mathbf{m}_f$  in (1). We can write the ‘‘Yukawa couplings’’ on the right hand side of (3) in terms of the corresponding couplings in the four-component notation by introducing

$$\vec{\psi} \equiv \begin{pmatrix} \psi_L \\ \psi_R \\ \psi_M \end{pmatrix} ,$$

and replacing  $\mathbf{Y}^a$  with a  $(3 \times 3)$  block matrix containing  $\mathbf{U}_a^1, \mathbf{U}_a^2, \mathbf{V}_a, \mathbf{W}_a, \mathbf{X}_a^1$  and  $\mathbf{X}_a^2$  as worked out in Paper I.

The fermion mass matrix can similarly be written (in this same basis) as,

$$\mathbf{m}_f = \begin{pmatrix} \mathbf{0} & (\mathbf{m}_U^T - i\mathbf{m}'_U{}^T) & (\mathbf{m}_W^T - i\mathbf{m}'_W{}^T) \\ (\mathbf{m}_U - i\mathbf{m}'_U) & \mathbf{0} & (\mathbf{m}_V - i\mathbf{m}'_V) \\ (\mathbf{m}_W - i\mathbf{m}'_W) & (\mathbf{m}_V^T - i\mathbf{m}'_V{}^T) & (\mathbf{m}_X - i\mathbf{m}'_X) \end{pmatrix} , \quad (4)$$

where in the context of the  $R$ -parity-conserving MSSM, all the entries except  $(\mathbf{m}_X - i\mathbf{m}'_X)$  vanish because gauge invariance precludes the corresponding fermion bilinears. From now on, we retain just  $\mathbf{m}_X$  and  $\mathbf{m}'_X$  in our analysis. We can now substitute  $\mathbf{m}_f$  as well as the form of the ‘‘Yukawa’’ matrices from Paper I into (3) to obtain the RGEs for the matrices

$\mathbf{m}_X$  and  $\mathbf{m}'_X$ . We find,

$$\begin{aligned}
(4\pi)^2 \frac{d\mathbf{m}_X}{dt} = & \frac{1}{4} \left[ \left( \mathbf{W}_b \mathbf{W}_b^\dagger + \mathbf{V}_b^T \mathbf{V}_b^* + \mathbf{X}_b^1 \mathbf{X}_b^{1\dagger} + \mathbf{X}_b^2 \mathbf{X}_b^{2\dagger} \right) (\mathbf{m}_X - i\mathbf{m}'_X) \right. \\
& + (\mathbf{m}_X + i\mathbf{m}'_X) \left( \mathbf{W}_b \mathbf{W}_b^\dagger + \mathbf{V}_b^T \mathbf{V}_b^* + \mathbf{X}_b^1 \mathbf{X}_b^{1\dagger} + \mathbf{X}_b^2 \mathbf{X}_b^{2\dagger} \right) \\
& + (\mathbf{m}_X - i\mathbf{m}'_X) \left( \mathbf{W}_b^* \mathbf{W}_b^T + \mathbf{V}_b^\dagger \mathbf{V}_b + \mathbf{X}_b^{1\dagger} \mathbf{X}_b^1 + \mathbf{X}_b^{2\dagger} \mathbf{X}_b^2 \right) \\
& \left. + \left( \mathbf{W}_b^* \mathbf{W}_b^T + \mathbf{V}_b^\dagger \mathbf{V}_b + \mathbf{X}_b^{1\dagger} \mathbf{X}_b^1 + \mathbf{X}_b^{2\dagger} \mathbf{X}_b^2 \right) (\mathbf{m}_X + i\mathbf{m}'_X) \right] \\
& + \left[ \mathbf{X}_b^1 (\mathbf{m}_X + i\mathbf{m}'_X) \mathbf{X}_b^2 + \mathbf{X}_b^2 (\mathbf{m}_X + i\mathbf{m}'_X) \mathbf{X}_b^1 \right. \\
& \left. + \mathbf{X}_b^{2\dagger} (\mathbf{m}_X - i\mathbf{m}'_X) \mathbf{X}_b^{1\dagger} + \mathbf{X}_b^{1\dagger} (\mathbf{m}_X - i\mathbf{m}'_X) \mathbf{X}_b^{2\dagger} \right] \\
& + \frac{1}{4} \left[ \mathbf{X}_b^1 \text{Tr} \left\{ \mathbf{X}_b^{1\dagger} (\mathbf{m}_X - i\mathbf{m}'_X) + (\mathbf{m}_X + i\mathbf{m}'_X) \mathbf{X}_b^2 \right\} \right. \\
& + \mathbf{X}_b^2 \text{Tr} \left\{ \mathbf{X}_b^{2\dagger} (\mathbf{m}_X - i\mathbf{m}'_X) + (\mathbf{m}_X + i\mathbf{m}'_X) \mathbf{X}_b^1 \right\} \\
& + \mathbf{X}_b^{1\dagger} \text{Tr} \left\{ (\mathbf{m}_X + i\mathbf{m}'_X) \mathbf{X}_b^1 + \mathbf{X}_b^{2\dagger} (\mathbf{m}_X - i\mathbf{m}'_X) \right\} \\
& \left. + \mathbf{X}_b^{2\dagger} \text{Tr} \left\{ (\mathbf{m}_X + i\mathbf{m}'_X) \mathbf{X}_b^2 + \mathbf{X}_b^{1\dagger} (\mathbf{m}_X - i\mathbf{m}'_X) \right\} \right] \\
& - 6g^2 \mathbf{C}_2^M(F) \mathbf{m}_X,
\end{aligned} \tag{5}$$

and

$$\begin{aligned}
(4\pi)^2 \frac{d\mathbf{m}'_X}{dt} = & \frac{i}{4} \left[ \left( \mathbf{W}_b \mathbf{W}_b^\dagger + \mathbf{V}_b^T \mathbf{V}_b^* + \mathbf{X}_b^1 \mathbf{X}_b^{1\dagger} + \mathbf{X}_b^2 \mathbf{X}_b^{2\dagger} \right) (\mathbf{m}_X - i\mathbf{m}'_X) \right. \\
& - (\mathbf{m}_X + i\mathbf{m}'_X) \left( \mathbf{W}_b \mathbf{W}_b^\dagger + \mathbf{V}_b^T \mathbf{V}_b^* + \mathbf{X}_b^1 \mathbf{X}_b^{1\dagger} + \mathbf{X}_b^2 \mathbf{X}_b^{2\dagger} \right) \\
& + (\mathbf{m}_X - i\mathbf{m}'_X) \left( \mathbf{W}_b^* \mathbf{W}_b^T + \mathbf{V}_b^\dagger \mathbf{V}_b + \mathbf{X}_b^{1\dagger} \mathbf{X}_b^1 + \mathbf{X}_b^{2\dagger} \mathbf{X}_b^2 \right) \\
& \left. - \left( \mathbf{W}_b^* \mathbf{W}_b^T + \mathbf{V}_b^\dagger \mathbf{V}_b + \mathbf{X}_b^{1\dagger} \mathbf{X}_b^1 + \mathbf{X}_b^{2\dagger} \mathbf{X}_b^2 \right) (\mathbf{m}_X + i\mathbf{m}'_X) \right] \\
& + i \left[ \mathbf{X}_b^1 (\mathbf{m}_X + i\mathbf{m}'_X) \mathbf{X}_b^2 + \mathbf{X}_b^2 (\mathbf{m}_X + i\mathbf{m}'_X) \mathbf{X}_b^1 \right. \\
& \left. - \mathbf{X}_b^{2\dagger} (\mathbf{m}_X - i\mathbf{m}'_X) \mathbf{X}_b^{1\dagger} - \mathbf{X}_b^{1\dagger} (\mathbf{m}_X - i\mathbf{m}'_X) \mathbf{X}_b^{2\dagger} \right] \\
& + \frac{i}{4} \left[ \mathbf{X}_b^1 \text{Tr} \left\{ \mathbf{X}_b^{1\dagger} (\mathbf{m}_X - i\mathbf{m}'_X) + (\mathbf{m}_X + i\mathbf{m}'_X) \mathbf{X}_b^2 \right\} \right. \\
& + \mathbf{X}_b^2 \text{Tr} \left\{ \mathbf{X}_b^{2\dagger} (\mathbf{m}_X - i\mathbf{m}'_X) + (\mathbf{m}_X + i\mathbf{m}'_X) \mathbf{X}_b^1 \right\} \\
& - \mathbf{X}_b^{1\dagger} \text{Tr} \left\{ (\mathbf{m}_X + i\mathbf{m}'_X) \mathbf{X}_b^1 + \mathbf{X}_b^{2\dagger} (\mathbf{m}_X - i\mathbf{m}'_X) \right\} \\
& \left. - \mathbf{X}_b^{2\dagger} \text{Tr} \left\{ (\mathbf{m}_X + i\mathbf{m}'_X) \mathbf{X}_b^2 + \mathbf{X}_b^{1\dagger} (\mathbf{m}_X - i\mathbf{m}'_X) \right\} \right] \\
& - 6g^2 \mathbf{C}_2^M(F) \mathbf{m}'_X,
\end{aligned} \tag{6}$$

where  $t = \ln Q$ ,  $\mathbf{C}_2^M(F)$  is the quadratic Casimir for the Majorana fermions as defined in Ref. [14], and there is a sum over all gauge group factors in the final term of both (5) and

(6). Note also that in the MSSM with  $R$ -parity conservation, the trace terms in (5) and (6) vanish. This is because, as seen in Eq. (2),  $\mathbf{X}$  only connects higgsinos to gauginos, while  $\mathbf{m}_X^{(\prime)}$  never connects higgsinos to gauginos. Therefore, a trace of the product of these two matrices is always zero.

Turning to the RGE for the trilinear scalar couplings, we first write the one-loop RGE for these couplings in (1) as [22],

$$(4\pi)^2 \beta_{\mathbf{h}_{abc}}|_{1-loop} = \Lambda_{abc}^2 - 4\mathcal{H}_{abc} + \Lambda_{abc}^Y - 3g^2\Lambda_{abc}^S, \quad (7)$$

with

$$\Lambda_{abc}^2 = \frac{1}{2} \sum_{\text{perms}} \lambda_{abef} \mathbf{h}_{efc}, \quad (8)$$

$$\mathcal{H}_{abc} = \frac{1}{2} \sum_{\text{perms}} \text{Tr} \{ \mathbf{m}_f \mathbf{Y}_a^\dagger \mathbf{Y}_b \mathbf{Y}_c^\dagger + \mathbf{Y}_a \mathbf{m}_f^\dagger \mathbf{Y}_b \mathbf{Y}_c^\dagger \}, \quad (9)$$

$$\Lambda_{abc}^Y = \frac{1}{2} \left[ \text{Tr} \left\{ \mathbf{Y}_{a'}^\dagger \mathbf{Y}_a + \mathbf{Y}_a^\dagger \mathbf{Y}_{a'} \right\} \mathbf{h}_{a'bc} + \text{Tr} \left\{ \mathbf{Y}_{b'}^\dagger \mathbf{Y}_b + \mathbf{Y}_b^\dagger \mathbf{Y}_{b'} \right\} \mathbf{h}_{ab'c} \right. \\ \left. + \text{Tr} \left\{ \mathbf{Y}_{c'}^\dagger \mathbf{Y}_c + \mathbf{Y}_c^\dagger \mathbf{Y}_{c'} \right\} \mathbf{h}_{abc'} \right], \quad (10)$$

$$\Lambda_{abc}^S = [C_2(a) + C_2(b) + C_2(c)] \mathbf{h}_{abc}, \quad (11)$$

where  $a'$ ,  $b'$ ,  $c'$ , and the indices  $e$  and  $f$ , are summed over all the scalars in the theory. Also, there is an implied sum over all gauge group factors in the final term of (7), and  $C_2(S) = \mathbf{t}^{\mathbf{A}} \mathbf{t}^{\mathbf{A}}$  is the quadratic Casimir operator for the scalars. All this is exactly as in Ref. [22] except that we have written the expression in (10) in a more transparent form. We note that the  $\beta$ -function in (7) is manifestly symmetric under any permutation of the three indices.

In order to convert this into our complex, four-component notation, we first expand out the trilinear scalar term in (2) in terms of real spin-zero fields (*i.e.* the real and imaginary parts of our complex fields), and compare this with (1) in order to obtain  $\mathbf{H}_{abc}$  in terms of  $\mathbf{h}_{abc}$  as,

$$\mathbf{H}_{abc} = \frac{1}{\sqrt{2}} [-\mathbf{h}_{a_R b_R c_R} + \mathbf{h}_{a_R b_I c_I} + i\mathbf{h}_{a_R b_R c_I} + i\mathbf{h}_{a_R b_I c_R}]. \quad (12)$$

We can now write down the RGE for  $\mathbf{H}_{abc}$  using the same relations for the two-component Yukawa matrices as before, and substituting the trilinear and quartic scalar couplings  $\mathbf{h}_{abc}$  and  $\lambda_{abcd}$  in terms of the corresponding couplings  $\mathbf{H}_{abc}$  and  $\Lambda_{abcd}$  or  $\Lambda'_{abcd}$  on the right hand

side of (7), taking care to sum over real and imaginary components of the scalar fields. This RGE then becomes,

$$\begin{aligned}
(4\pi)^2 \frac{d\mathbf{H}_{abc}}{dt} = & \left[ 2 (\Lambda_{afbe} + \Lambda'_{fabe}) \mathbf{H}_{ecf} + \Lambda'_{abef} \mathbf{H}_{cef}^* + (b \leftrightarrow c) \right] \\
& + \Lambda_{efbc} \mathbf{H}_{aef} + 2\Lambda'_{ebcf} (\mathbf{H}_{eaf}^* + \mathbf{H}_{fae}) \\
& + 2\text{Tr} \left\{ (\mathbf{m}_X - i\mathbf{m}'_X) \left[ (\mathbf{V}_a^\dagger \{ \mathbf{U}_b^1 \mathbf{W}_c^\dagger + \mathbf{V}_b \mathbf{X}_c^{2\dagger} \}) + (\mathbf{X}_a^{1\dagger} + \mathbf{X}_a^{2\dagger}) \mathbf{X}_b^1 \mathbf{X}_c^{2\dagger} \right. \right. \\
& \quad \left. \left. + \mathbf{W}_b^* \mathbf{W}_a^T \mathbf{X}_c^{2\dagger} + \mathbf{X}_b^{2\dagger} \{ \mathbf{W}_a \mathbf{W}_c^\dagger + (\mathbf{X}_a^1 + \mathbf{X}_a^2) \mathbf{X}_c^{2\dagger} \} \right. \right. \\
& \quad \left. \left. + \mathbf{W}_b^* \mathbf{U}_c^{1T} \mathbf{V}_a + \mathbf{X}_b^{2\dagger} \{ \mathbf{V}_c^T \mathbf{V}_a^* + \mathbf{X}_c^1 (\mathbf{X}_a^{1\dagger} + \mathbf{X}_a^{2\dagger}) \} \right) \right. \\
& \quad \left. + (b \leftrightarrow c) \right\} \\
& + 2\text{Tr} \left\{ (\mathbf{W}_a^T (\mathbf{m}_X + i\mathbf{m}'_X) \{ \mathbf{V}_b^T \mathbf{U}_c^{2*} + \mathbf{X}_b^1 \mathbf{W}_c^* \} \right. \\
& \quad \left. + (\mathbf{X}_a^1 + \mathbf{X}_a^2) (\mathbf{m}_X + i\mathbf{m}'_X) \mathbf{X}_b^1 \mathbf{X}_c^{2\dagger} + \mathbf{V}_b (\mathbf{m}_X + i\mathbf{m}'_X) \mathbf{W}_a \mathbf{U}_c^2 \right. \\
& \quad \left. + \mathbf{X}_b^1 (\mathbf{m}_X + i\mathbf{m}'_X) \{ \mathbf{W}_a \mathbf{W}_c^\dagger + (\mathbf{X}_a^1 + \mathbf{X}_a^2) \mathbf{X}_c^{2\dagger} \} \right. \\
& \quad \left. + \mathbf{V}_b (\mathbf{m}_X + i\mathbf{m}'_X) \mathbf{X}_c^1 \mathbf{V}_a^\dagger \right. \\
& \quad \left. + \mathbf{X}_b^1 (\mathbf{m}_X + i\mathbf{m}'_X) \{ \mathbf{V}_c^T \mathbf{V}_a^* + \mathbf{X}_c^1 (\mathbf{X}_a^{1\dagger} + \mathbf{X}_a^{2\dagger}) \} \right) \\
& \quad \left. + (b \leftrightarrow c) \right\} \\
& + \text{Tr} \left\{ \mathbf{U}_{a'}^{2\dagger} (\mathbf{U}_a^1 + \mathbf{U}_a^2) + (\mathbf{U}_a^{1\dagger} + \mathbf{U}_a^{2\dagger}) \mathbf{U}_{a'}^1 + \mathbf{V}_a^\dagger \mathbf{V}_{a'} + \mathbf{W}_{a'}^\dagger \mathbf{W}_a \right. \\
& \quad \left. + \frac{1}{2} \left\{ \mathbf{X}_{a'}^{2\dagger} (\mathbf{X}_a^1 + \mathbf{X}_a^2) + (\mathbf{X}_a^{1\dagger} + \mathbf{X}_a^{2\dagger}) \mathbf{X}_{a'}^1 \right\} \right\} \mathbf{H}_{a'bc} \\
& + \text{Tr} \left\{ \mathbf{U}_{b'}^{1\dagger} \mathbf{U}_b^1 + \mathbf{U}_b^{2\dagger} \mathbf{U}_{b'}^2 + \mathbf{V}_{b'}^\dagger \mathbf{V}_b + \mathbf{W}_{b'}^\dagger \mathbf{W}_b + \frac{1}{2} \left\{ \mathbf{X}_{b'}^{1\dagger} \mathbf{X}_b^1 + \mathbf{X}_b^{2\dagger} \mathbf{X}_{b'}^2 \right\} \right\} \mathbf{H}_{ab'c} \\
& + \text{Tr} \left\{ \mathbf{U}_{b'}^{2\dagger} \mathbf{U}_b^1 + \mathbf{U}_b^{2\dagger} \mathbf{U}_{b'}^1 + \frac{1}{2} \left\{ \mathbf{X}_{b'}^{2\dagger} \mathbf{X}_b^1 + \mathbf{X}_b^{2\dagger} \mathbf{X}_{b'}^1 \right\} \right\} (\mathbf{H}_{b'ac} + \mathbf{H}_{cab'}^*) \\
& + \text{Tr} \left\{ \mathbf{U}_{c'}^{1\dagger} \mathbf{U}_c^1 + \mathbf{U}_c^{2\dagger} \mathbf{U}_{c'}^2 + \mathbf{V}_{c'}^\dagger \mathbf{V}_c + \mathbf{W}_{c'}^\dagger \mathbf{W}_c + \frac{1}{2} \left\{ \mathbf{X}_{c'}^{1\dagger} \mathbf{X}_c^1 + \mathbf{X}_c^{2\dagger} \mathbf{X}_{c'}^2 \right\} \right\} \mathbf{H}_{ac'b} \\
& + \text{Tr} \left\{ \mathbf{U}_{c'}^{2\dagger} \mathbf{U}_c^1 + \mathbf{U}_c^{2\dagger} \mathbf{U}_{c'}^1 + \frac{1}{2} \left\{ \mathbf{X}_{c'}^{2\dagger} \mathbf{X}_c^1 + \mathbf{X}_c^{2\dagger} \mathbf{X}_{c'}^1 \right\} \right\} (\mathbf{H}_{c'ab} + \mathbf{H}_{bac'}^*) \\
& - 3g^2 [C_2(a) + C_2(b) + C_2(c)] \mathbf{H}_{abc} ,
\end{aligned} \tag{13}$$

where, as with (5) and (6), a sum over all gauge group factors is implied in the last term. The origin of the various terms in this long equation when compared with the two-component form of (7) should be clear. The terms involving the quartic couplings clearly originate in the first term of (7), the next set of terms involving the mass matrices for the Majorana spinors



in the second term, the terms with the summation over  $\{a', b', c'\}$  appear in both forms, and the last term involving the gauge couplings is clearly the corresponding term in (7). In the context of the MSSM, where we can without loss of generality choose for the index  $a$  in  $\mathbf{H}_{abc}$  to always refer to a sfermion, the RGE can be somewhat simplified. This is because, when  $a$  is a sfermion index,  $\mathbf{U}_a^{1,2}$  and  $\mathbf{X}_a^{1,2}$  are always zero, and the corresponding terms drop out from the equation. We remark that the first trace term not involving Majorana fermion masses in (13) is clearly symmetric under  $b \leftrightarrow c$  while the last two trace terms (*i.e.* those with  $c'$  as a dummy index) are simply the  $b \leftrightarrow c$  equivalent of the previous two trace terms involving the dummy index  $b'$ . Thus the RGE for  $\mathbf{H}_{abc}$  preserves the  $b \leftrightarrow c$  symmetry of this coupling noted below Eq. (2).

The RGE for the real scalar mass squared parameters in (1) reads [22],

$$(4\pi)^2 \beta_{\mathbf{m}_{ab}^2} \Big|_{1\text{-loop}} = \boldsymbol{\lambda}_{abef} \mathbf{m}_{ef}^2 + \mathbf{h}_{aef} \mathbf{h}_{bef} - 2\mathcal{H}_{ab} - 3g^2 \boldsymbol{\Lambda}_{ab}^S + \boldsymbol{\Lambda}_{ab}^Y, \quad (14)$$

with

$$\begin{aligned} \mathcal{H}_{ab} = \text{Tr} \left\{ \left( \mathbf{Y}_a \mathbf{Y}_b^\dagger + \mathbf{Y}_b \mathbf{Y}_a^\dagger \right) \mathbf{m}_f \mathbf{m}_f^\dagger + \left( \mathbf{Y}_a^\dagger \mathbf{Y}_b + \mathbf{Y}_b^\dagger \mathbf{Y}_a \right) \mathbf{m}_f^\dagger \mathbf{m}_f \right. \\ \left. + \mathbf{Y}_a \mathbf{m}_f^\dagger \mathbf{Y}_b \mathbf{m}_f^\dagger + \mathbf{m}_f \mathbf{Y}_a^\dagger \mathbf{m}_f \mathbf{Y}_b^\dagger \right\}, \end{aligned} \quad (15)$$

$$\boldsymbol{\Lambda}_{ab}^S = [C_2(a) + C_2(b)] \mathbf{m}_{ab}^2, \quad (16)$$

$$\boldsymbol{\Lambda}_{ab}^Y = \frac{1}{2} \left[ \text{Tr} \left\{ \mathbf{Y}_{a'}^\dagger \mathbf{Y}_a + \mathbf{Y}_a^\dagger \mathbf{Y}_{a'} \right\} \mathbf{m}_{a'b}^2 + \text{Tr} \left\{ \mathbf{Y}_{b'}^\dagger \mathbf{Y}_b + \mathbf{Y}_b^\dagger \mathbf{Y}_{b'} \right\} \mathbf{m}_{ab'}^2 \right], \quad (17)$$

where in (17) we have once again made the notation more explicit. Writing the complex fields  $\Phi_a$  as  $\Phi_a = \frac{\phi_{aR} + i\phi_{aI}}{\sqrt{2}}$  and comparing the coefficients of the bilinear terms in the *real* scalar fields  $\phi_\bullet$  then gives,

$$\mathbf{m}_{ab}^2 - \mathcal{B}_{ab} = \mathbf{m}_{a_R b_R}^2 - i \mathbf{m}_{a_R b_I}^2, \quad (18a)$$

$$\mathbf{m}_{ab}^2 + \mathcal{B}_{ab} = \mathbf{m}_{a_I b_I}^2 + i \mathbf{m}_{a_I b_R}^2. \quad (18b)$$

In the  $R$ -parity conserving MSSM, we never have non-zero entries in the Lagrangian corresponding to both  $\mathbf{m}_{ab}^2$  and  $\mathcal{B}_{ab}$  for the same  $a, b$ . It suffices, therefore, to write the RGE for

just one of these combinations, which we take to be the first one. We then have,

$$\begin{aligned}
(4\pi)^2 \frac{d[\mathbf{m}_{ab}^2 - \mathcal{B}_{ab}]}{dt} = & \left\{ 2 (\Lambda_{afbe} + \Lambda'_{fabe}) \mathbf{m}_{ef}^2 - \Lambda'_{abef} \mathcal{B}_{ef}^* - (\Lambda_{efab} + \Lambda_{baef}^*) \mathcal{B}_{ef} \right\} \\
& + \left\{ \mathbf{H}_{aef} \mathbf{H}_{bef}^* + 2 (\mathbf{H}_{caf}^* + \mathbf{H}_{fae}) \mathbf{H}_{ebf} \right\} \\
& - 2 \left[ 2 \text{Tr} \left\{ \left[ \mathbf{V}_b^T \mathbf{V}_a^* + \mathbf{W}_a \mathbf{W}_b^\dagger + (\mathbf{X}_a^1 + \mathbf{X}_a^2) \mathbf{X}_b^{2\dagger} + \mathbf{X}_b^1 (\mathbf{X}_a^{1\dagger} + \mathbf{X}_a^{2\dagger}) \right] \right. \right. \\
& \qquad \qquad \qquad \left. \left. \times (\mathbf{m}_X - i\mathbf{m}'_X) (\mathbf{m}_X + i\mathbf{m}'_X) \right\} \right. \\
& \quad + \text{Tr} \left\{ (\mathbf{X}_a^1 + \mathbf{X}_a^2) (\mathbf{m}_X + i\mathbf{m}'_X) \mathbf{X}_b^1 (\mathbf{m}_X + i\mathbf{m}'_X) \right\} \\
& \quad \left. + \text{Tr} \left\{ (\mathbf{X}_a^{1\dagger} + \mathbf{X}_a^{2\dagger}) (\mathbf{m}_X - i\mathbf{m}'_X) \mathbf{X}_b^{2\dagger} (\mathbf{m}_X - i\mathbf{m}'_X) \right\} \right] \\
& - 3g^2 [C_2(a) + C_2(b)] (\mathbf{m}_{ab}^2 - \mathcal{B}_{ab}) \\
& + \left[ \text{Tr} \left\{ \mathbf{U}_{a'}^{2\dagger} (\mathbf{U}_a^1 + \mathbf{U}_a^2) + (\mathbf{U}_a^{1\dagger} + \mathbf{U}_a^{2\dagger}) \mathbf{U}_{a'}^1 + \mathbf{V}_a^\dagger \mathbf{V}_{a'} \right. \right. \\
& \quad \left. \left. + \mathbf{W}_{a'}^\dagger \mathbf{W}_a + \frac{1}{2} \mathbf{X}_{a'}^{2\dagger} (\mathbf{X}_a^1 + \mathbf{X}_a^2) + \frac{1}{2} (\mathbf{X}_a^{1\dagger} + \mathbf{X}_a^{2\dagger}) \mathbf{X}_{a'}^1 \right\} \mathbf{m}_{a'b}^2 \right. \\
& \quad - \text{Tr} \left\{ \mathbf{U}_{a'}^{1\dagger} (\mathbf{U}_a^1 + \mathbf{U}_a^2) + (\mathbf{U}_a^{1\dagger} + \mathbf{U}_a^{2\dagger}) \mathbf{U}_{a'}^2 + \mathbf{V}_{a'}^\dagger \mathbf{V}_a \right. \\
& \quad \left. \left. + \mathbf{W}_a^\dagger \mathbf{W}_{a'} + \frac{1}{2} \mathbf{X}_{a'}^{1\dagger} (\mathbf{X}_a^1 + \mathbf{X}_a^2) + \frac{1}{2} (\mathbf{X}_a^{1\dagger} + \mathbf{X}_a^{2\dagger}) \mathbf{X}_{a'}^2 \right\} \mathcal{B}_{a'b} \right. \\
& \quad + \text{Tr} \left\{ \mathbf{U}_{b'}^{1\dagger} \mathbf{U}_b^1 + \mathbf{U}_b^{2\dagger} \mathbf{U}_{b'}^2 + \mathbf{V}_{b'}^\dagger \mathbf{V}_b \right. \\
& \quad \left. \left. + \mathbf{W}_b^\dagger \mathbf{W}_{b'} + \frac{1}{2} \mathbf{X}_{b'}^{1\dagger} \mathbf{X}_b^1 + \frac{1}{2} \mathbf{X}_b^{2\dagger} \mathbf{X}_{b'}^2 \right\} (\mathbf{m}_{ab'}^2 - \mathcal{B}_{ab'}) \right. \\
& \quad \left. + \text{Tr} \left\{ \mathbf{U}_{b'}^{2\dagger} \mathbf{U}_b^1 + \mathbf{U}_b^{2\dagger} \mathbf{U}_{b'}^1 + \frac{1}{2} \mathbf{X}_{b'}^{2\dagger} \mathbf{X}_b^1 + \frac{1}{2} \mathbf{X}_b^{2\dagger} \mathbf{X}_{b'}^1 \right\} (\mathbf{m}_{ab'}^2 - \mathcal{B}_{ab'})^* \right], \tag{19}
\end{aligned}$$

where, as before, a sum over gauge group factors in the term proportional to  $C_2(S)$  is implied. Just as in the RGE of Eq. (13), we have ordered the terms in (19) to make evident the correspondence with the terms in (14). The length of this equation is somewhat deceptive because many terms vanish in the case of the  $R$ -parity conserving MSSM. In a similar manner to the RGE for  $H_{abc}$  earlier, and as also seen in Paper I, when  $a$  and  $b$  are sfermion indices,  $\mathbf{U}_{a,b}^{1,2}$  and  $\mathbf{X}_{a,b}^{1,2}$  are zero. Likewise, when  $a$  and  $b$  label Higgs fields,  $\mathbf{V}_{a,b}$  and  $\mathbf{W}_{a,b}$  are zero. The derivation of the MSSM RGEs is, therefore, considerably less cumbersome than it appears at first sight.

### III. PARTICLE DECOUPLING

In the previous section, we have obtained the RGEs for the Majorana fermion and scalar mass parameters, as well as the bilinear and trilinear scalar coupling parameters for a gauge field theory with spin-0 and spin-1/2 fields. While these RGEs are not applicable to a completely general gauge field theory, as we have explained in Sec. II, they certainly apply to the MSSM with a conserved  $R$ -parity quantum number. Since we did not assume supersymmetry in our derivation, it is straightforward to include SUSY-breaking threshold effects in essentially the same way as in Paper I. Specifically, we implement SUSY and Higgs particle thresholds as step functions in the evaluation of the  $\beta$ -functions; *i.e.* we include the particle  $\mathcal{P}$  in the effective theory only if the scale,  $Q$ , is larger than the mass of  $\mathcal{P}$ .

To implement particle decoupling using this procedure clearly requires a knowledge of the particle spectrum which, in many models, is obtained using the RGEs. Fortunately, because the results depend only logarithmically on the scale at which we decouple the particles, an approximate knowledge of the particle spectrum suffices in order to implement particle decoupling. Here, for reasons detailed in Sec. III of Paper I, we will decouple both higgsinos at  $Q = |\mu|$ , the gauginos at the scale  $|M_i|$ , and the heavy Higgs bosons at the scale  $m_H$ . The decoupling of sfermions, if mixing effects are negligible, is also straightforward. Since one of the main reasons for this analysis is to study flavour-physics in the squark sector [23], we clearly must include mixing among the squarks. We will, therefore, defer the discussion of squark threshold corrections to a later point in the paper.

It is evident that for any discussion of thresholds we need to know the mass parameters in the MSSM. In addition to the SSB scalar and gaugino bilinears given in (16) of Paper I, we have mass terms for the higgsinos as well as Higgs scalars from the superpotential. These higgsino terms are,

$$\begin{aligned} \mathcal{L} \ni & -\frac{1}{2} \left\{ \frac{1}{2} (\mu + \mu^*) \left[ \bar{\Psi}_{h_u^0} \Psi_{h_d^0} + \bar{\Psi}_{h_d^0} \Psi_{h_u^0} + \bar{\Psi}_{h_u^+} \Psi_{h_d^-} + \bar{\Psi}_{h_d^-} \Psi_{h_u^+} \right] \right\} \\ & + \frac{i}{2} \left\{ \frac{1}{2i} (\mu - \mu^*) \left[ \bar{\Psi}_{h_u^0} \gamma_5 \Psi_{h_d^0} + \bar{\Psi}_{h_d^0} \gamma_5 \Psi_{h_u^0} + \bar{\Psi}_{h_u^+} \gamma_5 \Psi_{h_d^-} + \bar{\Psi}_{h_d^-} \gamma_5 \Psi_{h_u^+} \right] \right\}, \end{aligned} \quad (20)$$

resulting in two Majorana higgsino states of mass  $|\mu|$ , in the approximation that any gaugino-higgsino mixing can be neglected.

The superpotential,  $\hat{f}$ , also leads to Higgs scalar bilinears along with trilinear and quartic scalar terms in the potential. The so-called  $D$ -term contributions to the Lagrangian density

also lead to quartic scalar couplings that, in the supersymmetric limit, are fixed by the gauge couplings. In the notation of Ref. [4], these scalar potential terms are given by,

$$\mathcal{L} \ni -\frac{1}{2} \sum_A \left| \sum_i \mathcal{S}_i^\dagger g_\alpha t_{\alpha A} \mathcal{S}_i \right|^2 - \sum_i \left| \frac{\partial \hat{f}}{\partial \hat{\mathcal{S}}_i} \right|_{\hat{\mathcal{S}}=\mathcal{S}}^2. \quad (21)$$

Superpotential interactions can result in scalar bilinear, trilinear and quartic terms. As an illustration, if we take the second term in (21) and choose to differentiate with respect to the up-type Higgs superfield, *i.e.*  $\hat{\mathcal{S}} = \hat{H}_u$ , we see that,

$$\begin{aligned} \mathcal{L} \ni & -|\tilde{\mu}|^2 h_d^{0\dagger} h_d^0 - \tilde{u}_{Rk}^\dagger \tilde{u}_{Ll}^\dagger (\mathbf{f}_u)_{kn}^T (\mathbf{f}_u)_{lm}^* \tilde{u}_{Rm} \tilde{u}_{Ln} \\ & - \left( \tilde{u}_{Lk}^\dagger (\tilde{\mu}^* \mathbf{f}_u^{h_u})_{kl}^* \tilde{u}_{Rl} h_d^0 + \text{h.c.} \right). \end{aligned} \quad (22)$$

Note that we have inserted a tilde over the  $\mu$  in writing these terms. This is to allow for the fact that the higgsino mass  $\mu$  and the corresponding superpotential parameter  $\tilde{\mu}$  in the scalar sector will, in general, evolve differently once SUSY-breaking threshold effects are included. This is the analogue of the corresponding situation for dimensionless parameters. As we saw in Paper I, gaugino-quark-squark couplings  $\tilde{\mathbf{g}}^q$  evolve differently from the corresponding gauge couplings (and in fact develop flavour-violating components), while higgsino-quark-squark coupling matrices  $\tilde{\mathbf{f}}_{u,d}^q$  evolve differently from the corresponding Yukawa coupling matrices  $\mathbf{f}_{u,d}$  once the renormalization scale  $Q$  is below the mass of the heaviest sparticle. We should emphasize that we can never get an RGE for the parameter  $\tilde{\mu}$  discussed above. It enters via the SSB Higgs squared mass parameters in the combination  $m_{h_{u,d}}^2 + |\tilde{\mu}|^2$  or, as in (22) above, via combinations like  $(\tilde{\mu}^* \mathbf{f}_u^{h_u})_{lk}^*$ , the coefficients of “non-analytic” trilinear scalar interactions [24], denoted generically by  $\mathbf{c}_{ij}$  in Ref. [4]. It is only for these combinations of coefficients that enter the Lagrangian that we can (and do) obtain an RGE, not for the separate pieces. Above all thresholds, the RGEs for these combinations agree with the RGEs obtained from their component pieces. Notice that we have added a superscript  $\Phi$  to the “Yukawa coupling constant” that enters the trilinear scalar interaction in (22). Here, where this term in the scalar potential originates in the derivative of the superpotential with respect to  $\hat{h}_u$ , we set  $\Phi = h_u$ .

The reader may legitimately wonder why we include a superscript  $h_u$  on the coupling  $\mathbf{f}_u^{h_u}$  in the trilinear scalar coupling term but write the quartic scalar coupling constant as the square of the usual quark Yukawa coupling even below the scale of SUSY breaking. The reason is that we are going to ignore the difference in the renormalization of the quartic

scalar couplings, which is also why we did not derive the corresponding RGEs in Paper I. These couplings are less important from a phenomenological perspective (even though some of them enter the squark and slepton mass matrices). It is possible that quartic squark couplings that arise from the first term in (21) may also develop a non-trivial flavour-structure. These couplings will not affect the two-body (flavour-violating) decays of squarks except at the loop-level, leading us to believe that threshold corrections to these couplings can be sensibly neglected. In the following, we have set *all* quartic scalar couplings, irrespective of whether they originate in the superpotential or in the  $D$ -term, to their supersymmetric values, *i.e.* equal to the “square” of the usual Yukawa coupling or of the corresponding gauge coupling, but have retained threshold effects in the trilinear couplings that cause phenomenologically important mixing between left- and right-squarks.<sup>1</sup> Since we do not, therefore, need independent RGEs for these quartic couplings, we have not listed here equations to convert the  $\Lambda$  and  $\Lambda'$  in (2) to the corresponding  $\lambda$  in (1), equivalent to (12) and (18). Of course, the inverse of these equations is needed in order to write the right hand sides of (13) and (19), but this is considerably simpler.

The decoupling of fields whose mixing can be ignored is straightforward: below their mass scale, we simply remove all contributions from these fields when evaluating any RGE. This covers: gauginos; higgsinos, because they are approximately degenerate [14]; and in many models, also sleptons.

Next, we turn to the decoupling of the spin-zero particles in the Higgs sector where we cannot disregard mixing effects, and then discuss how we treat decoupling in the squark sector where evaluation of flavour effects is one of our important goals. Before proceeding, we mention one more complication that arises because  $\mu$  does not necessarily equal  $\tilde{\mu}$ . This makes the determination of  $\mu$  more involved since the electroweak symmetry breaking conditions only depend on its bosonic cousin  $\tilde{\mu}$ ; we will defer the discussion of how  $\mu$  and  $\tilde{\mu}$  are determined to the next section.

---

<sup>1</sup> The quartic terms in the potential yield the so-called  $D$ -term contributions to squark masses, and also the term that makes the squark mass the same as the quark mass in the supersymmetric limit. In most cases these are both subdominant contributions to squark masses, giving further credence to our approximation.

## A. Higgs Boson Decoupling

As discussed in Paper I, the implementation of step-function decoupling requires us to write the Lagrangian density with the fields in their (approximate) mass eigenstate basis. This led us to rewrite the interactions of the MSSM Higgs fields in terms of the spin-zero fields  $(\mathbf{h}, \mathcal{H}, H^\pm)$  defined [14] in terms of the MSSM fields of the scalar Higgs sector by,

$$\begin{pmatrix} G^+ \\ \mathbf{h} \end{pmatrix} = s \begin{pmatrix} h_u^+ \\ h_u^0 \end{pmatrix} + c \begin{pmatrix} h_d^{-*} \\ h_d^{0*} \end{pmatrix} \quad (23)$$

$$\begin{pmatrix} H^+ \\ \mathcal{H} \end{pmatrix} = c \begin{pmatrix} h_u^+ \\ h_u^0 \end{pmatrix} - s \begin{pmatrix} h_d^{-*} \\ h_d^{0*} \end{pmatrix}, \quad (24)$$

where  $c = \cos \beta$  and  $s = \sin \beta$ . For  $m_H \gg M_Z$ , the physical Higgs bosons  $h, H, A$  and  $H^\pm$  are then approximately given by [14],<sup>2</sup>

$$\begin{aligned} \mathbf{h} &= \frac{h+iG^0}{\sqrt{2}} \\ \mathcal{H} &= \frac{-H+iA}{\sqrt{2}}. \end{aligned}$$

Here  $G^+$  and  $G^0$  are the would-be-Goldstone bosons that get dynamically rearranged to become the longitudinal components of the massive gauge bosons by the Higgs mechanism. If  $CP$  is violated in the Higgs boson sector, the neutral spin-zero states  $H$  and  $A$  will further mix with one another. When we eliminate the charged and neutral components of the scalar doublets  $H_u$  and  $H_d$  and rewrite the Lagrangian density in terms of  $(\mathbf{h}, \mathcal{H}, H^\pm)$ , new operator structures, and concomitantly new couplings, appear in the theory. For instance, the couplings of  $h$  to fermions are given by the SM Yukawa coupling matrices  $\lambda_{u,d}$ , and after decoupling of the heavy Higgs scalars, the matrices  $\tilde{\mathbf{f}}_{u,d}$  disappear altogether (though, depending on the spectrum, their tilde cousins may remain).

For  $Q > m_H$  where all Higgs fields are active in the RGEs, the rotation to the Higgs field “mass basis” makes no difference as it is just a field redefinition. For  $Q < m_H$ , however, this rotation is crucial since it determines the particular combinations of fields that decouple from the RGEs. In this case, only specific combinations of the parameters in the original

---

<sup>2</sup> If  $m_H$  is close to  $M_Z$ , all the bosons in the Higgs sector have masses close to  $M_Z$  and, as noted in Paper I, the resulting threshold corrections are small.

theory remain upon decoupling, while other combinations generally become irrelevant. For example, when the two trilinear terms which couple  $\tilde{u}_L$  and  $\tilde{u}_R$  to the Higgs bosons are rotated into the  $(\mathbf{h}, \mathcal{H})$  basis, we see that

$$\begin{aligned} \mathcal{L} &\ni \tilde{u}_{Rk}^\dagger (\mathbf{a}_u^T)_{kl} \tilde{u}_{Ll} h_u^0 - \tilde{u}_{Rk}^\dagger (\tilde{\mu}^* \mathbf{f}_u^{h_u})_{kl}^T \tilde{u}_{Ll} h_d^{0*} \\ &= \tilde{u}_{Rk}^\dagger (\mathbf{a}_u^T)_{kl} \tilde{u}_{Ll} (s\mathbf{h} + c\mathcal{H}) - \tilde{u}_{Rk}^\dagger (\tilde{\mu}^* \mathbf{f}_u^{h_u})_{kl}^T \tilde{u}_{Ll} (c\mathbf{h} - s\mathcal{H}) . \end{aligned} \quad (25)$$

Upon decoupling the field  $\mathcal{H}$ , this term becomes

$$\mathcal{L} \ni \tilde{u}_{Rk}^\dagger \left[ s(\mathbf{a}_u^T)_{kl} - c(\tilde{\mu}^* \mathbf{f}_u^{h_u})_{kl}^T \right] \tilde{u}_{Ll} \mathbf{h} . \quad (26)$$

Although in the complete MSSM case we can sensibly talk about the evolution of the constituent pieces  $(\mathbf{a}_u^T)_{kl}$  and  $\mu$  separately, for  $Q < m_H$ , it is no longer possible to write RGEs for both  $\mathbf{a}_u$  and  $\tilde{\mu}^* \mathbf{f}_u^{h_u}$ . We must instead talk only about the single combination  $\left[ s(\mathbf{a}_u^T)_{kl} - c(\tilde{\mu}^* \mathbf{f}_u^{h_u})_{kl}^T \right]$  that remains in the effective theory below  $Q = m_H$ . In the same vein, we should mention that the quartic scalar operators with  $\Lambda'_{abcd}$ -type couplings in (2) are absent above all SUSY thresholds in the  $R$ -parity conserving MSSM, since in this case the number of daggered and undaggered fields is always the same (remember that these originate in the absolute square of a quadratic operator). We will see below that these  $\Lambda'$ -type couplings arise because of the way we define specific linear combinations of fields to take into account threshold effects.

## B. Squark Decoupling

Squarks of different flavours and types ( $L$  or  $R$ ) can mix as long as they have the same electric charge. In the up-squark sector, squark mass eigenstates are, therefore, combinations of  $\tilde{u}_{L,R}$ ,  $\tilde{c}_{L,R}$  and  $\tilde{t}_{L,R}$  squarks, and likewise in the down-squark sector. It is these mass eigenstate fields that need to be decoupled for the evaluation of threshold effects.

The reader may have noticed that in Paper I, as well as in this paper, we have maintained manifest electroweak gauge invariance throughout, in that we decouple entire multiplets together. In keeping with this, we have specified the boundary conditions for the  $(3 \times 3)$  Yukawa coupling matrices at the scale  $Q = m_t$ , rather than at  $Q = M_Z$  where the top quark would have already been decoupled.<sup>3</sup> To avoid any complications that may arise

---

<sup>3</sup> Specifying the boundary conditions at  $Q = m_t$  is really only necessary if we insist on decoupling every

from splitting a multiplet, for the purposes of evaluating the squark thresholds, *and for this alone*, we will assume that left-right squark mixing effects which can arise only from  $SU(2)_L \times U(1)_Y$  breaking are not important.<sup>4</sup> This is clearly a sensible approximation when squark SSB parameters are larger than the weak scale. Remembering that the calculation is only logarithmically sensitive to the actual location of the threshold, we can see that this approximation breaks down significantly *only when the off-diagonal entries in the squark mass matrices cause large cancellations in the calculation of the lighter squark eigenvalue, leading to a physical mass squared much smaller than either diagonal entry*. For pathological parameter values where such a cancellation is operative and  $\tilde{q}_L - \tilde{q}_R$  mixing indeed causes one of the squarks to be much lighter than all other squarks of the same charge, our approximation will not apply. Hereafter, we will assume that any hierarchy in the squark mass spectrum has its origin in the values of squark SSB parameters, and *is not the result of an accidental cancellation* between the diagonal and off-diagonal parameters in the squark-mass matrix. We will, therefore, neglect left-right mixing, for, and only for, the purpose of determining the locations of the squark thresholds.

Squark thresholds are then determined only by the SSB mass squared matrices for the squarks. As with all other particles, we decouple any squark below the scale equal to its mass. Since (for the purpose of locating the squark mass thresholds) we are working in the approximation that  $SU(2) \times U(1)_Y$  breaking terms are neglected, the various left- and right-squark mass thresholds are determined by the eigenvalues of the corresponding SSB mass squared matrices. The associated technicalities are best explained by describing the step-wise procedure that we use.

1. We evolve the gauge and Yukawa couplings to the high scale (usually taken to be  $M_{\text{GUT}}$ ) where the boundary conditions for the SSB parameters are specified. Toward this end, we first eliminate the quark masses in favour of the diagonal SM Yukawa coupling matrices in the quark mass basis at  $Q = M_Z$  ( $Q = m_t$  for the top quark), and rotate to a current basis (related to the quark mass basis by Eq. (38) of Paper I) at  $Q =$

---

particle at the scale equal to its mass. Such a procedure is advantageous in many situations, but not compulsory. Indeed, as we will see in the next section, while we decouple all sparticles and heavy Higgs bosons at their mass scale, we decouple the top quark at  $Q = M_Z$ , below which the effective theory is an  $SU(3)_C \times U(1)_{\text{em}}$  gauge theory.

<sup>4</sup> To be specific, we will focus our discussion on squark thresholds, but exactly the same procedure applies for slepton thresholds.



$m_t$ .<sup>5</sup> We morph the SM coupling matrices  $\lambda_{u,d}$  to the MSSM Yukawa coupling matrices  $\mathbf{f}_{u,d}$  at  $Q = m_H$ , and include SUSY radiative corrections [25] as given by ISAJET [26] (*i.e* without flavour mixing among squarks) at  $Q = M_{\text{SUSY}}$ , before continuing to evolve to  $M_{\text{GUT}}$ .

2. All the dimensionless couplings and MSSM SSB parameters can now be evolved back to the low scale with Higgs bosons, higgsino and gaugino thresholds implemented as in Paper I. We must, however, be careful in implementing the squark thresholds. At each step in the integration, we find the eigenvalues of the SSB squark mass squared matrices, and carry on the evolution in the original current basis if the scale  $Q^2$  is larger than the highest of these eigenvalues, and none of the squarks are decoupled.
3. At some value of the scale,  $Q_0$ ,  $Q^2$  just crosses the largest eigenvalue of one of the SSB squark  $\mathbf{m}^2$  matrices, evaluated at the scale  $Q_0$ . We decouple that particular squark at this scale, but retain all other squarks in the evolution. The up and down type squarks in the same doublet decouple together of course, so that  $SU(2)$  is never broken by this procedure. To decouple the squark, we rotate to the basis (denoted here by the superscript  $M$ ) where the corresponding squark SSB matrix is diagonal at  $Q = Q_0$  using the appropriate one of,

$$\begin{pmatrix} \tilde{u}_L \\ \tilde{d}_L \end{pmatrix} = \mathbf{R}_Q \begin{pmatrix} \tilde{u}_L^M \\ \tilde{d}_L^M \end{pmatrix}, \quad (27a)$$

$$\tilde{u}_R = \mathbf{R}_u \tilde{u}_R^M, \quad (27b)$$

$$\tilde{d}_R = \mathbf{R}_d \tilde{d}_R^M, \quad \text{or one of} \quad (27c)$$

$$\begin{pmatrix} \tilde{e}_L \\ \tilde{\nu}_L \end{pmatrix} = \mathbf{R}_L \begin{pmatrix} \tilde{e}_L^M \\ \tilde{\nu}_L^M \end{pmatrix}, \quad (27d)$$

$$\tilde{e}_R = \mathbf{R}_e \tilde{e}_R^M \quad \text{when decoupling a slepton.} \quad (27e)$$

The unitary rotation matrices,  $\mathbf{R}_\bullet$ , are chosen to diagonalize the Hermitian SSB squark (or slepton) mass matrices, for example:

$$\left( \mathbf{R}_Q^\dagger \mathbf{m}_Q^2 \mathbf{R}_Q \right)_{ij} = \left( \mathbf{m}_Q^2 \right)_{ij}^{\text{diag}} \equiv \left( \mathbf{m}_Q^2 \right)_{ii}^{\text{diag}} \delta_{ij}. \quad (28)$$

---

<sup>5</sup> In our iterative procedure to solve the RGEs described below, it is important to remember that we retain the top quark all the way to  $Q = M_Z$  so that electroweak gauge invariance is preserved.

Decoupling this squark is now straightforward — as with all sparticles, we simply introduce a  $\theta_{\tilde{q}_k}$  for the decoupled squark  $\tilde{q}_k^M$  (where  $k$  is the mass basis index, and  $\tilde{q} = \tilde{Q}_L, \tilde{u}_R$  or  $\tilde{d}_R$ ) into the RGEs, since we are in the “mass basis” for this squark at least within the approximation that we have discussed.<sup>6</sup> Just for clarification, in any other basis these  $\theta_{\tilde{q}_k}$  would be matrices. For instance, the left-handed squark theta,  $\theta_{\tilde{Q}_k}$ , can be written in the original current basis as,

$$(\Theta_Q)_{ij} = (\mathbf{R}_Q \Theta_Q^{\text{diag}} \mathbf{R}_Q^\dagger)_{ij} = \theta_{\tilde{Q}_k} (\mathbf{R}_Q)_{ik} \delta_{kl} (\mathbf{R}_Q^\dagger)_{lj} . \quad (29)$$

We have checked that this same  $\Theta_Q$  matrix works for all terms involving doublet squark thresholds, and likewise for the other squarks and sleptons. We always write the RGEs in a current basis where the SSB squark mass matrices are diagonal (see the item immediately following this). This is why we have  $\theta$ 's rather than the matrices  $\Theta$  appearing. We rotate back to our original current basis when we present numerical results.

4. To evolve to lower values of  $Q$ , we must be in *some current basis*. We thus also rotate the corresponding quarks (or leptons for slepton decoupling) by the same amount as the decoupled squark (slepton), and continue the evolution in this new current basis. The “mass” and the “eigenvector” of the decoupled squark is frozen at its decoupled value at  $Q = Q_0$ . As a technical aside, we note that the same RGE (with  $(3 \times 3)$  mass squared matrices) can be used to continue the evolution in this new current basis. The  $\theta_{\tilde{q}_k}$ 's that we introduce into the RGEs ensure that the decoupled squark does not contribute to the evolution of the remaining squarks. In other words, in the new mass basis the decoupled squark *never* contributes to the evolution of the SSB matrix elements for the  $(2 \times 2)$  sub-matrix in the sub-space orthogonal to the decoupled squark state.<sup>7</sup> We use the RGEs to continue the evolution to lower scales, now obtaining the eigenvalues of the  $(2 \times 2)$  sub-matrix in the orthogonal sub-space just mentioned, and

---

<sup>6</sup> From now on, we will no longer write the superscript  $M$  for the squark mass eigenstates, but it will presumably be clear from the context whether we are referring to these, or to the states in the original basis.

<sup>7</sup> Rather than re-code new RGEs where we retain only the two active squarks for the subsequent evolution, we continue the evolution with all the squarks. Below the scale  $Q_0$ , just the elements of the  $(2 \times 2)$  sub-matrix in the vector space orthogonal to the decoupled squark are physical. The remaining elements, though calculated are never used, and their value does not affect the calculation.

once again decoupling the squark when the larger of the two eigenvalues just crosses  $Q^2$ . The corresponding eigenvector of this sub-matrix gives us the second squark state with the same gauge quantum numbers to be decoupled (remember that we are in the new current basis). As before we freeze its mass and wave function upon decoupling. Notice that, by construction, the two decoupled states are orthogonal to one another and to the single remaining active state, as they should be. The single remaining state may be decoupled in a straightforward way. Since we know the relation between the new current basis and our original current basis, it is straightforward to rotate the SSB parameters back to the latter basis.

5. We have described squark decoupling for any one set of squarks, *i.e.* doublet squarks, the up-type singlet squarks or the down-type singlet squarks, but it should be clear that the procedure that we have described works for all the squarks as well as for sleptons.
6. We must, likewise, decouple squark mass eigenstates obtained using our procedure during the evolution of all other parameters. However, for the scalar trilinear coupling parameters,  $\mathbf{a}$ , there is the added complication that we must decouple the heavy Higgs bosons at the scale  $Q = m_H$ . In this case particular combinations of parameters that include  $\mathbf{a}_{ij}$  need to be evolved, as we have already discussed.

#### IV. APPLICATION TO THE MSSM

We now apply the general results obtained in Sec. II to derive the RGEs for the dimensionful couplings of the  $R$ -parity conserving MSSM. As in Paper I, our strategy will be to read off the couplings in (2) from the MSSM couplings detailed in Eq. (16)-(22) of Paper I, and from (20)-(22) of this paper, and substituting these into the general RGEs obtained in Sec. II. The quartic scalar couplings not listed here may be derived from (21) above, and are also found in Ref. [4]. Once the couplings are all correctly identified, the derivation of the RGEs using (5), (6), (13) and (19) is tedious but straightforward.

We proceed by outlining how to go about deriving the RGEs for each group of dimensionful couplings: gaugino and higgsino mass parameters, trilinear couplings, and scalar soft mass parameters and their bilinear cousins. Our purpose is to guide the reader interested

in deriving the RGEs as to where the various terms come from, and to point out potential pitfalls that may be encountered on the way. The complete set of RGEs for the dimensionful parameters is listed in Appendix B.

### A. Gaugino and Higgsino Mass Parameters

The application to the MSSM of the general RGEs in (5) and (6) is straightforward. The matrices  $\mathbf{m}_X^{(\prime)}$  are constructed from the  $M_{1,2,3}^{(\prime)}$ , the SSB gaugino mass terms, and  $\mu$  which appears via the higgsino mass terms in (20). The parameter  $\tilde{\mu}$  that appears in the scalar Higgs sector should not be confused with the corresponding fermion mass parameter  $\mu$ .

As previously noted, the trace terms in (5) and (6) vanish so that we need only sum over the scalar index  $b$  and multiply out the terms. When the higgsinos are rotated as in Eq. (14) of Paper I,  $\mathbf{m}_X^{(\prime)}$  becomes diagonal and the derivation simplifies further. We find, for example, that the RGE for  $M_2$  is

$$\begin{aligned}
(4\pi)^2 \frac{dM_2}{dt} = & M_2 \theta_{\tilde{W}} \left[ 3\theta_{\tilde{Q}_k} (\tilde{\mathbf{g}}^Q)_{kl} (\tilde{\mathbf{g}}^Q)_{lk}^\dagger + \theta_{\tilde{L}_k} (\tilde{\mathbf{g}}^L)_{kl} (\tilde{\mathbf{g}}^L)_{lk}^\dagger + \theta_{\tilde{h}} |\tilde{g}^{h_u}|^2 (s^2\theta_h + c^2\theta_H) \right. \\
& \left. + \theta_{\tilde{h}} |\tilde{g}^{h_d}|^2 (c^2\theta_h + s^2\theta_H) \right] \\
& + 2sc(-\theta_h + \theta_H) \theta_{\tilde{h}} [\tilde{g}^{h_d} \mu^* \tilde{g}^{h_u} + (\tilde{g}^{h_d})^* \mu (\tilde{g}^{h_u})^*] - 12\theta_{\tilde{W}} M_2 g_2^2,
\end{aligned} \tag{30}$$

and draw the reader's attention to the following points:

1. The first term, which is  $M_2$  multiplied by a number of gaugino coupling terms, arises from the terms in (5) that have  $(\mathbf{m}_X \pm i\mathbf{m}'_X)$  on the extreme left or on the extreme right. When in this position the  $\mathbf{m}_X^{(\prime)}$  is connected to an external gaugino, and since  $\mathbf{m}_X^{(\prime)}$  is diagonal it contributes a gaugino mass term. This term includes a sum over scalar fields and corresponding fermion fields (that enter the RGE via 1-loop Feynman diagrams), with concomitant couplings such as  $\tilde{\mathbf{g}}^Q$  and  $\tilde{g}^{h_u}$  of fields that couple to the wino. This sum over *all* scalar fields includes all active sfermion flavours at the scale  $Q$ , *i.e.* sfermions with masses larger than  $Q$  are decoupled. As in Paper I, the decoupling of any particle is introduced into the RGEs via the  $\theta_{\mathcal{P}} = 1$  if  $Q$  is larger than the mass of  $\mathcal{P}$ , with  $\theta_{\mathcal{P}} = 0$  otherwise. Thus, for instance, in the first term  $\theta_{\tilde{Q}_k} (\tilde{\mathbf{g}}^Q)_{kl} (\tilde{\mathbf{g}}^Q)_{lk}^\dagger$ , the summation over  $k$  includes all *active* left-type squarks at the scale  $Q$  (as emphasized in the last section, this RGE is written in the basis where the corresponding squark

SSB matrix is diagonal), while the  $l$  sums over the quarks (that are all always assumed to be present in the effective theory we use to compute the RGE<sup>8</sup>) which is why we do not include the corresponding  $\theta$ 's. Below the highest sfermion threshold the sfermion gaugino coupling terms are, therefore, *truncated* traces.

2. In the RGEs, we write  $\theta_{\mathcal{P}}$ 's for, and only for, particles  $\mathcal{P}$  that enter via the internal lines of loop diagrams that contribute in the RGEs. Sometimes, this internal particle is the same as the particle on the external leg of the corresponding diagram, as illustrated by the appearance of  $\theta_{\tilde{W}}$  in the first and third terms of (30). Furthermore, since at any scale  $Q$ , we retain only those (non-SM) particles with masses larger than  $Q$  in the effective Lagrangian that we use to derive the RGEs, we stop evolving the coefficient of any (composite) field operator — these coefficients are just the Lagrangian parameters — when the scale  $Q$  falls below the mass of any of the fields that enter the operator. Thus, in the case of  $M_2(Q)$ , we freeze its evolution below the scale  $Q_0$  where  $Q_0 = M_2(Q_0)$ .
3. The reader may be struck by the second term on the right-hand-side, proportional to  $\mu$ , whose appearance seems odd at first sight. It originates in the terms in (5) where  $\mathbf{m}_X^{(\prime)}$  is sandwiched between two  $\mathbf{X}_b^{1,2}$  matrices. Since  $\mathbf{X}_b^{1,2}$  connects gauginos to higgsinos, and the external fields are gauginos, the  $\mathbf{m}_X^{(\prime)}$  is necessarily a higgsino mass term. Notice that this term is a threshold effect: it does not vanish only if  $|\mu| < Q < m_H$ . The light and heavy Higgs boson doublets in (23) and (24), respectively, make equal but opposite  $\mu$ -dependent contributions to the evolution of  $M_2$  which indeed cancel above all thresholds. The appearance of  $\mu$  is a general feature of the electroweak gaugino mass RGEs — listed in full in Appendix B, (B2)-(B5). For much the same reasons, for appropriate mass ordering, the RGE for the complex parameter  $\mu$ , (B1), develops a dependence on the electroweak gaugino mass parameters,  $M_1^{(\prime)}$  and  $M_2^{(\prime)}$ .
4. Despite the appearance of the complex  $\mu$ -dependent terms just discussed in the RGEs for the gaugino mass parameters, the reality of  $M_i$  and  $M_i'$  under renormalization group evolution is preserved, as it must.

---

<sup>8</sup> In this paper, we always assume that  $Q \geq M_Z$ , and retain all SM particles in the effective theory, but write an explicit  $\theta_h$  only for the light scalar doublet that includes the would-be-Goldstone bosons.

5. Finally, notice that above all thresholds, where the  $SU(2)$  gaugino coupling matrices  $\tilde{\mathbf{g}}^\bullet$  reduce to  $g_2$  times the unit matrix in the flavour space (see Paper I) and all  $\theta_i = 1$ , we recover the MSSM result upon summing over all flavours [18].

## B. Trilinear Couplings

For the  $R$ -parity conserving MSSM, the trilinear scalar couplings  $\mathbf{H}_{abc}$  involve couplings between one of the Higgs boson fields and two sfermion fields. In order to facilitate decoupling of the Higgs scalars, we saw that it is necessary to rotate these Higgs fields to their (approximate) mass basis given by (23) and (24), so that  $a, b$  and  $c$  run over the *complex* fields,  $\{\mathbf{h}, \mathcal{H}, G^+, H^+, \tilde{u}_{Li}, \tilde{d}_{Li}, \tilde{e}_{Li}, \tilde{\nu}_{Li}, \tilde{u}_{Ri}, \tilde{d}_{Ri}, \tilde{e}_{Ri}\}$ , and  $i$  runs over all three flavours. Unlike the charged would-be-Goldstone fields  $G^\pm$  that appear explicitly, the neutral would-be-Goldstone boson  $G^0$  is contained in the complex field  $\mathbf{h}$ . When fully expanded out in flavour space,  $\mathbf{H}_{abc}$  is a  $(25 \times 25 \times 25)$  array, whose entries are mostly all zero, and with many non-zero entries related by the  $SU(2)$  gauge symmetry of the interactions, that we can easily read off. For instance, from (26) we immediately see that,

$$\mathbf{H}_{\tilde{u}_{Rk}, \mathbf{h}, \tilde{u}_{Ll}} = \left[ s(\mathbf{a}_u^T)_{kl} - c(\tilde{\mu}^* \mathbf{f}_u^{h_u})_{kl}^T \right]. \quad (31)$$

As we mentioned below (13), we can without loss of generality in the RGEs, always choose the external index  $a$  to be a sfermion, since then several terms drop out in the derivation of the corresponding RGE for the trilinear parameter. Of course, we also need to work out the  $\mathbf{\Lambda}$  and  $\mathbf{\Lambda}'$  matrices. These are  $(25 \times 25 \times 25 \times 25)$  arrays in scalar field space, again with mostly zero entries and with most non-zero entries related by the gauge invariance of the interactions. As noted previously, these can be worked out from (21). The extraction of the  $\mathbf{\Lambda}$  terms is entirely straightforward, but care must be taken with the sfermion flavours and squark colours, which are implicitly summed over in (21). As alluded to at the end of Sec. III A, we note here that  $\mathbf{\Lambda}' = \mathbf{0}$  when the MSSM Lagrangian is written in terms of  $h_u$  and  $h_d$  Higgs fields. These couplings arise only when the Higgs boson doublets are rotated to their mass basis using (23) and (24) since only the conjugate fields  $h_d^{-*}$  and  $h_d^{0*}$  appear in the linear combinations with the unstarred fields  $h_u^+$  and  $h_u^0$ , respectively. In order to get only one daggered scalar field, lepton and baryon number conservation for the dimension four operators imply that we must have Higgs fields in the interactions. Moreover, we must

have both an up-type and a down-type Higgs field *before* the Higgs field rotation to the mass basis, and that the down-type Higgs fields must be  $h_d^{(0,-)*}$  while the up-type fields must be  $h_u^{(+,0)}$ . This only occurs in quartics in (21) that derive from differentiating the superpotential with respect to the superfields  $\hat{u}_L$  or  $\hat{d}_L$ , and so have a  $\tilde{u}_{iR}$  and a  $\tilde{d}_{jR}$  in the interaction. As a result, there are very few non-vanishing  $\Lambda'$ -type quartic interactions. Indeed, these are completely given by,

$$\mathcal{L} \ni (\mathbf{f}_u^T \mathbf{f}_d^*)_{kl} (\mathbf{h}H^+ - G^+\mathcal{H}) \tilde{u}_{Rk}^\dagger \tilde{d}_{Rl} + \text{h.c.} \quad (32)$$

In deriving the RGEs, we must remember to include the contributions from the would-be-Goldstone fields in the sum over *complex* scalar fields. The neutral Goldstone boson is automatically present in the field  $\mathbf{h}$  along with the (almost) SM-like Higgs boson, but the charged fields  $G^\pm$  must explicitly be included in the sum. For example, the RGE for  $\mathbf{H}_{\tilde{u}_{Ri}, \mathbf{h}, \tilde{u}_{Lj}}$  includes a term  $\Lambda_{e,f,\mathbf{h},\tilde{u}_{Lj}} \mathbf{H}_{\tilde{u}_{Ri},e,f}$  and we must sum  $e$  and  $f$  over *all* scalars in the theory for which  $\Lambda_{e,f,\mathbf{h},\tilde{u}_{Lj}} \mathbf{H}_{\tilde{u}_{Ri},e,f} \neq 0$ .

Using Eq. (13) to derive the RGE for the operator in (31), writing all internal threshold  $\theta_{\mathcal{P}}$ 's explicitly, we obtain:

$$\begin{aligned}
& (4\pi)^2 \frac{d[s(\mathbf{a}_u)_{ij} - c(\tilde{\mu}^* \mathbf{f}_u^{hu})_{ij}]}{dt} = \\
& \theta_{\tilde{u}_k} \left\{ \theta_h [s(\mathbf{a}_u)_{ik} - c(\tilde{\mu}^* \mathbf{f}_u^{hu})_{ik}] \left[ \frac{2g'^2}{3} (c^2 - s^2) \delta_{kj} + 2s^2 [(\mathbf{f}_u)^\dagger(\mathbf{f}_u)]_{kj} \right] \right. \\
& \quad \left. + \theta_{HSC} [c(\mathbf{a}_u)_{ik} + s(\tilde{\mu}^* \mathbf{f}_u^{hu})_{ik}] \left[ -\frac{4g'^2}{3} \delta_{kj} + 2 [(\mathbf{f}_u)^\dagger(\mathbf{f}_u)]_{kj} \right] \right\} \\
& + \theta_{\tilde{u}_l} \theta_{\tilde{Q}_k} \left[ -2 \left( \frac{g'^2}{9} + \frac{4g_3^2}{3} \right) \delta_{ik} \delta_{lj} + 6(\mathbf{f}_u)_{ij} (\mathbf{f}_u)_{lk}^\dagger \right] [s(\mathbf{a}_u)_{kl} - c(\tilde{\mu}^* \mathbf{f}_u^{hu})_{kl}] \\
& + 2\theta_{\tilde{Q}_k} \left\{ \theta_h \left[ \left( \frac{g'^2}{12} - \frac{3g_2^2}{4} \right) (s^2 - c^2) \delta_{ik} + 2s^2 [(\mathbf{f}_u)(\mathbf{f}_u)^\dagger]_{ik} - c^2 [(\mathbf{f}_d)(\mathbf{f}_d)^\dagger]_{ik} \right] \right. \\
& \quad \times [s(\mathbf{a}_u)_{kj} - c(\tilde{\mu}^* \mathbf{f}_u^{hu})_{kj}] + \theta_{HSC} \left[ \left( \frac{g'^2}{6} - \frac{3g_2^2}{2} \right) \delta_{ik} + 2 [(\mathbf{f}_u)(\mathbf{f}_u)^\dagger]_{ik} \right. \\
& \quad \left. \left. + [(\mathbf{f}_d)(\mathbf{f}_d)^\dagger]_{ik} \right] \times [c(\mathbf{a}_u)_{kj} + s(\tilde{\mu}^* \mathbf{f}_u^{hu})_{kj}] \right\} \\
& + 2\theta_H \theta_{\tilde{d}_k} [s(\mathbf{a}_d)_{ik} + c(\tilde{\mu}^* \mathbf{f}_d^{hd})_{ik}] [(\mathbf{f}_d)^\dagger(\mathbf{f}_u)]_{kj} \\
& + \frac{2}{3} \theta_{\tilde{B}} s (M_1 - iM'_1) \left( \theta_{\tilde{h}} (\tilde{g}^{hu})^* (\tilde{\mathbf{g}}'^Q)_{ik}^* (\tilde{\mathbf{f}}_u^{uR})_{kj} - \frac{4}{3} (\tilde{\mathbf{g}}'^Q)_{ik}^* (\mathbf{f}_u)_{kl} (\tilde{\mathbf{g}}'^{uR})_{kj}^* \right. \\
& \quad \left. - 4\theta_{\tilde{h}} (\tilde{\mathbf{f}}_u^Q)_{ik} (\tilde{\mathbf{g}}'^{uR})_{kj}^* (\tilde{g}^{hu})^* \right) - \frac{32}{3} \theta_{\tilde{g}} s (M_3 - iM'_3) (\tilde{\mathbf{g}}_s^Q)_{ik}^* (\mathbf{f}_u)_{kl} (\tilde{\mathbf{g}}_s^{uR})_{lj}^* \\
& \quad - 6\theta_{\tilde{W}} \theta_{\tilde{h}} s (M_2 - iM'_2) (\tilde{g}^{hu})^* (\tilde{\mathbf{g}}^Q)_{ik}^* (\tilde{\mathbf{f}}_u^{uR})_{kj} + \frac{2}{3} \theta_{\tilde{B}} \theta_{\tilde{h}} c \mu^* \tilde{g}^{hd} \left( 4(\tilde{\mathbf{f}}_u^Q)_{ik} (\tilde{\mathbf{g}}'^{uR})_{kj}^* - (\tilde{\mathbf{g}}'^Q)_{ik}^* (\tilde{\mathbf{f}}_u^{uR})_{kj} \right) \\
& \quad + 6\theta_{\tilde{h}} \theta_{\tilde{W}} c \mu^* \tilde{g}^{hd} (\tilde{\mathbf{g}}^Q)_{ik}^* (\tilde{\mathbf{f}}_u^{uR})_{kj} - 4\theta_{\tilde{h}} c \mu^* (\tilde{\mathbf{f}}_d^Q)_{ik} (\mathbf{f}_d^\dagger)_{kl} (\tilde{\mathbf{f}}_u^{uR})_{lj} \\
& \quad \left. + \theta_{\tilde{u}_k} [s(\mathbf{a}_u)_{ik} - c(\tilde{\mu}^* \mathbf{f}_u^{hu})_{ik}] \left[ \frac{8}{9} \theta_{\tilde{B}} (\tilde{\mathbf{g}}'^{uR})_{kl}^T (\tilde{\mathbf{g}}'^{uR})_{lj}^* + \frac{8}{3} \theta_{\tilde{g}} (\tilde{\mathbf{g}}_s^{uR})_{kl}^T (\tilde{\mathbf{g}}_s^{uR})_{lj}^* + 2\theta_{\tilde{h}} (\tilde{\mathbf{f}}_u^{uR})_{kl}^\dagger (\tilde{\mathbf{f}}_u^{uR})_{lj} \right] \right. \\
& \quad + \theta_h \left[ 3s^2 (\mathbf{f}_u^\dagger)_{kl} (\mathbf{f}_u)_{lk} + c^2 \left\{ 3(\mathbf{f}_d^\dagger)_{kl} (\mathbf{f}_d)_{lk} + (\mathbf{f}_e^\dagger)_{kl} (\mathbf{f}_e)_{lk} \right\} \right] [s(\mathbf{a}_u)_{ij} - c(\tilde{\mu}^* \mathbf{f}_u^{hu})_{ij}] \\
& \quad + \theta_{HSC} \left[ 3(\mathbf{f}_u^\dagger)_{kl} (\mathbf{f}_u)_{lk} - \left\{ 3(\mathbf{f}_d^\dagger)_{kl} (\mathbf{f}_d)_{lk} + (\mathbf{f}_e^\dagger)_{kl} (\mathbf{f}_e)_{lk} \right\} \right] [c(\mathbf{a}_u)_{ij} + s(\tilde{\mu}^* \mathbf{f}_u^{hu})_{ij}] \\
& \quad + \frac{1}{2} \theta_{\tilde{h}} \left\{ \theta_h \left[ c^2 \left( \theta_{\tilde{B}} |\tilde{g}^{hd}|^2 + 3\theta_{\tilde{W}} |\tilde{g}^{hd}|^2 \right) + s^2 \left( \theta_{\tilde{B}} |\tilde{g}^{hu}|^2 + 3\theta_{\tilde{W}} |\tilde{g}^{hu}|^2 \right) \right] \right. \\
& \quad \times [s(\mathbf{a}_u)_{ij} - c(\tilde{\mu}^* \mathbf{f}_u^{hu})_{ij}] + \theta_{HSC} \left[ - \left( \theta_{\tilde{B}} |\tilde{g}^{hd}|^2 + 3\theta_{\tilde{W}} |\tilde{g}^{hd}|^2 \right) \right. \\
& \quad \left. \left. + \left( \theta_{\tilde{B}} |\tilde{g}^{hu}|^2 + 3\theta_{\tilde{W}} |\tilde{g}^{hu}|^2 \right) \right] \times [c(\mathbf{a}_u)_{ij} + s(\tilde{\mu}^* \mathbf{f}_u^{hu})_{ij}] \right\} \\
& + \theta_{\tilde{Q}_l} \left[ \theta_{\tilde{h}} (\tilde{\mathbf{f}}_u^Q)_{ik} (\tilde{\mathbf{f}}_u^Q)_{kl}^\dagger + \theta_{\tilde{h}} (\tilde{\mathbf{f}}_d^Q)_{ik} (\tilde{\mathbf{f}}_d^Q)_{kl}^\dagger + \frac{1}{18} \theta_{\tilde{B}} (\tilde{\mathbf{g}}'^Q)_{ik}^* (\tilde{\mathbf{g}}'^Q)_{kl}^T + \frac{3}{2} \theta_{\tilde{W}} (\tilde{\mathbf{g}}^Q)_{ik}^* (\tilde{\mathbf{g}}^Q)_{kl}^T \right. \\
& \quad \left. + \frac{8}{3} \theta_{\tilde{g}} (\tilde{\mathbf{g}}_s^Q)_{ik}^* (\tilde{\mathbf{g}}_s^Q)_{kl}^T \right] [s(\mathbf{a}_u)_{lj} - c(\tilde{\mu}^* \mathbf{f}_u^{hu})_{lj}] \\
& - 3 \left\{ \left( \frac{1}{36} \theta_{\tilde{Q}_i} + \frac{4}{9} \theta_{\tilde{u}_j} + \frac{1}{4} \theta_h \right) g'^2 + \frac{3}{4} (\theta_{\tilde{Q}_i} + \theta_h) g_2^2 + \frac{4}{3} (\theta_{\tilde{Q}_i} + \theta_{\tilde{u}_j}) g_3^2 \right\} [s(\mathbf{a}_u) - c(\tilde{\mu}^* \mathbf{f}_u^{hu})]_{ij}
\end{aligned} \tag{33}$$

The first set of terms before the appearance of  $(M_1 - iM'_1)$  arises from the  $\Lambda$  and  $\Lambda'$  terms



in (13). All  $\mathbf{\Lambda}$  terms have a non-zero contribution but since most  $\mathbf{\Lambda}'$  entries are zero, only  $\mathbf{\Lambda}'_{abef}\mathbf{H}_{cef}^*$  contributes.

The second set of entries, containing gaugino mass terms, originate in the non-vanishing traces in (13) where  $(\mathbf{m}_X - i\mathbf{m}'_X)$  is on the extreme left. For our case,  $\Phi_a = \tilde{u}_{Rj}$ , so that  $\mathbf{V}_a$  has a quark/gaugino as the first/second index, while  $\mathbf{W}_a$  has the higgsino/quark as the first/second index. Remembering that taking the transpose, or the dagger, flip the order of these indices, it is quite straightforward to see that the first set of trace terms where  $(\mathbf{m}_X - i\mathbf{m}'_X)$  is located on the extreme left necessarily give contributions proportional to SSB gaugino masses. For this, we must keep in mind that the matrices  $\mathbf{X}_{\bullet}^{1,2}$  connect gauginos to higgsinos, and vice-versa. A similar analysis of the next set of trace terms in (13), with  $(\mathbf{m}_X + i\mathbf{m}'_X)$  enclosed by other fermion matrices, shows that the altered location of the Majorana fermion mass matrix now results in the appearance of the ‘‘higgsino mass’’,  $\mu^*$  (without any tilde).

The remaining terms, except for the very last one which obviously arises from  $C_2(S)\mathbf{H}_{abc}$ , are from the traces with primed scalar indices. The important thing to note is that the trace in (13) denotes a sum over fermion types, which sometimes, but not necessarily, becomes a trace over fermion flavours, since now a scalar may carry a flavour index. In the present case, the trace over the product of two  $\mathbf{U}_{\bullet}^{1,2}$  matrices does result in a trace over fermion flavours, since then the scalar index on the  $\mathbf{U}_{\bullet}^{1,2}$  necessarily corresponds to a Higgs field which does not carry any flavour. We refer the interested reader to the discussion below Eqs. (36) and (37) of Paper I where a completely analogous situation is discussed in more detail.

We have illustrated the derivation of the RGE for the trilinear scalar coupling of squarks to the lighter of the two Higgs doublets. The RGE for the corresponding coupling,  $\left[ c(\mathbf{a}_u)_{ij} + s(\tilde{\mu}^*\mathbf{f}_u^{h_u})_{ij} \right]$ , to the heavier doublet can be obtained in the same manner. By taking linear combinations of these RGEs, we can obtain the separate RGEs for  $\mathbf{a}_u$  and  $\tilde{\mu}^*\mathbf{f}_u^{h_u}$ .<sup>9</sup> Since the coupling  $\tilde{\mu}^*\mathbf{f}_u^{h_u}$  always occurs as a product, it is not possible to obtain the RGEs for the individual factors. Of course, above all thresholds, we must have  $\tilde{\mu} = \mu$  and

---

<sup>9</sup> The  $s$  and  $c$  can be taken out of the derivatives on the left-hand-side as noted in Paper I. For  $Q > m_H$ , when both doublets are in the theory, the rotation is irrelevant. Otherwise, the input value of  $\tan\beta$  corresponds to the ratio of VEVs at the scale  $Q = m_H$  when the two doublet model reduces to the one-doublet model. We may think about this as evolving the couplings  $\mathbf{a}_u$  and  $\mathbf{f}_u^{h_u}$  from the high scale down to the scale  $Q = m_H$ , at which we *must* do the Higgs rotations to reduce to the one-doublet model.

$\mathbf{f}_u^{h_u} = \mathbf{f}_u$ . We have checked that with these replacements, our RGEs reduce to the MSSM RGEs [18] if we put all  $\theta_i = 1$  and take care to sum over all internal flavours.

### C. Soft Masses

Finally, we turn to the RGEs for the SSB mass parameters and their bilinear cousins  $\mathcal{B}$ ; we have almost all the matrices necessary to use (19) to find the RGEs. The majority of the missing  $\mathbf{m}^2$  and  $\mathcal{B}$  terms appear in the SSB Lagrangian and so the required matrices can be written down directly. Note that when we write the Lagrangian in the rotated Higgs basis, there are no  $\mathcal{B}$  terms so that  $\mathcal{B}_{ef} = 0$ . In this case, several terms drop out of the RGE in (19).

#### 1. Higgs Mass Terms

Using (19) to derive the RGE for the coefficient of the  $h^\dagger h$  term in the Lagrangian we find that

$$\begin{aligned}
& (4\pi)^2 \frac{d[s^2 M_{H_u}^2 + c^2 M_{H_d}^2 - sc(b+b^*)]}{dt} \\
&= \frac{3}{2} \theta_h [g'^2 + g_2^2] (c^2 - s^2)^2 [s^2 M_{H_u}^2 + c^2 M_{H_d}^2 - sc(b+b^*)] \\
&\quad + \theta_H [g'^2 (-c^4 + 4s^2 c^2 - s^4) + 6s^2 c^2 g_2^2] [c^2 M_{H_u}^2 + s^2 M_{H_d}^2 + sc(b+b^*)] \\
&\quad - 6\theta_h \theta_H [g'^2 + g_2^2] sc (c^2 - s^2) \left[ sc \{M_{H_u}^2 - M_{H_d}^2\} - \frac{1}{2} (c^2 - s^2) (b+b^*) \right] \\
&\quad + \theta_{\tilde{u}_k} \theta_{\tilde{u}_l} [-2g'^2 (s^2 - c^2) \delta_{lk} + 6s^2 [(\mathbf{f}_u)^T (\mathbf{f}_u)^*]_{lk}] (\mathbf{m}_U^2)_{kl} \\
&\quad + \theta_{\tilde{Q}_k} \theta_{\tilde{Q}_l} [g'^2 (s^2 - c^2) \delta_{lk} + 6s^2 [(\mathbf{f}_u)^* (\mathbf{f}_u)^T]_{lk} + 6c^2 [(\mathbf{f}_d)^* (\mathbf{f}_d)^T]_{lk}] (\mathbf{m}_Q^2)_{kl} \\
&\quad + \theta_{\tilde{d}_k} \theta_{\tilde{d}_l} [g'^2 (s^2 - c^2) \delta_{lk} + 6c^2 [(\mathbf{f}_d)^T (\mathbf{f}_d)^*]_{lk}] (\mathbf{m}_D^2)_{kl} \\
&\quad + \theta_{\tilde{L}_k} \theta_{\tilde{L}_l} [-g'^2 (s^2 - c^2) \delta_{lk} + 2c^2 [(\mathbf{f}_e)^* (\mathbf{f}_e)^T]_{lk}] (\mathbf{m}_L^2)_{kl} \\
&\quad + \theta_{\tilde{e}_k} \theta_{\tilde{e}_l} [g'^2 (s^2 - c^2) \delta_{lk} + 2c^2 [(\mathbf{f}_e)^T (\mathbf{f}_e)^*]_{lk}] (\mathbf{m}_E^2)_{kl} \\
&\quad + 6\theta_{\tilde{u}_k} \theta_{\tilde{Q}_l} [s(\mathbf{a}_u)_{lk} - c(\tilde{\mu}^* \mathbf{f}_u^{h_u})_{lk}] \left[ s(\mathbf{a}_u)_{kl}^\dagger - c(\tilde{\mu}^* \mathbf{f}_u^{h_u})_{kl}^\dagger \right] \\
&\quad + 6\theta_{\tilde{Q}_k} \theta_{\tilde{d}_l} \left[ c(\mathbf{a}_d)_{lk} - s(\tilde{\mu}^* \mathbf{f}_d^{h_d})_{lk} \right] \left[ c(\mathbf{a}_d)_{kl}^\dagger - s(\tilde{\mu}^* \mathbf{f}_d^{h_d})_{kl}^\dagger \right] \\
&\quad + 2\theta_{\tilde{L}_k} \theta_{\tilde{e}_l} \left[ c(\mathbf{a}_e)_{lk} - s(\tilde{\mu}^* \mathbf{f}_e^{h_e})_{lk} \right] \left[ c(\mathbf{a}_e)_{kl}^\dagger - s(\tilde{\mu}^* \mathbf{f}_e^{h_e})_{kl}^\dagger \right] \\
&\quad - 2\theta_{\tilde{h}} |\mu|^2 \left\{ \theta_{\tilde{B}} \left[ s^2 |\tilde{g}^{h_u}|^2 + c^2 |\tilde{g}^{h_d}|^2 \right] + 3\theta_{\tilde{W}} \left[ s^2 |\tilde{g}^{h_u}|^2 + c^2 |\tilde{g}^{h_d}|^2 \right] \right\} \\
&\quad - 2\theta_{\tilde{h}} \left\{ \theta_{\tilde{B}} (M_1^2 + M_1'^2) \left[ s^2 |\tilde{g}^{h_u}|^2 + c^2 |\tilde{g}^{h_d}|^2 \right] + 3\theta_{\tilde{W}} (M_2^2 + M_2'^2) \left[ s^2 |\tilde{g}^{h_u}|^2 + c^2 |\tilde{g}^{h_d}|^2 \right] \right\} \\
&\quad - \frac{1}{2} \left\{ -4\theta_{\tilde{h}} \theta_{\tilde{B}} sc \mu^* \tilde{g}^{h_u} \tilde{g}^{h_d} (M_1 + iM_1') - 12\theta_{\tilde{h}} \theta_{\tilde{W}} sc \mu^* \tilde{g}^{h_u} \tilde{g}^{h_d} (M_2 + iM_2') \right\} \\
&\quad - \frac{1}{2} \left\{ -4\theta_{\tilde{h}} \theta_{\tilde{B}} sc \mu (\tilde{g}^{h_u})^* (\tilde{g}^{h_d})^* (M_1 - iM_1') - 12\theta_{\tilde{h}} \theta_{\tilde{W}} sc \mu (\tilde{g}^{h_u})^* (\tilde{g}^{h_d})^* (M_2 - iM_2') \right\} \\
&\quad - \theta_h \left( \frac{3g'^2}{2} + \frac{9g_2^2}{2} \right) [s^2 M_{H_u}^2 + c^2 M_{H_d}^2 - sc(b+b^*)] \\
&\quad + \theta_h \left\{ s^2 [6\mathbf{f}_u^* \mathbf{f}_u^T]_{kk} + c^2 [6\mathbf{f}_d^* \mathbf{f}_d^T + 2\mathbf{f}_e^* \mathbf{f}_e^T]_{kk} + \theta_{\tilde{B}} \theta_{\tilde{h}} \left[ s^2 |\tilde{g}^{h_u}|^2 + c^2 |\tilde{g}^{h_d}|^2 \right] \right. \\
&\quad \quad \left. + 3\theta_{\tilde{W}} \theta_{\tilde{h}} \left[ s^2 |\tilde{g}^{h_u}|^2 + c^2 |\tilde{g}^{h_d}|^2 \right] \right\} [s^2 M_{H_u}^2 + c^2 M_{H_d}^2 - sc(b+b^*)] \\
&\quad + \theta_H sc \left\{ [6\mathbf{f}_u^* \mathbf{f}_u^T]_{kk} - [6\mathbf{f}_d^* \mathbf{f}_d^T + 2\mathbf{f}_e^* \mathbf{f}_e^T]_{kk} + \theta_{\tilde{B}} \theta_{\tilde{h}} \left[ |\tilde{g}^{h_u}|^2 - |\tilde{g}^{h_d}|^2 \right] \right. \\
&\quad \quad \left. + 3\theta_{\tilde{W}} \theta_{\tilde{h}} \left[ |\tilde{g}^{h_u}|^2 - |\tilde{g}^{h_d}|^2 \right] \right\} \left[ sc \{M_{H_u}^2 - M_{H_d}^2\} - \frac{1}{2} (c^2 - s^2) (b+b^*) \right], \tag{34}
\end{aligned}$$

where  $M_{H_u}^2 \equiv (m_{H_u}^2 + |\tilde{\mu}|^2)$  and  $M_{H_d}^2 \equiv (m_{H_d}^2 + |\tilde{\mu}|^2)$ .

All terms up to the trilinear scalar couplings derive from the single term,  $\mathbf{\Lambda}_{afbe} \mathbf{m}_{ef}^2$ , in (19). All other quartic terms are zero, either because  $\mathbf{\Lambda}'$  vanishes when  $a = b$ , or because

$\mathcal{B}_{ef} = 0$ . Since this operator has no flavour indices, all flavours are internal and, therefore, summed over. Extra care should be applied when dealing with sums over squarks since there are additional factors of 3 arising from a sum over colours. Once the entries of the  $\mathbf{A}$  matrix have been worked out, this contribution should not pose any special difficulty. The so-called  $S$ -term is also contained in the terms proportional to  $g'^2$  from this contribution.

The terms containing the trilinear scalar couplings obviously come from the  $(\mathbf{H}_{caf}^* + \mathbf{H}_{fae}) \mathbf{H}_{ebf}$  term in (19). Since we have chosen the first index of  $\mathbf{H}_{abc}$  to always be a sfermion,  $\mathbf{H}_{aef} = 0$  for  $a = \mathbf{h}$ . For the contributions from the squark-Higgs scalar trilinear interactions the factor 2 changes to a factor 6 due to a colour sum.

Next, we turn to the contributions from the Majorana fermion mass terms from the  $\mathbf{m}_X^{(\prime)}$  matrices in (19). When the two factors of  $(\mathbf{m}_X \pm i\mathbf{m}'_X)$  are next to one another, it should be clear that we should obtain either a  $|\mu|^2$  or an  $(M_{1,2}^2 + M_{1,2}'^2)$  term. On the other hand, when the factors of  $(\mathbf{m}_X \pm i\mathbf{m}'_X)$  are separated by an  $\mathbf{X}_b^{1,2}$ -matrix, we obtain a product of gaugino and higgsino mass parameters because  $\mathbf{X}_b^{1,2}$  only connects gauginos with higgsinos. The trace, of course, is a sum over all gauginos and higgsinos in the theory.

The terms that derive from the next term,  $\mathbf{C}_2(S)\mathbf{m}_{ab}^2$ , should be obvious. Following these, we have the set of traces with primed scalar indices,  $a'$  and  $b'$ . As discussed earlier, many of these terms are zero when  $a$  and  $b$  are Higgs scalars. We are left with traces over only  $\mathbf{U}_\bullet^{1,2}$  and  $\mathbf{X}_\bullet^{1,2}$ . The trace over the  $\mathbf{U}_\bullet^{1,2}$  matrices leads to a trace over matter fermion flavours, of which the quark traces acquire an additional colour factor of 3.

The Higgs scalar mass term for which we just obtained the RGE written above is the only combination which remains in the effective theory for  $Q < m_H$ . The complete set of mass terms in the rotated Higgs basis are,

$$\begin{aligned}
\mathcal{L} \ni & - [s^2 (m_{H_u}^2 + |\tilde{\mu}|^2) + c^2 (m_{H_d}^2 + |\tilde{\mu}|^2) - sc (b + b^*)] \mathbf{h}^\dagger \mathbf{h} \\
& - [c^2 (m_{H_u}^2 + |\tilde{\mu}|^2) + s^2 (m_{H_d}^2 + |\tilde{\mu}|^2) + sc (b + b^*)] \mathcal{H}^\dagger \mathcal{H} \\
& - [sc (m_{H_u}^2 + |\tilde{\mu}|^2) - sc (m_{H_d}^2 + |\tilde{\mu}|^2) - c^2 b + s^2 b^*] \mathbf{h}^\dagger \mathcal{H} \\
& - [sc (m_{H_u}^2 + |\tilde{\mu}|^2) - sc (m_{H_d}^2 + |\tilde{\mu}|^2) + s^2 b - c^2 b^*] \mathcal{H}^\dagger \mathbf{h} ,
\end{aligned} \tag{35}$$

and the RGEs for these coefficients can be obtained in a similar manner. We can then obtain the separate RGEs for the real parameters  $(m_{H_u}^2 + |\tilde{\mu}|^2)$ ,  $(m_{H_d}^2 + |\tilde{\mu}|^2)$  and the complex parameter  $b$ , valid for  $Q > m_H$ , by taking appropriate linear combinations.

It is important to note that since the terms  $m_{H_u}^2$  and  $|\tilde{\mu}|^2$  only appear in the Lagrangian

in the combination  $(m_{H_u}^2 + |\tilde{\mu}|^2)$ , we cannot derive an RGE for them separately. Of course, above all thresholds, supersymmetry requires  $\mu = \tilde{\mu}$ , so that we can use the RGE for  $\mu$ , (B1), to extract the RGE for the soft mass parameters  $m_{H_u}^2$  and  $m_{H_d}^2$ , but these will cease to be valid once any one particle is decoupled from the theory. We have checked that these RGEs reduce to the standard ones [18] once all  $\theta_i$  are set equal to unity, and that our RGE for  $m_{\text{H}}^2$  reduces to the RGE for the SM Higgs boson mass parameter [27] if we set the quartic scalar coupling in the SM to be the appropriate combination of gauge couplings.

## 2. Sfermion Mass Terms

The RGEs for sfermion soft mass terms are somewhat simpler on account of the fact that they have no Higgs fields in their operator in the Lagrangian. Otherwise, the derivation follows in a similar fashion to the Higgs mass terms, with the obvious differences in the terms in (19) that contribute to the RGE. There is still only one  $\mathbf{A}$  term (because again the  $\mathbf{A}'$  and  $\mathbf{B}$  are zero), and this contributes a large proportion of the RGE including terms with, and terms without, traces over sfermion mass matrices. These terms include the  $S$ -term as for the Higgs mass RGE above. When  $e$  and  $f$  are both Higgs fields, this gives a  $b$ -parameter dependence in the RGEs for the sfermions listed in Appendix B for  $Q < m_H$ . Since the external fields are sfermions, both trilinear terms in (19) now contribute, and in the trace terms, only  $\mathbf{V}_\bullet$  and  $\mathbf{W}_\bullet$  terms are non-zero. These terms yield the contributions that depend on the square of the gaugino mass parameters, and also on  $|\mu|^2$ . Above all thresholds, these latter contributions cancel with  $\tilde{\mu}^2$  contributions arising from Higgs boson loops.

There is one point about the RGEs for the sfermion SSB mass parameters that we ought to draw attention to. For  $Q < m_H$ , where we only have the light Higgs doublet in the theory, we would expect that the couplings  $\mathbf{f}_u$  can occur only in the combination  $s\mathbf{f}_u$ . A look at the term just before the trilinear coupling terms in (B25) shows, however, that this is not the case. (There are analogous terms in the RGEs for  $\mathbf{m}_{U,D}^2$ , and also for  $\mathbf{m}_{L,E}^2$ .) The ‘‘product of Yukawa couplings’’ that appears in these terms (without accompanying  $s^2$  or  $c^2$  factors) is really a  $\mathbf{\Lambda}_{ijkl}$ -type coupling for the quartic interaction of squarks which, as we have already explained, we have approximated by its supersymmetric limit and set equal to the product of the corresponding elements of the Yukawa coupling matrix, each frozen at

the scale  $Q = m_H$ ; *e.g.*  $\mathbf{\Lambda}_{\tilde{Q}_i \tilde{u}_{Rk} \tilde{u}_{Rl} \tilde{Q}_j} \sim (\mathbf{f}_u)_{ik}^* (\mathbf{f}_u)_{lj}^T$  in the first of such terms in (B25).

We have checked that, except for terms involving couplings and mass parameters of Higgs boson fields, the RGEs that we obtain agree with those in Ref. [17]. Indeed the RGEs in Ref. [17] do reduce to the MSSM RGEs if we set all the  $\theta$ 's to be one. However, since the RGEs of Ref. [17] appear to have been written *without any rotation* of the Higgs boson fields, we found it impossible to compare contributions involving thresholds for Higgs boson fields. For these same reasons, we are unable to see how their RGEs for Yukawa couplings reduce to the corresponding RGEs for the SM [14] when all new particles are decoupled. Likewise, we are not able to obtain the RGE for the SM Higgs boson mass parameter using the RGEs for the Higgs scalar SSB parameters as given in Ref. [17].

## V. SOLUTIONS TO THE RGEs AND FLAVOUR-VIOLATING SSB PARAMETERS

While the *quark mass basis*, where both up and down quark Yukawa matrices are diagonal (at a chosen scale), may be the most physical basis to work in, as we saw in Paper I, it is more convenient to work in a *current basis* where either the up or the down, but not both, Yukawa matrices are diagonal. In this case, we rotate the entire quark doublet (in the flavour space) thereby preserving the  $SU(2)$  gauge symmetry. To similarly preserve the underlying supersymmetry, we should also rotate the squark multiplets the same way that we rotate the quarks; *i.e.* we should rotate the quark (and also lepton) superfields. Of course, just as the Yukawa coupling matrices transform under this change of basis (see (38) and (39) of Paper I to set the notation), the SSB mass and  $\mathbf{a}$ -parameter matrices in a arbitrary basis are related to the corresponding matrices in the basis where the up (or the down) quark Yukawa coupling matrix is diagonal at  $Q = m_t$  (the matrices in this special basis are denoted with the superscript  $M$ ) according to,

$$(\mathbf{a}_{u,d})^T = \mathbf{V}_R(u, d) (\mathbf{a}_{u,d}^M)^T \mathbf{V}_L^\dagger(q), \quad (36)$$

$$\mathbf{m}_Q^2 = \mathbf{V}_L(q) (\mathbf{m}_Q^2)^M \mathbf{V}_L^\dagger(q), \quad (37)$$

$$\mathbf{m}_{U,D}^2 = \mathbf{V}_R(u, d) (\mathbf{m}_{U,D}^2)^M \mathbf{V}_R^\dagger(u, d), \quad (38)$$

where we set  $q = u(d)$  in  $\mathbf{V}_L(q)$  in the basis where up (down) type quark Yukawa coupling matrices are diagonal at  $Q = m_t$ . The matrices  $\mathbf{V}_{L,R}(u, d)$ , defined via (38) of Paper I,

are the linear transformations that connect any current basis to the quark mass basis. The SSB matrices  $\mathbf{a}_{u,d}^M$  and  $(m_{\bullet}^2)^M$  in the basis where up quark Yukawa couplings are diagonal are related to the corresponding matrices in which the down quark Yukawa couplings are diagonal by,

$$(\mathbf{a}_{u,d}^M)^T(u) = (\mathbf{a}_{u,d}^M)^T(d)\mathbf{K}^\dagger, \quad (39)$$

$$(\mathbf{m}_Q^2)^M(u) = \mathbf{K}(\mathbf{m}_Q^2)^M(d)\mathbf{K}^\dagger, \quad (40)$$

$$(\mathbf{m}_{U,D}^2)^M(u) = (\mathbf{m}_{U,D}^2)^M(d). \quad (41)$$

Here  $u$  and  $d$  in the parenthesis denote whether the up or down type Yukawa coupling matrices, respectively, are diagonal at  $Q = m_t$ , after the complete transformation (38) of Paper I; *i.e.* when we go to the basis where the up-type Yukawa matrix is diagonal, we also transform the singlet down sector by the matrix  $\mathbf{V}_R(d)$ , and likewise if we transform to the basis where the down-type Yukawa coupling matrix is diagonal. The matrix  $\mathbf{K}$  that appears in (39) and (40) is the Kobayashi-Maskawa matrix [28] given by,

$$\mathbf{K} = \mathbf{V}_L^\dagger(u)\mathbf{V}_L(d). \quad (42)$$

There is no *a priori* preference for the one or the other basis. However, if in a process there are only up, or only down, type quarks in the initial and final states, it makes sense to use the mass basis for these quarks. In the next section, we will apply the considerations of this paper to the rate for the decay of the lightest up-type squark to the final state  $c\tilde{Z}_1$ . For this reason, other than where explicitly stated, we will work in a basis where the up-type quark Yukawa couplings are diagonal at  $Q = m_t$ , *i.e.* we will take  $\mathbf{V}_{L,R}(u) = \mathbf{1}$ . We then have  $\mathbf{V}_L(d) = \mathbf{K}$ . Finally, to fully specify a current basis we must also choose  $\mathbf{V}_R(d)$  — the matrix for the rotation of the right-handed down-type quarks.<sup>10</sup> Except when we illustrate results for extensions of the mSUGRA model, we also set  $\mathbf{V}_R(d) = \mathbf{1}$ .

Since the boundary conditions for the dimensionless couplings of SM particles are specified at the weak scale, while those for the dimensionful parameters of the MSSM are usually given at a high scale, we solve the RGEs using an iterative procedure. This is, of course, quite standard, but the incorporation of threshold effects entails some new complications. We

---

<sup>10</sup> Within the SM, physics is independent of our choice of the matrices  $\mathbf{V}_R(u)$  and  $\mathbf{V}_R(d)$ , and depends on  $\mathbf{V}_L(u,d)$  only through the KM matrix. This is also the case for the MSSM with mSUGRA boundary conditions, but more generally, physics also depends on the right-handed quark rotation matrices.

begin by evolving the measured gauge and Yukawa couplings of quarks and leptons, specified in a chosen current basis, from  $Q = M_Z$  to the high scale (usually  $Q = M_{\text{GUT}}$ ) where the SSB parameters of the MSSM are specified.<sup>11</sup> We can now evolve *all* the MSSM parameters down to the weak scale, decoupling the particles one-by-one as described in Sec. III. In the course of this downward evolution, we must split the SM couplings  $g_i$  and  $\mathbf{f}_{u,d,e}$  from their SUSY cousins  $\tilde{\mathbf{g}}_i^\bullet$  and  $\tilde{\mathbf{f}}_{u,d,e}^\bullet$  as discussed in Paper I, and also incorporate the distinction between  $\mu$  and  $\tilde{\mu}$ . As we will see shortly, this complicates the introduction of the electroweak symmetry breaking conditions which are incorporated at  $M_{\text{SUSY}}$ . Finally, below the scale  $m_H$  where the two Higgs doublet MSSM transitions to the one Higgs doublet model, we switch from the MSSM quark and lepton Yukawa couplings  $\mathbf{f}_\bullet$  to the corresponding SM couplings  $\boldsymbol{\lambda}_\bullet$ , which we reset along with the gauge couplings, after evolving these to  $Q = M_Z$  ( $Q = m_t$  for the top quark Yukawa coupling). We then evolve back to the GUT scale where we re-set  $\mu = \tilde{\mu}$  as discussed below, and iterate the solution to the system of RGEs until convergence is obtained to the specified precision.

### 1. Weak scale boundary conditions

For the gauge sector, we take as our input at the weak scale the current PDG values [29]  $\alpha_{em}$ ,  $\alpha_s$  and  $\sin^2 \theta_W$ , which are

$$\alpha_{em}^{-1}(M_Z) = 127.925 \pm 0.016 ; \alpha_s(M_Z, \overline{\text{MS}}) = 0.1176 \pm 0.002 ;$$

$$\sin^2 \theta_W(M_Z, \overline{\text{MS}}) = 0.23119 \pm 0.00014.$$

These are the couplings extracted using the effective theory with the electroweak gauge bosons as well as the top quark integrated out at  $Q = M_Z$ . In order to use the SM for evolution for  $Q > M_Z$ , we must match these couplings to those of the full SM, which, to two-loop accuracy implies that the SM gauge couplings in the  $\overline{\text{MS}}$  scheme are given by

---

<sup>11</sup> Although the gauge and Yukawa coupling RGEs along with their tilde cousins form a closed system, the solution to these RGEs may be sensitive to sparticle thresholds through particle decoupling effects. We will see that these effects can be especially important in non-universal models where squark mass matrices are non-diagonal (in the basis where the corresponding quark Yukawa couplings are diagonal) and the squark mass eigenvalues have substantial splitting.



[30, 31],

$$\frac{1}{\alpha_1(M_Z)} = \frac{3}{5} \left[ \frac{1 - \sin^2 \theta_W(M_Z)}{\alpha_{em}(M_Z)} \right] + \frac{3}{5} [1 - \sin^2 \theta_W(M_Z)] 4\pi\Omega(M_Z), \quad (43a)$$

$$\frac{1}{\alpha_2(M_Z)} = \frac{\sin^2 \theta_W(M_Z)}{\alpha_{em}(M_Z)} + \sin^2 \theta_W(M_Z) 4\pi\Omega(M_Z), \quad (43b)$$

$$\frac{1}{\alpha_3(M_Z)} = \frac{1}{\alpha_s(M_Z)} + 4\pi\Omega_3(M_Z), \quad (43c)$$

where

$$\Omega(\mu) = \frac{1}{24\pi^2} \left[ 1 - 21 \ln \left( \frac{M_W}{\mu} \right) \right] + \frac{2}{9\pi^2} \ln \left( \frac{m_t}{\mu} \right), \quad (44a)$$

$$\Omega_3(\mu) = \frac{2}{24\pi^2} \ln \left( \frac{m_t}{\mu} \right). \quad (44b)$$

Notice that in order to preserve the  $SU(2)$  symmetry of the effective theory down to  $Q = M_Z$ , we have, as mentioned earlier, integrated out the top quark at  $Q = M_Z$  rather than at its mass as we do for all other particles. This is the origin of the  $\ln(m_t/\mu)$  terms in the matching conditions for the gauge couplings above. We emphasize that we decouple all SUSY particles as well as the additional Higgs bosons at the scale of their mass: as a result, we do not get corresponding jumps in the gauge couplings as these decouple. Our method — which is also used in ISAJET — has an important advantage in that it “sums the logs of the ratio of any large mass to  $M_Z$ ”, in contrast to the frequently used procedure that uses MSSM evolution down to  $M_Z$ , and then corrects for this via a “single step evolution” (between the heavy scale and  $M_Z$ ) to take into account the difference between the running in the MSSM and in the SM.

Next, we convert the values of these gauge couplings in the  $\overline{\text{MS}}$  scheme to their corresponding values in the  $\overline{\text{DR}}$  scheme using the relations [32]:

$$\frac{1}{\alpha_1(\overline{\text{DR}})} = \frac{1}{\alpha_1(\overline{\text{MS}})}, \quad (45a)$$

$$\frac{1}{\alpha_2(\overline{\text{DR}})} = \frac{1}{\alpha_2(\overline{\text{MS}})} - \frac{1}{6\pi}, \quad (45b)$$

$$\frac{1}{\alpha_3(\overline{\text{DR}})} = \frac{1}{\alpha_3(\overline{\text{MS}})} - \frac{1}{4\pi}, \quad (45c)$$

and use the results as boundary conditions at  $Q = M_Z$  when solving the RGEs.

For the Yukawas, we begin with the quark masses at  $Q = M_Z$  (the masses of the light quarks and leptons at  $M_Z$  can be found in Ref. [33]), and convert to SM Yukawas using

$v_{SM} = 248.6/\sqrt{2}$  as in Ref. [25]. The masses of the first two generations of quarks have substantial error, which leads to a corresponding error in their Yukawa couplings. The third generation quark masses are more precisely known — we take the top pole mass  $m_t = 172$  GeV, and  $m_b(M_Z) = 2.83$  GeV [34]. We rotate the diagonal Yukawa couplings, which are in the “quark mass basis” to a current basis using (39) of Paper I at  $Q = m_t$ . We include SUSY radiative corrections [25] (from ISAJET), with inter-generation quark mixing neglected, at  $Q = M_{\text{SUSY}}$ . Finally, for the numerical results that we present in the rest of the paper, we parametrize the Kobayashi-Maskawa matrix as in (50) below, and take  $\sin \alpha = 0.2243$ ,  $\sin \beta = 0.0037$  and  $\sin \gamma = 0.0413$ ,  $\delta_\beta = 60^\circ$  and  $\delta_\alpha = \delta_\gamma = 0$ .

## 2. Electroweak symmetry breaking

It is traditional to use the observed value of  $M_Z^2$  to determine the value of  $\mu^2$  from the minimization conditions for the scalar potential in the Higgs sector. The inclusion of threshold effects causes additional complications for this program. Recall that the electroweak symmetry breaking conditions are imposed at  $M_{\text{SUSY}} = \sqrt{m_{\tilde{t}_L} m_{\tilde{t}_R}}$  which is always smaller than the mass of the heaviest SUSY particle. As a result,  $\mu^2$  is now conceptually and numerically different from  $|\tilde{\mu}|^2$ , which is of course the parameter that enters in the Higgs boson potential. Moreover, the Higgs potential depends only on  $M_{H_u}^2 \equiv (m_{H_u}^2 + |\tilde{\mu}|^2)$  and  $M_{H_d}^2 \equiv (m_{H_d}^2 + |\tilde{\mu}|^2)$ , so that it is not possible to separate  $\tilde{\mu}^2$  from the SSB parameters  $m_{H_u}^2$  and  $m_{H_d}^2$  that are specified at the high scale. Using the combinations,

$$\begin{aligned} (M_{H_u}^2 + M_{H_d}^2) &= m_{H_u}^2 + m_{H_d}^2 + 2|\tilde{\mu}|^2 \quad \text{and} \\ (M_{H_d}^2 - M_{H_u}^2) &= m_{H_d}^2 - m_{H_u}^2, \end{aligned}$$

the tree level minimisation conditions of the Higgs potential can be written as,

$$(M_{H_u}^2 + M_{H_d}^2) = -\frac{1}{\cos 2\beta} (M_{H_d}^2 - M_{H_u}^2) - \frac{1}{2} (g'^2 + g^2) (v_u^2 + v_d^2), \quad (46)$$

$$b = sc (M_{H_u}^2 + M_{H_d}^2). \quad (47)$$

The first of these fixes the sum  $(M_{H_u}^2 + M_{H_d}^2)$  in terms of the difference  $(M_{H_u}^2 - M_{H_d}^2)$ . Since we know the difference at the GUT scale, we can evolve this down to  $M_{\text{SUSY}}$  (along with other SSB parameters) during the iterative process that we use to solve the RGEs. At  $Q = M_{\text{SUSY}}$  we use (46) to solve for  $M_{H_u}^2 + M_{H_d}^2$ , which can be evolved back to the GUT

scale. We then use the sum to fix  $\tilde{\mu} = \mu$  at the GUT scale, reset the difference to its input value, and iterate. The value of the higgsino parameter  $\mu$  can then be obtained at all scales using (B1). The  $b$ -parameter can, as usual, be eliminated in favour of  $\tan \beta$  using (47).<sup>12</sup>

In our discussion up to this point we have ignored another potential complication that arises if  $m_H > M_{\text{SUSY}}$ . In this case, the heavy particles of the Higgs sector decouple, and for  $M_{\text{SUSY}} < Q < m_H$ , we only have the light doublet in the effective theory that we use to calculate the RGEs. In this case, the heavy Higgs doublet mass term  $[c^2 (m_{H_u}^2 + |\tilde{\mu}|^2) + s^2 (m_{H_d}^2 + |\tilde{\mu}|^2) + sc(b + b^*)]$  and the Higgs mixing term,  $[sc(m_{H_u}^2 + |\tilde{\mu}|^2) - sc(m_{H_d}^2 + |\tilde{\mu}|^2) + s^2 b - c^2 b^*]$  (and its complex conjugate) in Eq. (35), together with  $\tan \beta$ , are frozen at their values at  $Q = m_H$ , while the light doublet mass parameter,  $[s^2 (m_{H_u}^2 + |\tilde{\mu}|^2) + c^2 (m_{H_d}^2 + |\tilde{\mu}|^2) - sc(b + b^*)]$ , along with  $v_{\text{SM}} = \sqrt{v_u^2 + v_d^2}$ , continues to evolve to  $M_{\text{SUSY}}$ . The three frozen coefficients together with the evolved mass term for the light doublet can now be used to solve for  $(m_{H_d}^2 + |\tilde{\mu}|^2)$ ,  $(m_{H_u}^2 + |\tilde{\mu}|^2)$  and the complex  $b$ -parameter. We can now find an iterative solution in the same manner as for  $M_{\text{SUSY}} > m_H$ .

Before closing this section, we should add that although we have discussed EWSB conditions only at tree-level, in practice, we minimize the one-loop effective potential including effects of third generation Yukawa couplings, but ignoring all flavour-mixing effects in this computation. These corrections, which effectively shift the Higgs boson SSB mass squared parameters by  $\Sigma_u$  and  $\Sigma_d$ , respectively, are evaluated by replacing  $f_{t,b,\tau}$  in the relations by the (3,3) element of the corresponding Yukawa matrices, and with the dimensionful parameters also replaced by the (3,3) element of the corresponding matrix (or the appropriate

---

<sup>12</sup> The alert reader will notice that something is amiss in (47): the  $b$ -parameter is complex, while the right-hand-side is manifestly real. The point is that at any one scale, chosen here to be  $M_{\text{SUSY}}$ , the  $b$ -parameter can always be made real. Indeed, the very fact that we have written positive values for the VEVs  $v_u$  and  $v_d$  mandates that  $b$  is real and positive at  $Q = M_{\text{SUSY}}$ . To be specific, we can always make a gauge transformation such that just the lower component of the scalar doublet  $H_u$  has a VEV, and that this VEV is real and positive. Then the minimization of the scalar potential in the Higgs sector requires that the VEV of  $H_d$  is aligned; *i.e.* it is also only in its lower component. This alignment is a result of the dynamics. Finally, we can redefine the phase of the doublet superfield  $\hat{H}_d$  so that  $v_d$  is real and positive. This is not compulsory, but is the customary practice that allows us to define  $\tan \beta$  to be real and positive. If instead we write the VEV of the down type Higgs field as  $|v_d| \exp(i\theta_d)$  and  $\tan \beta = \frac{v_u}{|v_d|}$ , the left-hand-side of (47) would have to be amended to  $b \exp i\theta_b$ . So, although we choose real VEVs and a concomitantly real  $b$ -parameter at  $Q = M_{\text{SUSY}}$ , we retain the complex  $b$  in the RGEs, since  $b$  will not remain real at other scales.

frozen value).

### 3. *SSB parameters at the high scale*

Since our purpose in these papers is to address flavour physics of sparticles in as general a way as possible, subject to experimental constraints that seem to suggest that flavour physics is largely restricted by the structure of the Yukawa coupling matrices, we thought it would be useful to first seek a general parametrization for SSB parameters that does not introduce a new source of flavour-violation, but allows for non-universality of model parameters. Additional, but uncontrolled, flavour-violation can easily be incorporated by allowing for other contributions to the SSB mass and trilinear parameter matrices. We use the (s)quark sector to illustrate our arguments, but almost identical considerations will apply to (s)leptons, except that in this case we would also have to include additional lepton number and lepton-flavour violating matrices in the singlet (s)neutrino sector.

Within the framework of the  $R$ -parity conserving MSSM, the SSB matrices  $\mathbf{m}_{U,D,Q}^2$  and  $\mathbf{a}_{u,d}$  potentially include new sources of flavour-violation, not included in the superpotential Yukawa couplings. In order not to introduce a new source of flavour-violation, these SSB matrices must be diagonal in the same superfield basis (where the SM fermions and their scalar superpartners are rotated by the same matrices) that the superpotential Yukawa interactions (renormalized at the same high scale as the SSB parameters) are diagonal.<sup>13</sup> Of course, it is impossible to simultaneously diagonalize  $\mathbf{f}_u$  and  $\mathbf{f}_d$ , but what we mean is that the SSB mass matrices that describe the mixing of both left- and right-up type squarks, and their trilinear couplings must be diagonal in the basis that the matrix  $\mathbf{f}_u$  is diagonal, and likewise for the down sector. However, since  $SU(2)$  symmetry dictates that the  $\mathbf{m}_{\tilde{u}_L}^2$  and  $\mathbf{m}_{\tilde{d}_L}^2$  SSB matrices must be the identical, this doublet squark mass-squared matrix must be proportional to the unit matrix,  $\mathbf{1}$ , in order to remain diagonal, both when the up- or the down-type Yukawa coupling matrix is diagonal. In contrast, the matrices  $\mathbf{m}_{\tilde{U}}^2$  and  $\mathbf{a}_u$  ( $\mathbf{m}_{\tilde{D}}^2$  and  $\mathbf{a}_d$ ) can be functions of the up (down) type Yukawa coupling matrices (and their Hermitian adjoints) chosen in such a way that these matrices

---

<sup>13</sup> This is *not equivalent* to the requirement that the Yukawa coupling matrix commute with the corresponding  $\mathbf{a}$ -parameter matrix because these non-Hermitian matrices are diagonalized by bi-unitary rather than by unitary transformations.

are simultaneously diagonal when we transform these to the basis where the corresponding superpotential Yukawa coupling matrix is diagonal.

To find the most general parametrization of the  $\mathbf{m}_{U,D}^2$  and  $\mathbf{a}_{u,d}$  matrices of the type that we are looking for, we first note that these, respectively, transform in the same way as the matrices  $(\mathbf{f}_{u,d}^T \mathbf{f}_{u,d}^*)^n$  and  $\mathbf{f}_{u,d} (\mathbf{f}_{u,d}^\dagger \mathbf{f}_{u,d})^n$ , where  $n$  is any integer. Thus any linear combination of these matrices (with  $n = 0, 1, 2 \dots$ ) is guaranteed to be diagonal in the basis that  $\mathbf{f}_{u,d}$  is diagonal (at the high scale at which we input the SSB parameters). The only question, then, is just how many terms we need to allow in the linear combinations that make up  $\mathbf{m}_{U,D}^2$  or  $\mathbf{a}_{u,d}$ , to guarantee the most general form for these SSB matrices, so that flavour violation enters only through the superpotential Yukawa coupling matrices? This is easiest to see in the diagonal basis for the Yukawa couplings. The SSB matrices are also diagonal in this basis, and so are completely specified by  $n_g$  diagonal elements, where  $n_g$  is the number of generations. Transforming to a general basis does not alter the number of parameters that we need: we thus know that we must have  $n_g$  terms in each of the linear combinations for  $\mathbf{m}_{U,D}^2$  and for  $\mathbf{a}_{u,d}$  that we discussed above. For the MSSM with  $n_g = 3$  generations, we thus parametrize the SSB sfermion mass and  $\mathbf{a}$ -parameter matrices at the high scale as,

$$\mathbf{m}_{Q,L}^2 = m_{\{Q,L\}0}^2 \mathbf{1} + \mathbf{T}_{Q,L} , \quad (48a)$$

$$\mathbf{m}_{U,D,E}^2 = m_{\{U,D,E\}0}^2 [c_{U,D,E} \mathbf{1} + R_{U,D,E} \mathbf{f}_{u,d,e}^T \mathbf{f}_{u,d,e}^* + S_{U,D,E} (\mathbf{f}_{u,d,e}^T \mathbf{f}_{u,d,e}^*)^2] + \mathbf{T}_{U,D,E} , \quad (48b)$$

$$\mathbf{a}_{u,d,e} = \mathbf{f}_{u,d,e} [A_{\{u,d,e\}0} \mathbf{1} + W_{u,d,e} \mathbf{f}_{u,d,e}^\dagger \mathbf{f}_{u,d,e} + X_{u,d,e} (\mathbf{f}_{u,d,e}^\dagger \mathbf{f}_{u,d,e})^2] + \mathbf{Z}_{u,d,e} , \quad (48c)$$

where  $\mathbf{f}_{u,d,e}$  are the superpotential Yukawa coupling matrices *in an arbitrary current basis* at the same scale at which the SSB parameters of the model are specified. Here,  $c_{U,D,E} = 0$  or 1 is introduced only to allow the facility to “switch off” the universal term if desired. The matrices  $\mathbf{T}_{Q,L,U,D,E}$  and  $\mathbf{Z}_{u,d,e}$  have been introduced only to allow for additional sources of flavour-violation not contained in the Yukawa couplings. Setting  $\mathbf{T}_{Q,L,U,D,E} = \mathbf{Z}_{u,d,e} = \mathbf{0}$  gives us the most generation parametrization of the three-generation  $R$ -parity conserving MSSM where the superpotential Yukawa interactions are the sole source of flavour violation. In other words, any top-down theory of flavour, will specify the form of the matrices  $\mathbf{T}_{Q,L,U,D,E}$  and  $\mathbf{Z}_{u,d,e}$  along with the coefficients  $m_{\bullet 0}^2$ ,  $A_{\bullet 0}$ ,  $c_{\bullet}$ ,  $R_{\bullet}$ ,  $S_{\bullet}$ ,  $W_{\bullet}$  and  $X_{\bullet}$  that appear above.

The physics behind our ansatz (48) for SSB parameters, with  $\mathbf{T}_{\bullet} = \mathbf{Z}_{\bullet} = \mathbf{0}$ , is that we assume that the SUSY breaking mechanism, for reasons that are not understood today, does

not introduce a new source of flavour violation.<sup>14</sup> We stress that this differs from the minimal flavour violation [36] assumption, where the new physics may introduce an additional flavour violation in a controlled way. Our ansatz is thus a special case of the minimal flavour violation scenario. Of course, the form of (48) is not invariant under renormalization group evolution, and at the weak scale we will end up with the same form for the SSB parameters as the minimal flavour violation ansatz (suitably generalized from the first paper of Ref. [36] to include higher order terms in the Yukawa couplings), but with appropriate relations between the coefficients of the various terms in the minimal flavour violation formulae for SSB parameters. We will return to the difference between minimal flavour violation and (48) in Sec. VI.

We have created a code (to be incorporated into ISAJET) that allows the reader to choose the arbitrary values for the various coefficients as well as the matrices  $\mathbf{T}_{Q,L,U,D,E}$  and  $\mathbf{Z}_{u,d,e}$  that appear in (48) as boundary conditions for the RGEs for the SSB parameters of the MSSM. This code provides a tool for a study of (s)quark flavour violation in sparticle processes in a arbitrary theory that reduces to the MSSM at the scale where the SSB parameters are specified. We can evolve the gauge and Yukawa couplings from the weak scale to this high scale, use the boundary conditions (48) as inputs for the SSB parameters, and proceed to determine the iterative solution to the RGEs as described above. The familiar universal mSUGRA boundary conditions are reproduced by setting  $c_{U,D,E} = 1$ ;  $m_{\{Q,L\}0}^2 = m_{\{U,D,E\}0}^2 = m_0^2$ ;  $A_{\{u,d,e\}0} = A_0$ ;  $R_{U,D,E} = S_{U,D,E} = W_{u,d,e} = X_{u,d,e} = 0$ ;  $\mathbf{T}_{Q,L} = \mathbf{T}_{U,D,E} = \mathbf{Z}_{u,d,e} = \mathbf{0}$  in (48).

### A. Quark Yukawa Couplings

We begin the discussion of our numerical results by showing the magnitude of the complex elements of the up quark Yukawa coupling matrix  $\mathbf{f}_u$  above  $Q = m_H$ , and  $\boldsymbol{\lambda}_u/\sin\beta$  below  $Q = m_H$ , for the mSUGRA model with  $m_0 = 200$  GeV,  $m_{1/2} = -400$  GeV,  $A_0 = -200$  GeV,  $\tan\beta = 10$  and  $\mu > 0$  in Fig. 1.<sup>15</sup> The approximate spectrum for this illustrative scenario is

<sup>14</sup> For a complementary approach, where supersymmetry breaking is the origin of fermion flavour, see Ref. [35], and the extensive bibliography therein.

<sup>15</sup> The reader may well wonder why we choose the gaugino mass to be negative and of the opposite sign to that of the  $\mu$  parameter, a relative sign that is “apparently disfavoured” by the Brookhaven  $g_\mu - 2$  measurement. The reason is that our convention for the sign of  $\mu$  [4] (as well as the one used in ISAJET)

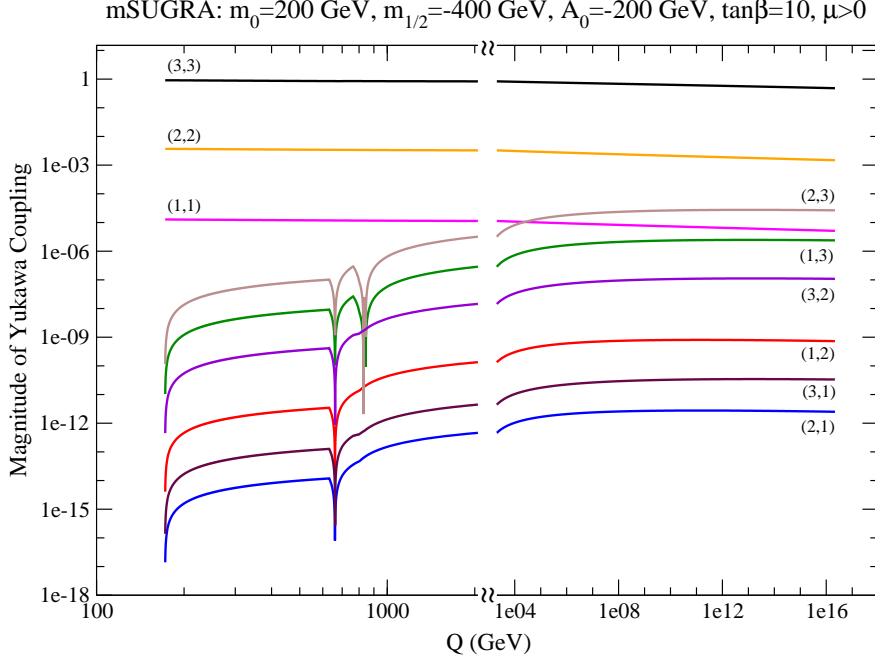


FIG. 1: Evolution of the magnitudes of the complex elements of the up-quark Yukawa coupling matrix of the mSUGRA model with  $m_0 = 200$  GeV,  $m_{1/2} = -400$  GeV,  $A_0 = -200$  GeV,  $\tan\beta = 10$  and  $\mu > 0$  in the basis where this matrix is diagonal at  $Q = m_t$ . For  $Q > m_H$  ( $\simeq 631$  GeV) we plot  $|(\mathbf{f}_u)_{ij}|$  whereas for  $Q < m_H$ , where the effective theory includes just one scalar Higgs doublet, we plot  $|(\boldsymbol{\lambda}_u)_{ij}|/\sin\beta$  which is equal to  $|(\mathbf{f}_u)_{ij}|$  at  $Q = m_H$ . In all the figures we take  $m_t = 172$  GeV.

shown in Table I. Fig. 1 should be compared with Fig. 1 of Paper I, where we had shown the evolution of the same Yukawa coupling, but in a simplified scenario where the SUSY thresholds were clustered in two regions, one at 600 GeV and the other at 2 TeV.

The most striking feature of the figure are the dips in the off-diagonal elements of the

---

is opposite the one that is usually used. To compensate for this, ISAJET internally (and unknown to the user) flips the sign of the gaugino masses relative to what the user uses as an input. Since the physics depends only on the relative sign between the gaugino masses and  $\mu$ , this sign flip is equivalent to a flipped sign for  $\mu$  (together with sign flips for  $A_0$  and  $b$ ), making it appear that the ISAJET output is in accord with the usual convention for the sign of  $\mu$ . We should also mention that here and in Ref. [4], the convention for the sign of the  $\mathbf{a}$  is opposite that to the one in Ref. [18] and of ISAJET. To reproduce the results with the sign conventions for mSUGRA parameters that we use in this paper (and in Ref. [4]) using ISAJET, we should merely switch the sign of the gaugino masses in the ISAJET inputs. Our results (except for inter-generation mixing effects) can thus be obtained by running ISAJET with  $m_0 = 200$  GeV,  $m_{1/2} = 400$  GeV,  $A_0 = -200$  GeV  $\tan\beta = 10$  and  $\mu > 0$ .

|   |                           |
|---|---------------------------|
| $M_{\text{SUSY}}$   | 703 GeV                   |
| Higgsinos ( $\mu$ )   | 538 GeV                   |
| Gluinos ( $m_{\tilde{g}}$ )   | 941 GeV                   |
| $\mathcal{H}, H^\pm$ ( $m_H$ )  | 631 GeV                   |
| Bino ( $ M_1 $ )  | 166 GeV                   |
| Winos ( $ M_2 $ )   | 315 GeV                   |
| $(\tilde{u}_L, \tilde{d}_L), (\tilde{c}_L, \tilde{s}_L), (\tilde{t}_L, \tilde{b}_L)$                            | 837 GeV, 837 GeV, 763 GeV |
| $\tilde{u}_R, \tilde{c}_R, \tilde{t}_R$   | 809 GeV, 809 GeV, 645 GeV |
| $\tilde{d}_R, \tilde{s}_R, \tilde{b}_R$   | 806 GeV, 806 GeV, 801 GeV |
| $(\tilde{\nu}_{eL}, \tilde{e}_L), (\tilde{\nu}_{\mu L}, \tilde{\mu}_L), (\tilde{\nu}_{\tau L}, \tilde{\tau}_L)$ | 331 GeV, 331 GeV, 329 GeV |
| $\tilde{e}_R, \tilde{\mu}_R, \tilde{\tau}_R$  | 249 GeV, 249 GeV, 245 GeV |

TABLE I: The location of the thresholds for our canonical mSUGRA case in Fig. 1 and in several subsequent figures.

$\mathbf{f}_u$  matrix. The aligned dips at  $Q \sim 650$  GeV, common to *all* the off-diagonal elements, occur because of the change in the sign of the coefficient of the  $\mathbf{f}_d \mathbf{f}_d^\dagger$ -type terms that drive the growth of these off-diagonal elements from zero at  $Q = m_t$ . This has been discussed in detail in Paper I, where we have also explained why the magnitudes of all the off-diagonal Yukawa couplings vanish at essentially a common value of  $Q$ . The presence of the second zero at the higher value of  $Q$ , just in the (2,3) and (1,3) elements, is accidental. It occurs because of conspiracies between terms in the corresponding  $\beta$ -function as the left-type squarks are decoupled. Notice that the lowest four curves, though they do not have this additional dip, show kinks at these same values of  $Q$ , corresponding to the decoupling of these squarks. For several other mSUGRA cases, we have checked that while squark decoupling causes kinks in the curves, the coupling does not drop to even close to zero for a second time, in contrast to the behaviour in our illustrative example in the figure.

The evolution of the down-quark Yukawa coupling matrix for the same mSUGRA point is shown in Fig. 2. We have shown these couplings both in what we will subsequently refer to as our “standard” current basis where the up-type Yukawa couplings are diagonal at  $Q = m_t$  in the left frame, and in the basis where the down-type Yukawa coupling matrix is diagonal at  $Q = m_t$  in the right frame. The matrices in the two bases are connected by the KM



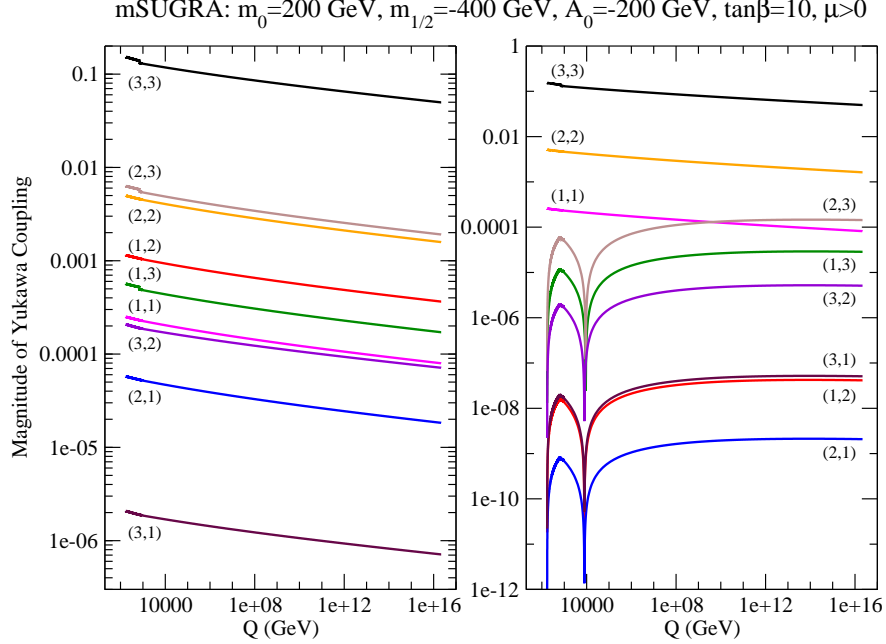


FIG. 2: Evolution of the magnitudes of the complex elements of the down-quark Yukawa coupling matrix of the mSUGRA model with  $m_0 = 200$  GeV,  $m_{1/2} = -400$  GeV,  $A_0 = -200$  GeV,  $\tan\beta = 10$  and  $\mu > 0$ . In the left-frame, we show the elements of the matrix in the same basis as in Fig. 1, where  $\lambda_u$  is diagonal at  $Q = m_t$ , whereas in the right frame, we show these elements in the basis where the  $\lambda_d$  is diagonal at  $Q = m_t$ . For  $Q > m_H$  ( $\simeq 631$  GeV) we plot  $|(\mathbf{f}_d)_{ij}|$  whereas for  $Q < m_H$ , where the effective theory includes just one scalar Higgs doublet, we plot  $|(\lambda_d)_{ij}| / \cos\beta$  which is equal to  $|(\mathbf{f}_d)_{ij}|$  at  $Q = m_H$ .

matrix, in an analogous way to (39). The curves in the left frame are all smooth (except for the small kink in the curves for  $|(\mathbf{f}_d)_{i3}|$  that occurs because of the SUSY correction to the bottom quark Yukawa coupling [25]), and do not show the dip to zero that appeared in the previous figure. This is not surprising because underlying the explanation of this dip was the fact that the off-diagonal elements evolved from zero at  $Q = m_t$  [14]. Notice also that in this frame the off-diagonal elements are not necessarily smaller than the diagonal elements even for  $Q \lesssim 1$  TeV. The magnitudes of the off-diagonal matrix elements in the frame on the right, which do start at zero at  $Q = m_t$  show the anticipated aligned dips, except that the location of the dip is shifted considerably to the right, relative to Fig. 1. This shift is not difficult to understand. The large top quark Yukawa coupling in the SM governs the evolution of the off-diagonal elements of the down-type Yukawa couplings, causing them to

evolve much more rapidly from zero in the right-hand frame of Fig. 2, so that in order to evolve back to zero after the sign flip in the  $\beta$ -function due to the additional Higgs and SUSY particles, a longer evolution distance is needed in the present case. Furthermore, beyond the Higgs boson threshold the off-diagonal elements of  $\mathbf{f}_u$  in Fig. 1 are accelerated to zero on account of the fact that the down-type Yukawa couplings  $\mathbf{f}_d$ , that enter in the evolution of these elements, are enhanced by a factor  $\sim 1/\cos\beta$ , pushing the dip in this figure to a low value of  $Q$ .

We now turn to briefly discuss what happens when we allow non-universality of GUT scale squark mass parameters, so as to split the squarks more than in mSUGRA. Recall that if the squarks all decouple together, all that happens is a change in the slope of the  $\beta$ -function. If, however, the squark masses are not all the same, our decoupling procedure entails an additional rotation to the squark mass basis. If this basis differs significantly from our “standard” basis in which the quark Yukawa coupling matrix is diagonal (at  $Q = m_t$ ), one may expect considerable deviation in the evolution of the off-diagonal elements from the mSUGRA case for  $Q$  values in between the highest and lowest squark thresholds. The introduction of non-universal squark mass parameters via non-vanishing values of  $R_\bullet$  and  $S_\bullet$  in (48) never leads to significant effects because the rotation from the “standard” basis to the squark mass basis is small by construction.

The question then is whether we can have large deviations from Fig. 1 and 2 via the  $\mathbf{T}_\bullet$  (or  $\mathbf{Z}_\bullet$ ) matrices. To examine this, we set all GUT scale inputs to be the same as the mSUGRA case in Fig. 1 except that we now take,

$$m_{\{U,D\}0}^2 = 0, \quad \text{and} \quad (49a)$$

$$\mathbf{T}_{U,D} = \text{diag} \{10000, 40000, 90000\} \text{ GeV}^2. \quad (49b)$$

We need, of course, to specify the basis in which the squark mass matrix is diagonal. If this is the “standard” current basis, we have checked that although the right squark masses are now significantly split relative to the mSUGRA case, except for detailed changes in the evolution for  $Q$  values in between the squark thresholds (*e.g.* the dip at the higher value of  $Q$  in the upper curves in Fig. 1 develops more structure, and there are jumps in the (1,2) and (2,1) elements), the evolution is not altered in any important way at large values of  $Q$ . This is because the rotation between the “standard” basis and the squark mass basis is again small.

If we take instead the right-squark matrices in (49) to be diagonal in a completely different basis specified by unitary matrices  $\mathbf{V}_L(u)$ ,  $\mathbf{V}_R(u)$  and  $\mathbf{V}_R(d)$  that take us to our “standard” basis, and specified to be of the form,

$$\mathbf{V} = \begin{pmatrix} c_\alpha c_\beta & s_\alpha c_\beta e^{-i\delta_\alpha} & s_\beta e^{-i\delta_\beta} \\ -s_\alpha c_\gamma e^{i\delta_\alpha} - c_\alpha s_\beta s_\gamma e^{i(\delta_\beta - \delta_\gamma)} & c_\alpha c_\gamma - s_\alpha s_\beta s_\gamma e^{i(-\delta_\alpha + \delta_\beta - \delta_\gamma)} & c_\beta s_\gamma e^{-i\delta_\gamma} \\ s_\alpha s_\gamma e^{i(\delta_\alpha + \delta_\gamma)} - c_\alpha s_\beta c_\gamma e^{i\delta_\beta} & -c_\alpha s_\gamma e^{i\delta_\gamma} - s_\alpha s_\beta c_\gamma e^{i(-\delta_\alpha + \delta_\beta)} & c_\beta c_\gamma \end{pmatrix}, \quad (50)$$

(where  $s_\alpha = \sin \alpha$ ,  $c_\alpha = \cos \alpha$ , *etc.*) with randomly chosen values of  $\alpha$ ,  $\beta$ ,  $\gamma$  and  $\delta_\beta$  (we take  $\delta_\alpha = \delta_\gamma = 0$  for simplicity), we may expect the evolution of Yukawa couplings to depart from the corresponding evolution in mSUGRA.<sup>16</sup> We emphasize that this scenario (which is only of pedagogical interest) where  $\mathbf{m}_{U,D}^2$  are diagonal in the basis where the corresponding Yukawa coupling matrices have large off-diagonal elements includes potentially very large flavour-violation in the singlet squark SSB mass matrices, and is likely excluded.

In Fig. 3 we illustrate the evolution of the magnitudes of the elements of the up-quark Yukawa coupling matrix with,

$$\mathbf{V}_L(u) : \alpha = 2.053, \beta = 0.254, \gamma = 2.030, \delta_\beta = 0.4829, \quad (51a)$$

$$\mathbf{V}_R(u) : \alpha = 1.188, \beta = 2.218, \gamma = 0.763, \delta_\beta = 0.87, \quad (51b)$$

$$\mathbf{V}_R(d) : \alpha = 1.904, \beta = 2.947, \gamma = 1.847, \delta_\beta = 1.14. \quad (51c)$$

Note that, just as in Fig. 1, we have plotted these elements in our “standard” basis where the Yukawa coupling matrix is diagonal at  $Q = m_t$ . The GUT scale matrices  $\mathbf{m}_U^2$  and  $\mathbf{m}_D^2$  will be random-looking Hermitian matrices in our “standard” basis. We see that the evolution of the diagonal elements is not significantly altered from mSUGRA. This is because although there is a large mismatch between the squark mass basis and our “standard” basis, this mismatch is operative over the small range of  $Q$  between the highest and lowest thresholds and so has little impact on the largest elements. The two largest off-diagonal entries (i.e.  $(\mathbf{f}_u)_{23}$  and  $(\mathbf{f}_u)_{13}$ ) similarly do not change significantly from Fig. 1, but all other entries are

---

<sup>16</sup> The matrices  $\mathbf{V}_{L,R}(u)$  should be numerically unitary to high accuracy. Otherwise, numerical errors from inverting the up Yukawa couplings from this new current basis to our “standard” basis will leave residual off-diagonal elements rather than zero even at  $Q = m_t$ . If the size of these elements is comparable to the values of the smallest off-diagonal elements at values of  $Q$  substantially away from  $m_t$ , it is clear that our solutions will be dominated by the error from the non-unitarity of the  $\mathbf{V}_{L,R}(u)$  matrices. A similar consideration applies to  $\mathbf{V}_R(d)$ .

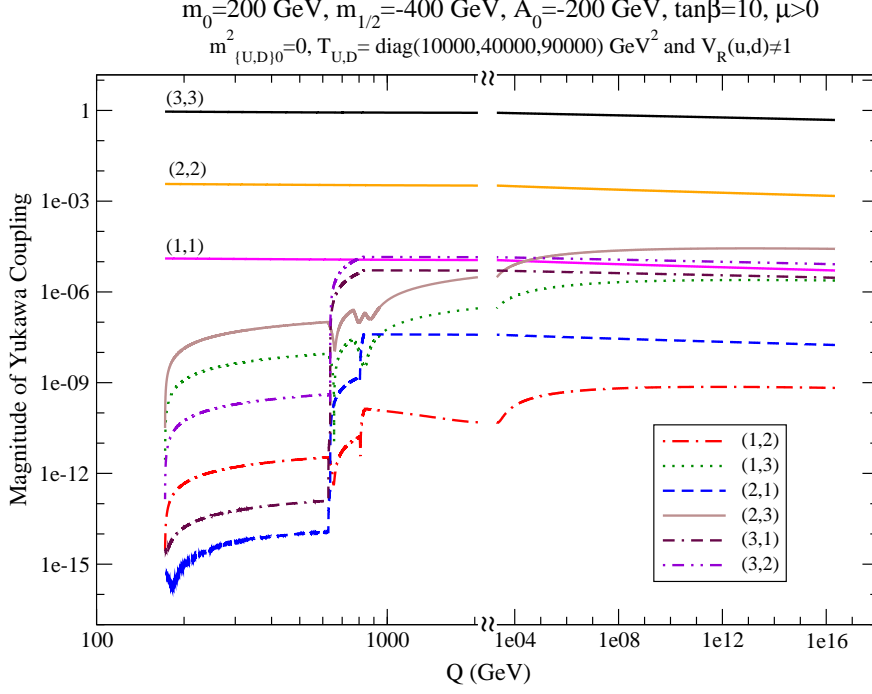


FIG. 3: The same as Fig. 1 except that the GUT scale right-squark mass matrices are now given by (49) in the basis specified by (51) of the text. Note, however, that these matrix elements are shown in the “standard” current basis where the matrix is diagonal at  $Q = m_t$ .

greatly altered. While it may seem that the values of these matrix elements at a large scale is quite irrelevant phenomenologically, the altered form of the Yukawa coupling matrix at the high scale could be of relevance to model-builders.

We have seen that the magnitudes of the off-diagonal elements in Fig. 3 remain small because the splitting in the squark spectrum is limited to  $\mathcal{O}(100 - 1000)$  GeV. The natural question then is whether we can get these to be larger by choosing extreme intra-generational squark splitting. Even putting aside potentially unacceptable flavour-changing effects that might result, this is not easy. In general, such a GUT scale splitting also has a large value for  $S = m_{H_u}^2 - m_{H_d}^2 + Tr [\mathbf{m}_Q^2 - \mathbf{m}_L^2 - 2\mathbf{m}_U^2 + \mathbf{m}_D^2 + \mathbf{m}_E^2]$ , which pulls the other squarks also to large masses, so the squark mass splitting is reduced by RGE effects. It may be possible to obtain split squarks by adjusting  $S$  to be zero ( $S$  is then invariant under renormalization group evolution), but we have not investigated this here.

## B. Gaugino Mass Parameters in Split SUSY Models

We have seen in Sec. IV A that the evolution of the electroweak gaugino mass parameters acquires a dependence on the  $\mu$ -parameter and *vice-versa*, once threshold effects from splitting in the Higgs boson sector are included. In models where  $m_H \gg |\mu|, |M_{1,2}|, |M'_{1,2}|$ , the effect of the term explicitly dependent on  $\mu$  in (B2)-(B5) (and the corresponding terms dependent on the gaugino mass parameters in the RGE for  $\mu$ ) may be significant, so that the relation  $M_2/M_1 = \alpha_2/\alpha_1$  expected in many models is modified. We should keep in mind that two loop terms will, in general, also alter this relation. Our point is that we should expect threshold corrections, from the  $\mu$  term in the RGE, as well as from the decoupling of sfermions, to be comparable to (or even larger than) the two loop modifications, and so need to be included in a quantitative analysis. Within the mSUGRA context, we have small values of  $|\mu|$ , and hence,  $m_H \gg |\mu|$  in the hyperbolic branch/focus point (HB/FP) region [37] which occurs for large values of  $m_0$ , and is one of the regions selected out [38] by the relic-density measurement [39]. We mention here that *the location of this HB/FP region is significantly altered by the inclusion of the threshold corrections.*

These considerations led us to examine the evolution of the gauge couplings and the electroweak gaugino parameters for a relic-density-consistent mSUGRA model point in the HB/FP region with  $m_0 = 3075$  GeV,  $m_{1/2} = -600$  GeV,  $A_0 = 0$ ,  $\tan\beta = 10$  and  $\mu > 0$ , for which  $(\mu, M_1, M_2) \simeq (306, -258, -496)$  GeV at the weak scale.<sup>17</sup> We found that at the two loop level with all threshold effects included,  $M_2/M_1 = 1.919$  to be compared to  $M_2/M_1 = 1.881$  obtained without including threshold effects. Thus, although threshold effects actually bring us closer to  $\alpha_2/\alpha_1 = 1.964$ , their inclusion is clearly necessary for a quantitative analysis of mass parameters that may be extracted at an  $e^+e^-$  linear collider, where a precision of better than 1% will be possible if charginos are kinematically accessible.

The threshold corrections to gaugino mass parameters can be much larger in the so-called split SUSY model [40] that has received considerable attention in the recent literature. In this scenario, the naturalness of the scalar Higgs sector (which we view as one of the primary motivations for weak scale SUSY) is abandoned, while gauge coupling unification and the neutralino dark matter candidate of  $R$ -parity violating models are preserved. Gaugino mass

---

<sup>17</sup> Without threshold corrections, ISAJET gives a similar spectrum for  $m_0 \simeq 3660$  GeV.

## Split Supersymmetry

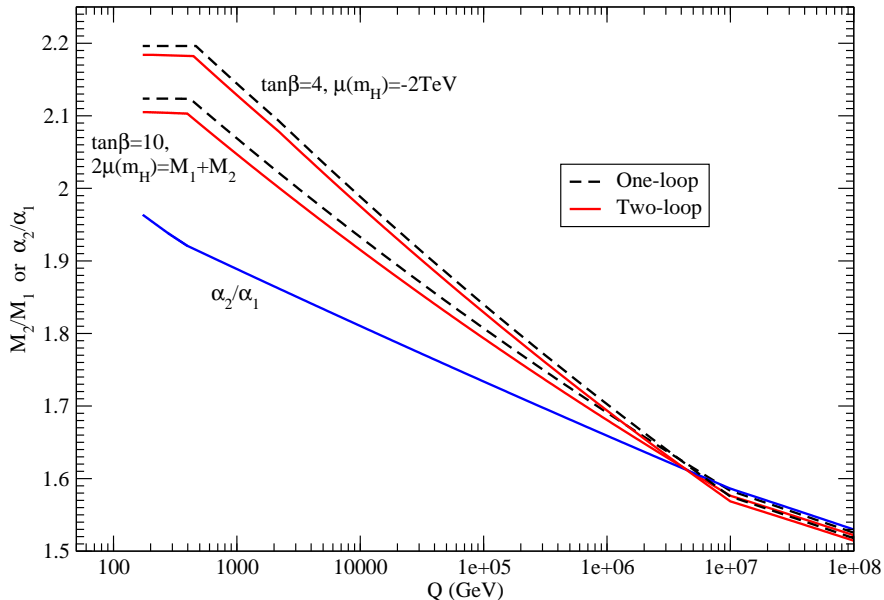


FIG. 4: The evolution of the gaugino mass ratio  $M_2/M_1$  at the one (dashed) and two (solid) loop levels, along with the two-loop evolution of  $\alpha_2/\alpha_1$ , for a split SUSY model where scalar masses are around  $10^7$  GeV, with gauginos and higgsinos at the weak scale. Gaugino mass unification is assumed and as everywhere else in this paper, the gaugino mass parameters are negative. The other parameters are as mentioned in the text.

parameters and  $|\mu|$  are assumed to be at the weak scale, while scalar mass parameters are set to be at an intermediate scale. This means that sfermion masses as well as  $m_H$  are very large (with the SM Higgs doublet fine-tuned to be light), so that charginos and neutralinos are the only new particles (other than a SM Higgs boson) at the weak scale.

As an illustration, in Fig. 4 we plot the variation of the ratio  $M_2/M_1$  at the one-loop level (dashed), as well as at the two-loop level (solid), with the renormalization scale  $Q$ , along with the two-loop value of  $\alpha_2/\alpha_1$ . We show results, first where the value of  $|\mu|$  is set exactly in between  $|M_1|$  and  $|M_2|$  so that the lightest neutralino acquires a significant higgsino component, to qualitatively mimic mixed higgsino dark matter.<sup>18</sup> We have checked

<sup>18</sup> In the absence of a real theory of split SUSY, we should view this figure only as a qualitative illustration of potentially large threshold effects. Here, we take the sfermion mass parameters to be  $10^7$  GeV at  $Q = M_{\text{GUT}}$ ,  $m_{1/2} = -350$  GeV and  $A_0 = 0$ . Since it is not possible to satisfy the EWSB conditions except when  $\tan\beta$  is hierarchically large — this would cause down-type Yukawa couplings to become

that the  $M_2/M_1$  values do not change in a significant way for yet larger values of  $\tan\beta$ . It is clear that the relation  $\frac{M_2}{M_1} = \frac{\alpha_2}{\alpha_1}$  is violated at the several percent level by the threshold corrections, without which the  $M_2/M_1$  lines would have continued with the same slope that they have above  $10^7$  GeV to low values. For this point, the  $2sc \times \mu$  term that explicitly appears in the RGE is very small so that the result is independent of the sign of  $\mu$ : most of the difference is an effect of the sfermion loop contributions being switched off below  $10^7$  GeV. To gain some idea of how large the effect of this  $\mu$  term might be, we have also shown  $M_2/M_1$  for  $\mu = -2$  TeV, with  $\text{sign}(\mu M_2) > 0$  and  $\tan\beta = 4$ . Since such a large value of  $\mu$  would be totally incompatible with the measured relic density and small values of  $\tan\beta$  are unnatural in these models without some modification to the EWSB sector, the reader should view these curves only as a guide to how much the gaugino mass ratio may deviate from its “unification value”. The difference between the two cases is almost entirely due to the different choice of  $\mu$ . We see that the gaugino mass unification condition will, in this case, be violated by  $\sim 10\%$ . If instead we choose the opposite sign for  $M_2\mu$ , but keep  $|\mu| = 2$  TeV, this “large  $|\mu|$  line” would be *lower* than the corresponding line with  $\mu = (M_1 + M_2)/2$  by about the same amount that it is higher than this line in the figure. Clearly, increasing the splitting between the scalar and the gaugino/higgsino sector of the theory will cause even further violation of the unification condition, and  $\sim 20\%$  effects appear to be plausible if the scalars are instead at the  $10^{11}$  GeV scale.

### C. Trilinear Couplings

We begin our discussion of the trilinear couplings by returning to the mSUGRA case considered in Figs. 1 and 2. The magnitudes of the individual entries of the trilinear coupling matrices  $\mathbf{a}_u$  and  $\mathbf{a}_d$  are shown in Fig. 5, where we plot (a)  $|(\mathbf{a}_u)_{ij}|$  and (b)  $|(\mathbf{a}_d)_{ij}|$  in our “standard” current basis where the up-type quark Yukawa coupling matrix is diagonal at  $Q = m_t$ , along with  $|(\mathbf{a}_d)_{ij}|$  in the basis where the down-type quark Yukawa coupling matrix is diagonal at  $Q = m_t$  in frame (c). We terminate the curves at  $Q = m_H$  since below this

---

non-perturbative — we treat  $\mu$  and  $\tan\beta$  as phenomenological parameters, and fix  $m_H$  to be  $10^7$  GeV in this figure. The parameters  $m_{H_u}^2$  and  $m_{H_d}^2$  (indeed all scalar mass parameters) are never needed since the RGEs for gaugino masses,  $\mu$  and the  $\mathbf{a}$ -parameters, and the dimensionless couplings, form a closed set even at the two-loop level. Sfermion masses only enter via the location of thresholds.

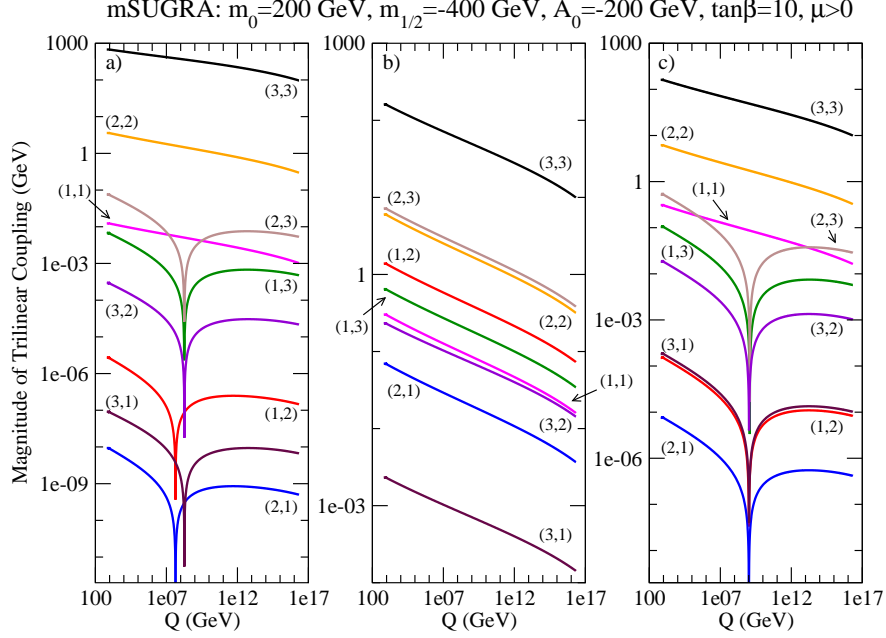


FIG. 5: The magnitude of the elements of the trilinear coupling matrix  $\mathbf{a}_\bullet$  for the mSUGRA model in Fig. 1. We show (a)  $|(\mathbf{a}_u)_{ij}|$ , (b)  $|(\mathbf{a}_d)_{ij}|$ , in the basis where up-quark Yukawa couplings are diagonal at  $Q = m_t$ , and (c)  $|(\mathbf{a}_d)_{ij}|$  in the basis where down-quark Yukawa couplings are diagonal at  $Q = m_t$ . The curves extend between  $Q = m_H$  and  $Q = M_{\text{GUT}}$ .

scale we have a single Higgs scalar doublet model, and the trilinear couplings  $\mathbf{a}_{u,d}$  evolve only as part of a linear combination with  $\tilde{\mu}^* \mathbf{f}_{u,d}^{h_{u,d}}$  as discussed in Sec. IV B. We see that the curves in frame (a) show a simple dip structure indicating that the real and imaginary parts of  $\mathbf{a}_{u,d}$  are really monotonic functions of  $Q$  that pass through zero together, in a manner similar to the elements of the Yukawa coupling matrix [14]. The actual location of the zero is somewhat harder to analyse because even though  $\mathbf{a}_u$  obtains off-diagonal components only because the down-quark Yukawa matrix is not diagonal at  $Q = m_t$ , the matrix  $\mathbf{a}_u$  is off-diagonal even at the GUT scale. The off-diagonal elements of  $\mathbf{a}_d$  in frame (b) start off with a much larger magnitude in the “standard” Yukawa basis at  $Q = M_{\text{GUT}}$  because the corresponding Yukawa coupling matrix has large off-diagonal pieces. In this case, the evolution of these off-diagonal elements receives significant contributions from *all* entries in the RGE (unlike the evolution of the off-diagonal elements in frame (a) or of the off-diagonal Yukawa couplings discussed at length in Paper I where contributions from the off-diagonal down-type Yukawa matrices govern the evolution), and never go through zero; the situation is similar to that in the first frame of Fig. 2. We see from frame (c) that the magnitudes of  $(\mathbf{a}_d)_{ij}$ , in the basis that the



down-type Yukawa coupling matrix is diagonal at  $Q = m_t$ , again show the characteristic dip structure indicating that the off-diagonal elements increase in magnitude from their value at  $Q = M_{\text{GUT}}$  to some maximum magnitude at an intermediate scale, but then smoothly reverse direction and thereafter evolve monotonically through zero to the low scale. The elements in frames (b) and (c) are, of course related by, (39). We note that because the off-diagonal elements in frame (c), are driven by the larger (and significantly off-diagonal) “up-type” Yukawa couplings, these are bigger than those in frame (a) where it is the down-type Yukawa coupling matrix that has the significant off-diagonal elements, and so largely determines the entries.

Finally, in Fig. 6 we consider a model with non-universal values of  $\mathbf{a}$ -parameters, but where these are not a new source of flavour violation. Specifically, we consider a model with the same values for mSUGRA parameters as in Fig. 5, but with non-zero values for  $W$  and  $X$  in (48c) (with  $A_{\{u,d\}0} = A_0$ ), and illustrate the evolution of (a)  $\text{Re}(\mathbf{a}_u)_{23}$  and (b)  $\text{Re}(\mathbf{a}_u)_{32}$ . We have checked that the imaginary parts of these matrix elements are about four orders of magnitude smaller. The striking feature of frame (a) is that the various curves which start with very different values of  $\text{Re}(\mathbf{a}_u)_{23}$  at  $Q = M_{\text{GUT}}$ , appear to focus to a common value at the low scale. We have checked, however, that although they all cross at  $Q \simeq 1.5$  TeV, they do not all converge at precisely the same value of  $Q$ . This apparent convergence, which persists for other values of mSUGRA parameters, is sensitively dependent on the special GUT scale boundary conditions for  $\mathbf{a}_u$  that we have used. We have checked that if instead we use a general matrix  $\mathbf{Z}_u$  in (48c), the corresponding evolution is completely different. We do not have a good explanation for the seeming convergence in frame (a), and only note that it is not generic to *all* elements of  $\mathbf{a}_u$  as evidenced, for example, by the corresponding evolution of  $\text{Re}(\mathbf{a}_u)_{32}$  in frame (b) of the figure.

#### D. Soft Masses

We begin our discussion of the evolution of the scalar mass SSB parameters by showing in Fig. 7 the evolution of the magnitudes of  $\mathbf{m}_{\mathcal{I}}^2$  in our “standard” current basis for the mSUGRA model with the same parameters as in Fig. 1. The diagonal matrix elements start from a common value  $m_0$  and increase as we go to the weak scale because of gauge (and gaugino) interactions. The splitting between the (1,1) and (2,2) elements that occurs

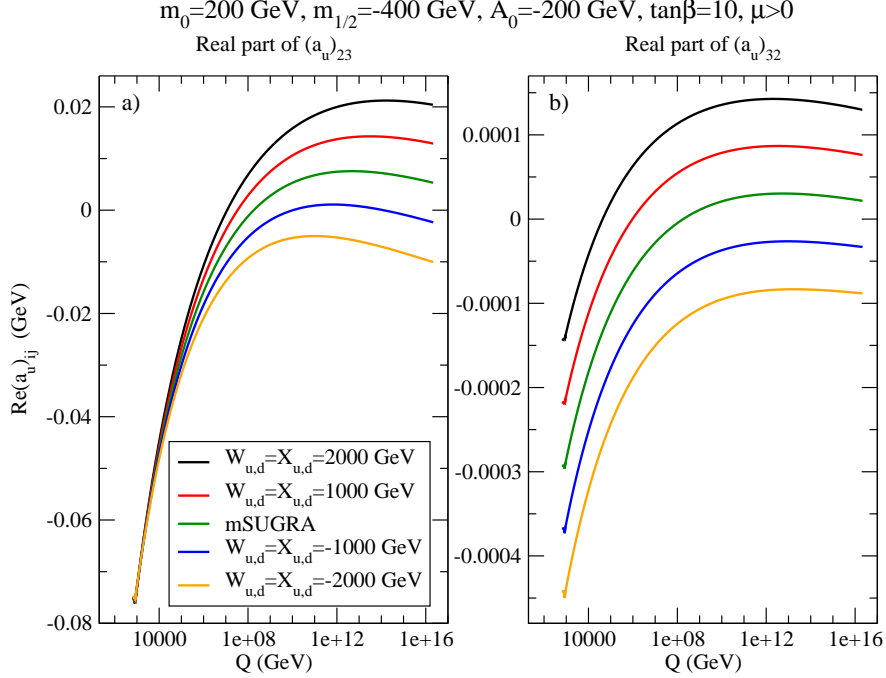


FIG. 6: The evolution of (a)  $\text{Re}(\mathbf{a}_u)_{23}$  and (b)  $\text{Re}(\mathbf{a}_u)_{32}$  for a model with the GUT scale values of  $\mathbf{a}$ -parameters set as in (48c) for several values of  $W$  and  $X$  shown in the legend (with  $A_{\{u,d\}0} = A_0$ ). The imaginary parts of the matrix elements are about four orders of magnitude smaller. The curves are in the same order as in the legend. The GUT scale SSB scalar and gaugino mass parameters are assumed to be universal, with the same value as in Fig. 5. We terminate the curves at  $Q = m_H$  at the lower end.

because of the Yukawa couplings is too small to be visible in the figure. The (3,3) element is, however, reduced significantly on account of the large (3,3) entry in  $\mathbf{f}_u$ . Notice that the curves become flat once the squarks are all decoupled. The magnitudes of the three independent off-diagonal elements of the Hermitian matrix  $\mathbf{m}_U^2$  start from zero at  $Q = M_{\text{GUT}}$ , and rapidly rise because  $\mathbf{f}_u$  has off-diagonal entries at  $Q = M_{\text{GUT}}$ : the much more off-diagonal  $\mathbf{f}_d$  matrix affects the evolution of  $\mathbf{m}_U^2$  only at the two-loop level. Note the break in the vertical scale in the figure. The ordering of the magnitudes of the off-diagonal elements of  $\mathbf{m}_U^2$  can be simply gauged from the up-type Yukawa coupling matrix. These off-diagonal elements start from zero at  $Q = M_{\text{GUT}}$ , evolve to a maximum magnitude, then smoothly reverse direction at an intermediate scale and then continue to evolve monotonically all the way to the weak scale. The dips in the figure occur where the real, and simultaneously the imaginary, part of  $(\mathbf{m}_U^2)_{ij}$  changes sign during the course of its evolution to  $Q = m_t$  where we terminate the

mSUGRA:  $m_0=200$  GeV,  $m_{1/2}=-400$  GeV,  $A_0=-200$  GeV,  $\tan\beta=10$ ,  $\mu>0$

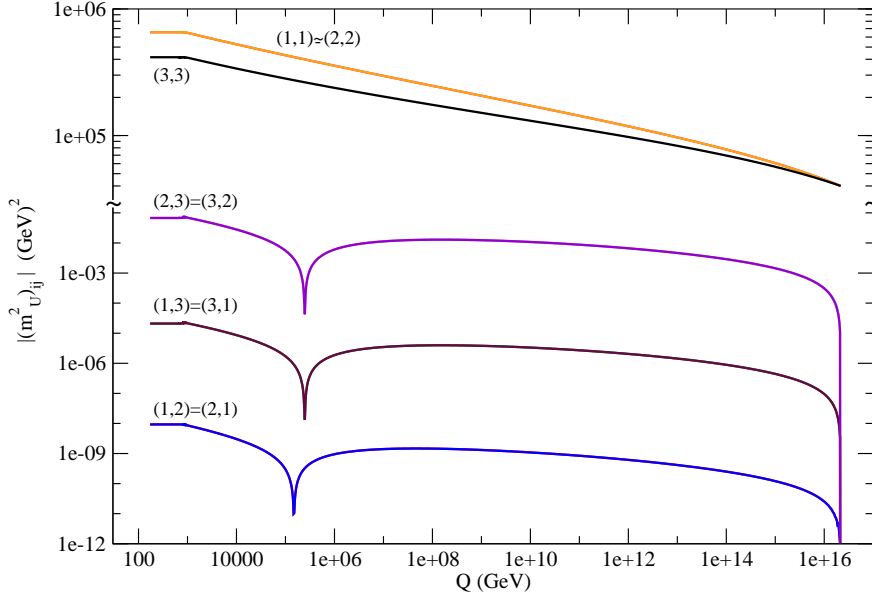


FIG. 7: The scale dependence of the magnitudes of the entries of the matrix  $\mathbf{m}_U^2$  for the mSUGRA model with parameters as in Fig. 1 in the basis where the up-type quark Yukawa coupling matrix is diagonal at  $Q = m_t$ . Note that we have broken the vertical scale at  $0.1 \text{ GeV}^2$  and also used a different scale above this to better show the splitting of the  $(3,3)$  entry from the other diagonal entries.

plot.

Before proceeding further we draw the reader’s attention to a technical point that is important for the numerical solution of the RGEs, once squark decoupling is included as described in Sec. III B. As we have already explained, in order to correctly implement the decoupling procedure for values of  $Q$  below the highest sfermion threshold, at each step we need to rotate to the basis where the SSB squark mass squared matrices are diagonal, which, in turn, requires us to obtain the unitary matrix  $\mathbf{R}$  that relates our “standard” basis to this “squark mass basis”. After evaluating the right-hand side of the RGEs, we always rotate back to our “standard” basis using  $\mathbf{R}^\dagger$ . While this is straightforward in principle, the practical problem is that when two squark eigenvalues become very close — this is always the case in mSUGRA because the up and charm squark mass parameters only evolve differently because of effects of the small first and second generation quark Yukawa couplings —  $\mathbf{R}\mathbf{R}^\dagger$  develops non-zero off-diagonal matrix elements due to numerical noise at the  $10^{-10}$  level (The

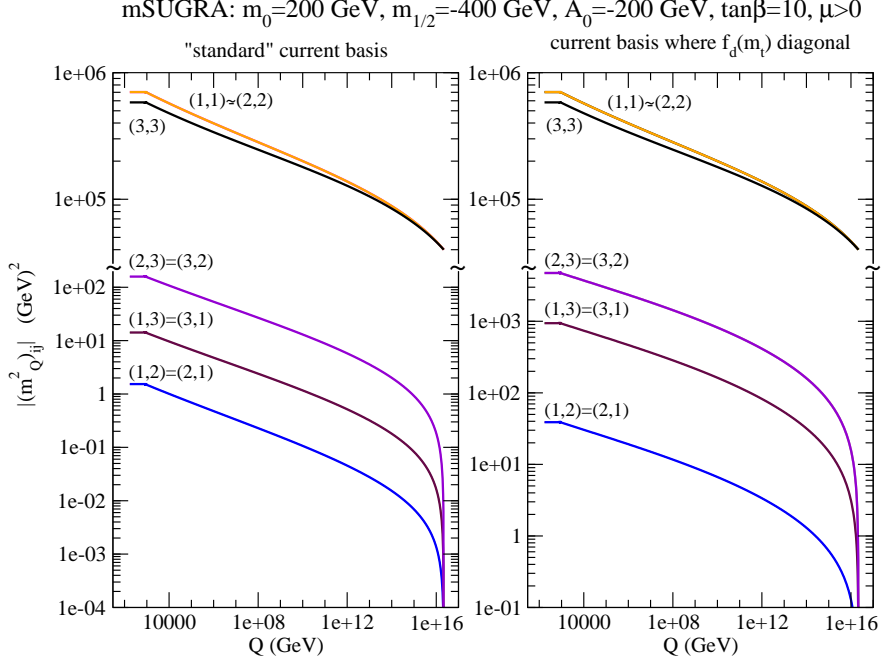


FIG. 8: The scale dependence of the magnitudes of the entries of the matrix  $\mathbf{m}_Q^2$  for the mSUGRA model with parameters as in Fig. 1 in the basis where the up-type (left frame), or the down-type (right frame), quark Yukawa coupling matrix is diagonal at  $Q = m_t$ . Note that we have broken the vertical scales to better display the matrix elements.

noise level depends on the computer system.). This then ruins the delicate cancellations that are necessary to obtain the tiny magnitude of  $(\mathbf{m}_U^2)_{12}$  seen in the bottom curve of Fig. 7. Our procedure for dealing with this is detailed in Appendix A. It is for essentially the same reason that we had to use the manifestly unitary form (as in (50)) for the matrices  $\mathbf{V}_L(u)$ ,  $\mathbf{V}_R(u)$  and  $\mathbf{V}_R(d)$  when we discussed the evolution of Yukawa couplings when the matrices  $\mathbf{m}_{U,D}^2$  were diagonal in a general current basis in Fig. 3; see the footnote just after Eq. (50).

Fig. 8 shows the evolution of  $\mathbf{m}_Q^2$  for the same mSUGRA point. In the left frame, we show the magnitudes of the elements in our “standard” basis, where the up quark Yukawa coupling matrix is diagonal at  $Q = m_t$ . The frame on the right shows the magnitudes of the elements of this same matrix, but in the basis where the down-type quark Yukawa coupling matrix is diagonal at  $m_t$ . We have checked that the large difference in the size of the off-diagonal elements in the two frames is indeed accounted for by the fact that the corresponding matrices are related by (40). Unlike in Fig. 7, there is no dip in the magnitudes of the off-diagonal elements because they evolve monotonically from zero at the GUT scale,

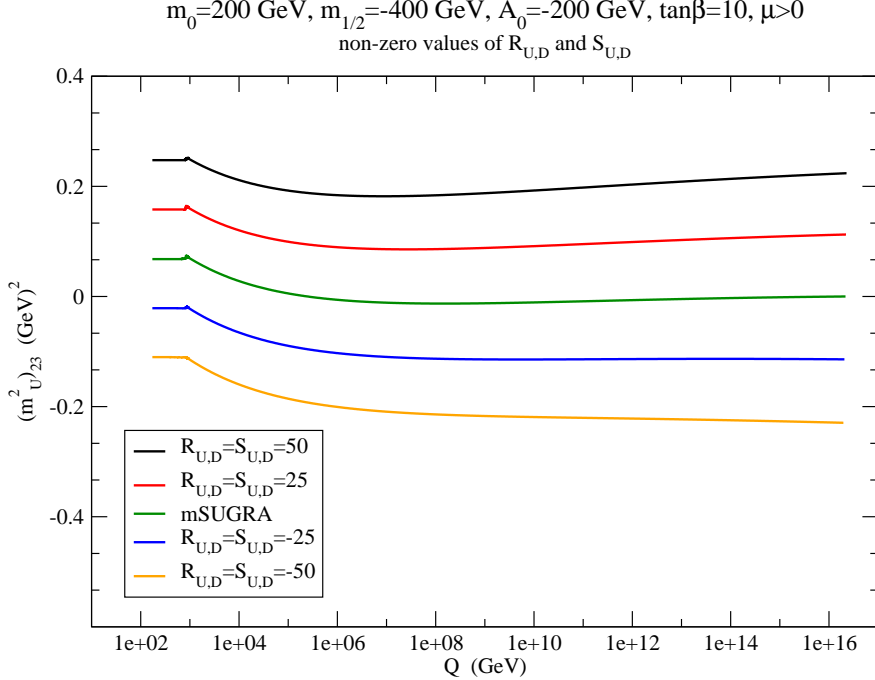


FIG. 9: The scale dependence of  $(\mathbf{m}_U^2)_{23}$  for several sets of values of  $R_{U,D}$  and  $S_{U,D}$  that appear in (48b) for the model with non-universal GUT scale SSB squark mass parameters, but  $c_{U,D} = 1$ . The curves are in the same order as the legend, and all the other parameters are set as in Fig. 7.

until the squarks are all decoupled.

To understand how the non-universal boundary conditions in (48b) impact the evolution of the squark mass matrices we examine a model with non-zero values of  $R_{U,D}$  and  $S_{U,D}$ , but with universal gaugino masses and  $\mathbf{a}$ -parameters. As an illustration we show in Fig. 9 the value of  $(\mathbf{m}_U^2)_{23}$  for the set of values of  $R_{U,D}$  and  $S_{U,D}$  shown in the figure, with all other parameters set as in Fig. 7 (including  $c_{U,D} = 1$ ) so that  $R_{U,D} = S_{U,D} = 0$  corresponds to mSUGRA model in this figure. We see that with non-zero values of  $R_{U,D}$  and  $S_{U,D}$ ,  $(\mathbf{m}_U^2)_{23}$  already starts off with a substantial value (positive or negative) at  $Q = M_{\text{GUT}}$ , and evolves slowly with  $Q$ . This situation is qualitatively similar to that in Fig. 7, once  $(\mathbf{m}_U^2)_{ij}$  has evolved away from its value at  $M_{\text{GUT}}$ , and has had a chance to grow from zero. However, because the curves start off with rather large values at the GUT scale (except for the middle mSUGRA curve) the evolution does not take them through zero for any value of  $Q > m_t$ . As a result, the dip which was the most prominent feature of Fig. 7 is absent, except in the middle curve which does cross zero for  $Q \sim 2.5 \times 10^5$  GeV.

Finally, in Fig. 10 we return to the non-mSUGRA case that we considered in Fig. 3.

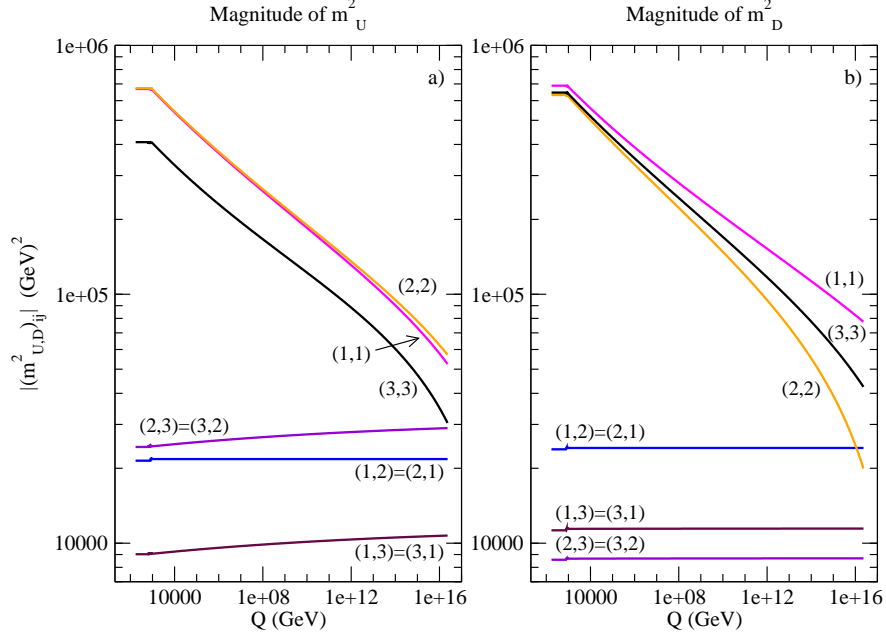


FIG. 10: (a) The same as Fig. 7 except for the non-universal model considered in Fig. 3, and (b) the magnitude of the corresponding elements of  $\mathbf{m}_D^2$  for the same scenario. The elements are plotted in our “standard” current basis but are exactly the same in the basis where the down quark Yukawa couplings are diagonal.

We emphasize again that in this case  $\mathbf{m}_U^2$  and  $\mathbf{m}_D^2$  are diagonal only in the basis where the superpotential Yukawa coupling matrices have large off-diagonal elements so that we would expect that this model includes new and potentially large sources of flavour-violation in the singlet squark SSB mass matrices that may well be excluded by data. As in Fig. 7, we show  $|(\mathbf{m}_U^2)_{ij}|$  in the basis where the up-quark Yukawa coupling matrix is diagonal at  $Q = m_t$ . We see from the figure that the matrix  $\mathbf{m}_U^2$  has large off-diagonal entries at  $Q = M_{GUT}$ . As expected, the gauge (and gaugino) interactions cause the diagonal entries to rapidly increase, whereas the off-diagonal elements which do not “feel these terms” evolve much more slowly with  $Q$ . Note also that because  $(\mathbf{m}_U^2)_{11} < (\mathbf{m}_U^2)_{22}$  at  $Q = M_{GUT}$ , Yukawa coupling effects draw them closer as we go to low scales. We also remark that the negative GUT scale value of  $S$  tends to reduce the diagonal elements of  $\mathbf{m}_U^2$  as we go to low scales but pulls up the corresponding elements of  $\mathbf{m}_D^2$ . Although the renormalization group evolution increases the gap between the off-diagonal and diagonal elements at the low scale, notice that the off-diagonal elements are separated by just one order of magnitude from the *difference between the diagonal elements*, so that we may expect large flavour mixing between the  $SU(2)$  singlet

up squarks. This mixing, if anything, is even larger in the down squark sector as can be seen in frame (b). A careful evaluation of inter-generation squark mixing is clearly necessary for any discussion of flavour-violation in squark decays, the subject of the next section.

## VI. FLAVOUR-CHANGING SQUARK DECAY: AN ILLUSTRATIVE APPLICATION

We are now ready to apply the considerations of our analysis to flavour violating decays of squarks. In models with additional sources of flavour violation in the SSB sector through non-vanishing values of the matrices  $\mathbf{T}_\bullet$  and/or  $\mathbf{Z}_\bullet$  in (48), at least some the SSB mass and  $\mathbf{a}$ -parameter matrices will not be diagonal in the basis that quarks are diagonal, and we will have flavour-violating decays of squarks at the “tree-level”, *i.e.* even without any renormalization group evolution of the SSB parameters. If the elements of these matrices take arbitrary values comparable to  $M_{\text{SUSY}}$ , flavour-violating quark-squark-neutralino and quark-squark-gluino couplings become comparable in magnitude to the corresponding flavour-conserving vertices, resulting in the well-known SUSY flavour problem. Minimal flavour violation [36] has been suggested as a way of introducing flavour violation into the SSB parameters in a controlled way. We present formulae for flavour violating couplings and partial widths for the corresponding decays of squarks, and then go on to a numerical analysis of these decays. For definiteness, we will focus on up-type squarks.

### A. Squark decay width

In the current basis the up-type squark mass terms in the Lagrangian are,

$$\mathcal{L} \ni - \left( \tilde{u}_{Ll}^\dagger, \tilde{u}_{Rr}^\dagger \right) (\mathcal{M}_{\tilde{u}}^2)_{(lr)(ms)} \begin{pmatrix} \tilde{u}_{Lm} \\ \tilde{u}_{Rs} \end{pmatrix}, \quad (52)$$

where the  $(6 \times 6)$  up-squark mass matrix takes the form,

$$(\mathcal{M}_{\tilde{u}}^2)_{(lr)(ms)} \equiv \begin{pmatrix} (\mathcal{M}_{LL}^2)_{lm} & (\mathcal{M}_{LR}^2)_{ls} \\ (\mathcal{M}_{LR}^2)_{rm}^\dagger & (\mathcal{M}_{RR}^2)_{rs} \end{pmatrix}. \quad (53)$$

Here, the indices  $l, m$  label left-handed squarks ( $\tilde{u}_{Ll} = (\tilde{u}_L, \tilde{c}_L, \tilde{t}_L)$ ), while  $r, s$  label right-handed squarks ( $\tilde{u}_{Rr} = (\tilde{u}_R, \tilde{c}_R, \tilde{t}_R)$ ). The elements of the squark mass matrix are given

by

$$(\mathcal{M}_{LL}^2)_{lm} = (\mathbf{m}_Q^2)_{lm} + v_u^2 (\mathbf{f}_u^* \mathbf{f}_u^T)_{lm} + \left( \frac{g'^2}{12} - \frac{g_2^2}{4} \right) (v_u^2 - v_d^2) \delta_{lm} , \quad (54a)$$

$$(\mathcal{M}_{RR}^2)_{rs} = (\mathbf{m}_U^2)_{rs} + v_u^2 (\mathbf{f}_u^T \mathbf{f}_u^*)_{rs} - \frac{g'^2}{3} (v_u^2 - v_d^2) \delta_{rs} , \quad (54b)$$

$$(\mathcal{M}_{LR}^2)_{ls} = -v_u (\mathbf{a}_u)_{ls}^* + v_d (\tilde{\mu}^* \mathbf{f}_u^{h_u})_{ls}^* . \quad (54c)$$

Of course, if we are evaluating  $(\mathcal{M}_{LR}^2)_{ls}$  for  $Q < m_H$ , it is the combination  $[-s (\mathbf{a}_u)_{ls}^* + c (\tilde{\mu}^* \mathbf{f}_u^{h_u})_{ls}^*]$  (for which the RGE is (B21) in Appendix B) that enters the mass matrix.

The physical squarks  $(\tilde{u}_\sigma^M, \sigma = 1 - 6)$  are obtained by diagonalizing the squark matrix (53) by a unitary transformation  $\mathbf{U}$ , and are given in terms of the current squarks by,

$$\begin{pmatrix} \tilde{u}_{Ll} \\ \tilde{u}_{Rr} \end{pmatrix} = \begin{pmatrix} \mathbf{U}_{Ll\sigma} \\ \mathbf{U}_{Rr\sigma} \end{pmatrix} \tilde{u}_\sigma^M , \quad (55)$$

where, for later convenience, we write the  $(6 \times 6)$  matrix  $\mathbf{U}$  in terms of two  $(3 \times 6)$  blocks  $\mathbf{U}_L$  and  $\mathbf{U}_R$ . We label the physical squarks in order of their mass, with  $\tilde{u}_1^M$  being the lightest, and  $\tilde{u}_6^M$  being the heaviest. Similar considerations hold for down-type squarks.

The couplings of the physical squarks to neutralinos can readily be evaluated by inserting the squark mass eigenstate fields obtained by inverting (55) into the obvious generalization,

$$\mathcal{L} \left( \tilde{q}_{Lm} q_a \tilde{Z}_i \right) = \tilde{q}_{Lm}^\dagger \tilde{Z}_i \left[ i \left( \mathbf{A}_{\tilde{Z}_i}^q \right)_{ma} P_L - (i)^{\theta_i} (\tilde{\mathbf{f}}_q^Q)_{ma}^* v_q^{(i)} P_R \right] q_a + \text{h.c.} \quad (56a)$$

$$\mathcal{L} \left( \tilde{q}_{Rs} q_a \tilde{Z}_i \right) = \tilde{q}_{Rs}^\dagger \tilde{Z}_i \left[ i \left( \mathbf{B}_{\tilde{Z}_i}^q \right)_{sa} P_R - (-i)^{\theta_i} (\tilde{\mathbf{f}}_q^{QR})_{sa}^T v_q^{(i)} P_L \right] q_a + \text{h.c.} \quad (56b)$$

of the quark-squark-neutralino couplings in Ref. [4] that incorporates the fact that the matrix couplings  $\tilde{\mathbf{g}}$  and  $\tilde{\mathbf{f}}$  are generally different from the usual gauge and Yukawa couplings. Here, we have used  $(\tilde{\mathbf{f}}_q^{QR})_{sa}$ ,  $(\tilde{\mathbf{f}}_q^Q)_{ma}$  and  $v_q^{(i)}$  to signify  $(\tilde{\mathbf{f}}_u^{QR})_{sa}$ ,  $(\tilde{\mathbf{f}}_u^Q)_{ma}$  and  $v_1^{(i)}$  for  $q = u$ . We have the same form for the interactions of down quarks and squarks, but we must then remember to use  $v_q^{(i)} = v_2^{(i)}$ . The matrices  $\mathbf{A}_{\tilde{Z}_i}^q$  and  $\mathbf{B}_{\tilde{Z}_i}^q$  that appear in the couplings generalize to,

$$\left( \mathbf{A}_{\tilde{Z}_i}^u \right)_{ma} \equiv \frac{(-i)^{\theta_i-1}}{\sqrt{2}} \left[ (\tilde{\mathbf{g}}^Q)_{ma} v_3^{(i)} + \frac{(\tilde{\mathbf{g}}'^Q)_{ma}}{3} v_4^{(i)} \right] , \quad (57a)$$

$$\left( \mathbf{A}_{\tilde{Z}_i}^d \right)_{ma} \equiv \frac{(-i)^{\theta_i-1}}{\sqrt{2}} \left[ -(\tilde{\mathbf{g}}^Q)_{ma} v_3^{(i)} + \frac{(\tilde{\mathbf{g}}'^Q)_{ma}}{3} v_4^{(i)} \right] , \quad (57b)$$

$$\left( \mathbf{B}_{\tilde{Z}_i}^u \right)_{sa} \equiv \frac{4}{3\sqrt{2}} (\tilde{\mathbf{g}}'^{uR\dagger})_{sa} (i)^{\theta_i-1} v_4^{(i)} , \quad (57c)$$

$$\left( \mathbf{B}_{\tilde{Z}_i}^d \right)_{sa} \equiv -\frac{2}{3\sqrt{2}} (\tilde{\mathbf{g}}'^{dR\dagger})_{sa} (i)^{\theta_i-1} v_4^{(i)} , \quad (57d)$$



in direct correspondence with (8.87) of Ref. [4]. The Lagrangian for physical squarks then takes the form,

$$\mathcal{L} \left( \tilde{q}_\sigma^M q_a \tilde{Z}_i \right) \ni \tilde{q}_\sigma^{M\dagger} \tilde{Z}_i \left[ \left( \boldsymbol{\alpha}_{\tilde{Z}_i}^q \right)_{\sigma a} P_L + \left( \boldsymbol{\beta}_{\tilde{Z}_i}^q \right)_{\sigma a} P_R \right] q_a + \text{h.c.}, \quad (58)$$

with

$$\left( \boldsymbol{\alpha}_{\tilde{Z}_i}^u \right)_{\sigma a} \equiv i(\mathbf{U}_L)_{\sigma m}^\dagger \left( \mathbf{A}_{\tilde{Z}_i}^u \right)_{ma} - (-i)^{\theta_i} v_1^{(i)} (\mathbf{U}_R)_{\sigma s}^\dagger (\tilde{\mathbf{f}}_u^{u_R})_{sa}^T, \quad (59a)$$

$$\left( \boldsymbol{\beta}_{\tilde{Z}_i}^u \right)_{\sigma a} \equiv i(\mathbf{U}_R)_{\sigma s}^\dagger \left( \mathbf{B}_{\tilde{Z}_i}^u \right)_{sa} - (i)^{\theta_i} v_1^{(i)} (\mathbf{U}_L)_{\sigma m}^\dagger (\tilde{\mathbf{f}}_u^Q)_{ma}^*, \quad (59b)$$

$$\left( \boldsymbol{\alpha}_{\tilde{Z}_i}^d \right)_{\sigma a} \equiv i(\mathbf{D}_L)_{\sigma m}^\dagger \left( \mathbf{A}_{\tilde{Z}_i}^d \right)_{ma} - (-i)^{\theta_i} v_2^{(i)} (\mathbf{D}_R)_{\sigma s}^\dagger (\tilde{\mathbf{f}}_d^{d_R})_{sa}^T, \quad (59c)$$

$$\left( \boldsymbol{\beta}_{\tilde{Z}_i}^d \right)_{\sigma a} \equiv i(\mathbf{D}_R)_{\sigma s}^\dagger \left( \mathbf{B}_{\tilde{Z}_i}^d \right)_{sa} - (i)^{\theta_i} v_2^{(i)} (\mathbf{D}_L)_{\sigma m}^\dagger (\tilde{\mathbf{f}}_d^Q)_{ma}^*. \quad (59d)$$

Here, the  $(3 \times 6)$  matrices  $\mathbf{D}_L$  and  $\mathbf{D}_R$ , which enter via the diagonalization of the  $(6 \times 6)$  down squark mass matrix, are the exact analogues of the matrices  $\mathbf{U}_L$  and  $\mathbf{U}_R$  in (55). The partial width for the  $\tilde{q}_\sigma^M \rightarrow q_a \tilde{Z}_i$  can then be written as,

$$\begin{aligned} \Gamma(\tilde{q}_\sigma^M \rightarrow q_a \tilde{Z}_i) = & \frac{1}{16\pi M_{\tilde{q}_\sigma^M}^3} \left\{ \left( \left| \left( \boldsymbol{\alpha}_{\tilde{Z}_i}^q \right)_{\sigma a} \right|^2 + \left| \left( \boldsymbol{\beta}_{\tilde{Z}_i}^q \right)_{\sigma a} \right|^2 \right) \left( M_{\tilde{q}_\sigma^M}^2 - m_{q_a}^2 - m_{\tilde{Z}_i}^2 \right) \right. \\ & \left. - 2m_{q_a} m_{\tilde{Z}_i} \left[ \left( \boldsymbol{\alpha}_{\tilde{Z}_i}^q \right)_{\sigma a} \left( \boldsymbol{\beta}_{\tilde{Z}_i}^q \right)_{\sigma a}^* + \left( \boldsymbol{\beta}_{\tilde{Z}_i}^q \right)_{\sigma a} \left( \boldsymbol{\alpha}_{\tilde{Z}_i}^q \right)_{\sigma a}^* \right] \right\} \\ & \times \lambda^{1/2} \left( M_{\tilde{q}_\sigma^M}^2, m_{q_a}^2, m_{\tilde{Z}_i}^2 \right), \end{aligned} \quad (60)$$

with

$$\lambda(x, y, z) = x^2 + y^2 + z^2 - 2xy - 2xz - 2yz.$$

## B. Flavour-Violating Squark Decay

Formula (60) is very general and applies to two body decays of squarks to neutralinos for an arbitrary flavour structure of SSB parameters. We would expect that except, possibly, in the cases where we have non-vanishing values of  $\mathbf{T}_{Q,U,D}$  and/or  $\mathbf{Z}_{u,d}$  in (48), rates for flavour-conserving decays to neutralinos will overwhelm the corresponding flavour-violating decays. In many SUSY models, flavour-violating decays of squarks are thus phenomenologically relevant only when all flavour-conserving two-body decays are kinematically inaccessible. Because of the small values of down-type squark masses, this is unlikely to be the case for

down-type squarks. In other words, these flavour-violating decays are likely to be most relevant for  $\tilde{u}_1^M$ , the lightest of the up-type squarks. In many models — certainly in models where the SSB parameters are given by the ansatz (48) with modest values of  $R_\bullet$ ,  $S_\bullet$ ,  $W_\bullet$  and  $X_\bullet$ , and  $c_\bullet = 1$  — the lightest charge  $\frac{2}{3}$  squark is likely to be  $\tilde{t}_1$ , the lighter of the two squarks with the greatest top-squark content, and only small admixtures of  $\tilde{u}_{L,R}$  and  $\tilde{c}_{L,R}$ . In models where the superpotential Yukawa interactions are the *sole source* of flavour-violation, the decay  $\tilde{t}_1 \rightarrow c\tilde{Z}_1$  has a larger rate than  $\tilde{t}_1 \rightarrow u\tilde{Z}_1$  because of the structure of the Kobayashi-Maskawa matrix. It is for this reason that this decay has received considerable attention in the literature [41–44]. Although other squark mass patterns are certainly possible, we will focus our attention on the  $\tilde{t}_1 \rightarrow c\tilde{Z}_1$  decay for the remainder of this section, assuming that the lightest up-type squark  $\tilde{u}_1^M = \tilde{t}_1$  and that the decays  $\tilde{t}_1 \rightarrow t\tilde{Z}_1$  as well as  $\tilde{t}_1 \rightarrow b\tilde{W}_1$  are kinematically forbidden.

Before turning to numerical details, we qualitatively estimate the various contributions to the effective flavour-changing coupling that causes the decay  $\tilde{t}_1 \rightarrow c\tilde{Z}_1$ , beginning with inter-generational squark mixing. For obvious reasons, we will work in the basis that up-type quark Yukawas are diagonal at the weak scale. We see from the RGEs in Appendix B that (above all thresholds) the mixing among singlet up-type squarks occurs only via the Yukawa coupling matrix  $\mathbf{f}_u$ , and so vanishes (except for two-loop RGE effects) if the first and second generation up Yukawa couplings are neglected. Up-type singlet squarks can still, however, mix with doublet up-type squarks via the  $\mathbf{a}$ -parameters. In contrast, inter-generation up squark mixing between doublet up squarks can occur via *down*-type Yukawa coupling matrices (which are not diagonal) even if the first two generations have vanishing Yukawa couplings. Thus, in models where, in the standard current basis, up squark mass matrices are (essentially) diagonal at the high scale, the dominant contribution to the mixing occurs via mixing between  $\tilde{t}_L$  or  $\tilde{t}_R$  with  $\tilde{c}_L$ . Within mSUGRA (or similar models), if we assume  $\mathbf{a}_d \sim A_0\mathbf{f}_d$ , with  $A_0 \sim m_0$ , we can estimate that the weak scale value of

$$\left| (\mathbf{m}_Q^2)_{23} \right| \sim \frac{8}{16\pi^2} m_0^2 f_b^2 |\mathbf{K}_{23}| |\mathbf{K}_{33}| \log(M_{\text{GUT}}/M_{\text{weak}}),$$

which leads to a “mixing angle”  $\theta_{\tilde{c}_L\tilde{t}_L} \sim \left| (\mathbf{m}_Q^2)_{23} \right| / (\text{few} \times m_0^2) \sim \text{few} \times 10^{-4}$  [41]. With similar assumptions, the  $\tilde{t}_R - \tilde{c}_L$  mixing angle has a comparable magnitude which, however, scales with the  $A_d$ -parameter. Indeed, the mixing parameter that determines the decay rate is given to an excellent approximation in models with small flavour mixings among squarks,

by,

$$\epsilon = \frac{(\mathcal{M}_{\tilde{u}})_{23} \left(\mathbf{u}_L^\dagger\right)_{13} + (\mathcal{M})_{26} \left(\mathbf{u}_R^\dagger\right)_{13}}{m_{\tilde{t}_1}^2 - \mathcal{M}_{22}}, \quad (61)$$

where the elements  $\left(\mathbf{u}_L^\dagger\right)_{13}$  and  $\left(\mathbf{u}_R^\dagger\right)_{13}$  (which are just  $\cos \theta_t$  and  $-\sin \theta_t$  [4] in the absence of flavour-mixing) can be reliably estimated using the  $(2 \times 2)$  submatrix of the full up-squark mass matrix for the mixing between  $\tilde{t}_L$  and  $\tilde{t}_R$ . More generally,  $|\epsilon| = \left| \left(\mathbf{u}_L^\dagger\right)_{12} \right|$ .

How does this “mixing contribution” compare to the “direct contribution” from the induced  $\tilde{\mathbf{g}}$ -type couplings? A similar analysis to that of the previous paragraph shows that the dominant contribution once again arises via the  $\mathbf{f}_d$  and  $\tilde{\mathbf{f}}_d^q$ -type couplings.<sup>19</sup> The main difference is that because off-diagonal elements of  $\tilde{\mathbf{g}}$  arise only below the scale of the heaviest sparticle, the large logarithm  $\log(M_{\text{GUT}}/M_{\text{weak}})$  is absent. Moreover, the combinatorial factor of 8 in the previous paragraph is about unity so that these direct contributions are typically two orders of magnitude smaller in models where all sparticles are at the TeV scale. We can also check this from the magnitudes of the Yukawa couplings in Fig. 2, since the difference between these and the  $\tilde{\mathbf{f}}_d^q$  couplings is small. We have also checked that the value of the width calculated, ignoring the difference between the tilde couplings and the true couplings, differs from the full calculation by a few percent, as the reader may well expect.

### C. Single-step RGE integration and the stop decay rate

The decay rate for the  $\tilde{t}_1 \rightarrow c\tilde{Z}_1$  was first estimated by Hikasa and Kobayashi [41] who were considering squarks of around 30 GeV that might have been accessible at the TRISTAN collider. They used what is essentially the equivalent of (60), but estimated the size of the off-diagonal elements of the up-squark mass matrix that enter (61) by a single step integration of the RGEs. Working within the mSUGRA framework, and using the approximation that  $\tilde{Z}_1 \simeq \tilde{\gamma}$ , they showed that if tree-level two body decays of  $\tilde{t}_1$  were kinematically forbidden,  $\tilde{t}_1 \rightarrow c\tilde{Z}_1$  would be the dominant decay mode of  $\tilde{t}_1$ . While their approximations<sup>20</sup> and analysis are certainly valid for  $m_{\tilde{t}_1}$  values that they considered twenty years ago, this is not the case for top squark masses in the range of interest today.

<sup>19</sup> Just to be sure there is no confusion, we reiterate that in models with non-vanishing values for  $\mathbf{T}$  and  $\mathbf{Z}$  matrices, this need not be the case.

<sup>20</sup> Effects of general mixing in the neutralino sector are simple to include [42].

|   | Method                      | Width (GeV)              |
|---|-----------------------------|--------------------------|
| $\Gamma(\tilde{t}_1 \rightarrow bW\tilde{Z}_1)$ |                             | $8.6 \times 10^{-8}$     |
| $\Gamma(\tilde{t}_1 \rightarrow c\tilde{Z}_1)$  | “single-step” approximation | $\sim 41 \times 10^{-8}$ |
|   | full calculation            | $3.3 \times 10^{-8}$     |

TABLE II: Partial widths for the two- and three-body decays of the  $\tilde{t}_1$  within the mSUGRA framework, with  $m_0 = 250$  GeV,  $m_{1/2} = -250$  GeV,  $A_0 = -930$  GeV  $\tan\beta = 20$  and  $\mu < 0$ , for which the decays  $\tilde{t}_1 \rightarrow b\tilde{W}_1$  and  $\tilde{t}_1 \rightarrow t\tilde{Z}_1$  are kinematically forbidden. The result for the two-body decay is calculated using two methods, the single-step integration of the RGE (see text) commonly used in the literature, and the full integration of the RGEs.

For top squarks in the TRISTAN range analysed in Ref. [41], the competing tree-level decays are four-body decays (we assume here that the sneutrinos are heavier than  $\tilde{t}_1$ ) of  $\tilde{t}_1$ , which are both higher order in the couplings and suppressed by four-body phase space. However, for  $m_{\tilde{t}_1}$  in the range of interest today, the three body decay  $\tilde{t}_1 \rightarrow bW\tilde{Z}_1$  may well be kinematically accessible and could compete with the flavour-changing two body decay. It is with this in mind that we are led to re-visit the rate for  $\tilde{t}_1 \rightarrow c\tilde{Z}_1$ , but this time integrating the RGEs numerically to obtain the off-diagonal elements of the up-squark mass matrix, as opposed to obtaining this via a single-step integration as is common practice in the literature [43, 44].

To illustrate the need for integrating the RGEs we compare the rates for the flavour-conserving three-body decay of  $\tilde{t}_1$  with the flavour-violating  $\tilde{t}_1 \rightarrow c\tilde{Z}_1$  decay for the mSUGRA point  $m_0 = 250$  GeV,  $m_{1/2} = -250$  GeV,  $A_0 = -930$  GeV  $\tan\beta = 20$  and  $\mu < 0$  (where we have chosen a large value of  $|A_0|$  to obtain a light  $\tilde{t}_1$ ) in Table II. For this point,  $m_{\tilde{t}_1} \simeq 181$  GeV,  $m_{\tilde{Z}_1} = 102$  GeV,  $m_{\tilde{\nu}_\tau} = 270$  GeV and  $\tilde{W}_1 = 197$  GeV so that tree level two-body decays of the  $\tilde{t}_1$  as well as three-body decays,  $\tilde{t}_1 \rightarrow b\ell\tilde{\nu}_\ell$ , to sneutrinos are kinematically forbidden, but both the two-body loop decay that we are considering and the three-body decay to  $bW\tilde{Z}_1$  [44] are allowed. We show the two-body decay rate, both for the single-step estimate as well as with the full integration of the RGEs. We see from Table II that the single-step approximation over-estimates the decay rate by about a factor of 13.6,<sup>21</sup> and would lead us to conclude that the branching ratio  $B(\tilde{t}_1 \rightarrow c\tilde{Z}_1) \simeq 0.83$ ,

<sup>21</sup> Since  $\tilde{t}_1$  is mainly  $\tilde{t}_R$ , we evaluate the decay rate using parameters at a scale equal to the lightest right-

whereas the full calculation shows that  $B(\tilde{t}_1 \rightarrow bW\tilde{Z}_1) \simeq 0.72$ , completely changing the qualitative picture of top squark decays! Admittedly, this striking change is because we are close to the kinematic boundary for the  $\tilde{t}_1 \rightarrow bW\tilde{Z}_1$  decay. We have checked, however, that the single-step approximation over-estimates  $\Gamma(\tilde{t}_1 \rightarrow c\tilde{Z}_1)$  by a factor of  $\sim 10 - 25$  in mSUGRA models where the decay  $\tilde{t}_1 \rightarrow b\tilde{W}_1$  is kinematically forbidden, and where the LSP is the lightest neutralino. This may make the four-body decay modes of  $\tilde{t}_1$  more competitive than previously thought.

#### D. Model dependence of $\Gamma(\tilde{t}_1 \rightarrow c\tilde{Z}_1)$

The rate for flavour-violating squark decays will sensitively depend on whether the SSB parameters include genuinely new sources of flavour violation. To illustrate this, we return to our sample mSUGRA point from the previous section, namely  $m_0 = 200$  GeV,  $m_{1/2} = -400$  GeV,  $A_0 = -200$  GeV  $\tan\beta = 10$  and  $\mu > 0$ , and include non-zero values for  $\mathbf{T}_{Q,U,D}$  to obtain a variety of scenarios. We mention that the scenarios we examine are unrealistic from the perspective of observing flavour-violating  $\tilde{t}_1$  decays: indeed for this sample mSUGRA scenario, tree-level decays of  $\tilde{t}_1$  are accessible. Our purpose here is to understand how  $\Gamma(\tilde{t}_1 \rightarrow c\tilde{Z}_1)$  is altered (and also the quantities that it is sensitive to) as we alter the scenarios, to systematically allow increased non-universality and/or flavour violation in the SSB sector. Our results are shown in Table III, beginning with Scenario (1) which is the reference mSUGRA case. In mSUGRA, any dependence of the width on the matrices  $\mathbf{V}_{L,R}(u, d)$  enters only via the KM matrix.

1. In Scenario (2), we allow (a) non-universality by allowing  $\mathbf{T}_{U,D} \neq \mathbf{0}$  but diagonal in our standard current basis where up-type Yukawas are diagonal at  $m_t$ , while in (b) we allow  $\mathbf{T}_Q \neq \mathbf{0}$  and diagonal. The up-type squark matrices are (approximately) aligned with the up-quark Yukawa couplings so we do not expect large flavour-violating effects in up-squark decays in this case. Nevertheless, we do see changes of  $\mathcal{O}(1)$  from mSUGRA predictions. We emphasize that the situation would be quite different for flavour-violating decays of down-type squarks, since the down-squark matrix is now

---

handed squark threshold. We have checked that the partial width changes by  $\sim 6\%$  if instead we had calculated it using parameters evaluated at the highest right-squark threshold.

| Scenario |   | Width                              |                          |
|----------|---|------------------------------------|--------------------------|
| (1)      | mSUGRA — no dependence on specific $\mathbf{V}_{L,R}(u, d)$   | $2.2 \times 10^{-9}$ GeV           |                          |
| (2a)     | $\mathbf{V}_R(u) = \mathbf{V}_R(d) = \mathbf{V}_L(u) = \mathbf{1}$                                  | $\mathbf{T}_{U,D} \neq \mathbf{0}$ | $3.9 \times 10^{-9}$ GeV |
| (2b)     |   | $\mathbf{T}_Q \neq \mathbf{0}$     | $1.6 \times 10^{-9}$ GeV |
| (3a)     | $\mathbf{V}_L(u) \neq \mathbf{1}, \mathbf{V}_R(u) = \mathbf{V}_R(d) = \mathbf{1}$                   | $\mathbf{T}_{U,D} \neq \mathbf{0}$ | $3.9 \times 10^{-9}$ GeV |
| (3b)     |   | $\mathbf{T}_Q \neq \mathbf{0}$     | $2.7 \times 10^{-5}$ GeV |
| (4a)     | $\mathbf{V}_R(d) \neq \mathbf{1}, \mathbf{V}_R(u) = \mathbf{V}_L(u) = \mathbf{1}$                   | $\mathbf{T}_{U,D} \neq \mathbf{0}$ | $3.6 \times 10^{-9}$ GeV |
| (4b)     |   | $\mathbf{T}_Q \neq \mathbf{0}$     | $1.6 \times 10^{-9}$ GeV |
| (5a)     | $\mathbf{V}_R(u) \neq \mathbf{1}, \mathbf{V}_R(d) = \mathbf{V}_L(u) = \mathbf{1}$                   | $\mathbf{T}_{U,D} \neq \mathbf{0}$ | $5.8 \times 10^{-3}$ GeV |
| (5b)     |   | $\mathbf{T}_Q \neq \mathbf{0}$     | $1.6 \times 10^{-9}$ GeV |
| (6a)     | $\mathbf{V}_R(u) \neq \mathbf{1}, \mathbf{V}_R(d) \neq \mathbf{1}, \mathbf{V}_L(u) \neq \mathbf{1}$ | $\mathbf{T}_{U,D} \neq \mathbf{0}$ | $5.8 \times 10^{-3}$ GeV |
| (6b)     |   | $\mathbf{T}_Q \neq \mathbf{0}$     | $2.7 \times 10^{-5}$ GeV |

TABLE III: A comparison of the two-body loop decay widths for six scenarios. For each scenario we list the basis used for our GUT scale inputs, with rotation matrices as specified by (51) in the text. In case (a) of each scenario, we take  $\mathbf{T}_Q = \mathbf{0}$  and  $\mathbf{T}_{U,D} = \text{diag}\{10000, 40000, 90000\}$  GeV<sup>2</sup>. In case (b),  $\mathbf{T}_{U,D} = \mathbf{0}$  and  $\mathbf{T}_Q = \text{diag}\{10000, 40000, 90000\}$  GeV<sup>2</sup>. When  $\mathbf{T}_{Q,U,D} \neq \mathbf{0}$ , the corresponding  $m_{\{Q,U,D\}0}^2 = 0$ . Here,  $\mathbf{V}_{L,R}(u, d)$  are the matrices needed to transform from the current basis in which the matrices  $\mathbf{T}_U$ ,  $\mathbf{T}_D$  or  $\mathbf{T}_Q$  are diagonal at  $Q = M_{\text{GUT}}$  to the basis where the up or the down quark Yukawa coupling matrices are diagonal at the weak scale. We have checked that  $m_{\tilde{t}_1}$  is constant to within about 5% across the Table, so its contribution to the variation of the partial width is small.

not aligned with the corresponding Yukawa coupling matrix.

2. This is exemplified in Scenario (3b) where the mass matrix for left type up squarks is completely unaligned with the up Yukawa couplings. Not surprisingly, this leads to a very large increase in the rate for the flavour-violating decay of  $\tilde{t}_1$ . In contrast, the width for this decay in Scenario (3a) coincides with that in (2a) because  $\mathbf{m}_U^2$  is unchanged when we transform to our standard basis, so that scenarios (2a) and (3a) are really identical.

3. In Scenario (4), the rotation matrices used mean that the boundary condition for Scenario (4a), the  $\mathbf{T}_{U,D} \neq \mathbf{0}$  case, differs from scenario (2a) only in the boundary condition for  $\mathbf{m}_D^2$  which, in turn, affects the running of the  $\mathbf{m}_{Q,U}^2$  matrices to a small extent through the RGEs. As a result, we see that the width is different from the other scenarios by a few percent. On the other hand, the boundary condition on  $\mathbf{m}_Q^2$  is not dependent on  $\mathbf{V}_R(d)$  so that scenarios (2b) and (4b) are identical, and the width is, therefore, the same in the two cases.
4. In Scenario (5a), the matrix  $\mathbf{m}_U^2$  is unaligned with  $\mathbf{f}_u$  resulting in a large flavour mixing among *singlet* up squarks in our standard basis, and a concomitantly large rate for the flavour-violating decay. It is only in this scenario that  $\tilde{t}_R - \tilde{c}_R$  mixing is the dominant source of the flavour-violation, since in all the other scenarios that we have considered up to now, this mixing was suppressed by the small size of the charm quark Yukawa coupling. The corresponding partial width is larger than in the other scenarios because  $\tilde{t}_1$  is still dominantly  $\tilde{t}_R$  as can be seen from Fig. 10. (See also the discussion in the vicinity of this figure.) Although one might expect significant contributions to (59) from off-diagonal entries in the higgsino and gaugino ‘Yukawa’ matrices, we have checked that the contribution from the  $(\mathbf{u}_R)_{\tilde{t}_1 2}^\dagger \left( \mathbf{B}_{\tilde{Z}_1}^u \right)_{22}$  term is still two orders of magnitude larger than any other entry in (59). In contrast, Scenario (5b) shows no change from (2b), because the boundary condition is exactly the same in the two cases.
5. Finally, the boundary condition for  $\mathbf{m}_D^2$  is the only difference between Scenarios (5a) and (6a). Since  $\mathbf{m}_D^2$  only affects the decay rate via its effect on  $\mathbf{m}_{U,Q}^2$  (see item 3. above), the change that it causes is too small to be seen in the Table for this case where the flavour-changing partial width is so large. Scenarios (6b) and (3b) coincide because the GUT scale boundary conditions coincide since  $\mathbf{m}_U^2$  and  $\mathbf{m}_D^2$  are unit matrices, and so unaffected by any rotations.

In our pedagogical examples in Table III, we considered the case with very large GUT scale splitting in the squark mass matrices which are likely excluded, especially when the squark mass matrices and the corresponding Yukawa couplings are unaligned. However, flavour-violation effects can be large even for very small GUT scale splitting in the squark mass matrices. We illustrate this for the compressed SUSY scenario, proposed by Martin [45]

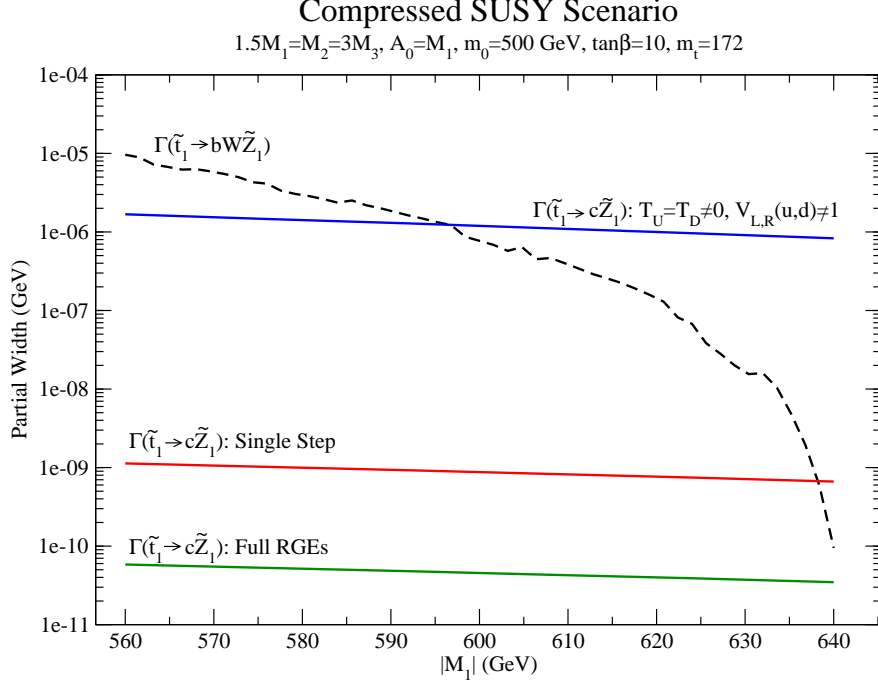


FIG. 11: Comparison of the partial width of the three-body tree level decay of the stop with the two-body loop decay in the compressed SUSY scenario discussed in the text. The dashed (black) line shows the partial width for the three-body decay  $\tilde{t}_1 \rightarrow bW\tilde{Z}_1$  while the other lines represent calculations of rates for  $\tilde{t}_1 \rightarrow c\tilde{Z}_1$  decay. For the red line in the range  $10^{-9}$  we use the single-step RGE integration, the green line around  $10^{-10}$  is the full calculation and the upper line in the range  $10^{-6}$  shows the enhancement as a result of taking  $\mathbf{T}_{U,D} = \text{diag}\{498^2, 500^2, 502^2\} \text{ GeV}^2$  in the general basis using (51).

where efficient neutralino annihilation to top pairs via the exchange of a light squark leads to the observed cold dark matter relic density. We use mSUGRA-like GUT scale inputs, where  $m_0 = 500 \text{ GeV}$ ,  $A_0 = M_1$ ,  $\tan\beta = 10$  and  $\mu > 0$ , but the gaugino masses are split so that  $1.5M_1 = M_2 = 3M_3$ , with  $\mathbf{m}_{U,D}^2 = \text{diag}\{498^2, 500^2, 502^2\} \text{ GeV}^2$  at  $Q = M_{\text{GUT}}$ . We show the partial widths for the three body and the flavour-violating two body decays of  $\tilde{t}_1$  as a function of  $|M_1|$  in Fig. 11. Over the whole of this region the two-body flavour-conserving decays of  $\tilde{t}_1$  as well as its decays to sneutrinos are kinematically forbidden, but the three-body decay  $\tilde{t}_1 \rightarrow bW\tilde{Z}_1$  is allowed until its kinematic boundary at  $|M_1| \sim 640 \text{ GeV}$ . The (black) dashed line in the figure shows the partial width for this three-body decay. The partial width for the two-body decay, for the case of universal GUT scale masses, calculated using the single-step approximation is in the range  $10^{-9} \text{ GeV}$  and competes with the three-



body decay near the extreme edge of phase space. However, the corresponding result of our complete calculation is essentially always smaller than the width for the three-body decay, although it may compete with the four-body decay rate of  $\tilde{t}_1$  at large  $|M_1|$  [43].

The highest horizontal line in Fig. 11 shows the result of the complete calculation of  $\Gamma(\tilde{t}_1 \rightarrow c\tilde{Z}_1)$  for a non-universal model with  $\mathbf{T}_{U,D} = \text{diag}\{498^2, 500^2, 502^2\}$  (in the general basis of (51)) and  $c_{U,D} = 0$ . We see that despite the very small splitting between diagonal entries of the squark mass matrices at  $Q = M_{\text{GUT}}$ , the rate for the flavour-violating two body decay is enhanced by three orders of magnitude, and can be competitive with the rate for the decay  $\tilde{t}_1 \rightarrow bW\tilde{Z}_1$ . We also mention that if we take this same splitting, but use  $\mathbf{V}_R(u, d) = \mathbf{V}_L(u) = \mathbf{1}$ , we recover the result with no splitting to within around 4%.

Our discussion of flavour-violating squark decays in this section has revolved around the introduction of flavour-violation via a completely arbitrary choice of the  $\mathbf{T}_{U,D,Q}$  matrices in (48). It has been suggested that flavour-violation can be introduced into the theory in a controlled way through the minimal flavour violation (MFV) ansatz [36]. The general idea stems from the observation that, except for Yukawa couplings, the Lagrangian of the Standard Model is invariant under *independent* rotations in flavour space of the electroweak singlet up-type, singlet down-type, and the doublet quarks (along with independent rotations among the singlet, and also doublet, lepton flavours). If we regard the Yukawa couplings as spurion fields, and assume that *these are the only source of flavour-violation* even in extensions of the SM, we obtain the MFV ansatz.

In the case of the MSSM, since  $\mathbf{m}_{U,D}^2$  and  $(\mathbf{f}_{u,d}^T \mathbf{f}_{u,d}^*)^n$  transform the same way under the flavour rotations just discussed, as do  $\mathbf{m}_Q^2$  and  $(\mathbf{f}_{u,d}^* \mathbf{f}_{u,d}^T)^n$ , it is easy to see that  $\mathbf{m}_{U,D}^2$  must take the same form (48b) with  $\mathbf{T}_{U,D} = \mathbf{0}$ . In contrast, for the doublet squark SSB mass matrix we would have,

$$\mathbf{m}_Q^2 = m_{Q0}^2 [\mathbf{1} + t_u \mathbf{f}_u^* \mathbf{f}_u^T + t_d \mathbf{f}_d^* \mathbf{f}_d^T + \dots] , \quad (62)$$

where the ellipses denote quartic and higher terms of the form,  $(\mathbf{f}_{u,d}^* \mathbf{f}_{u,d}^T)^2$ ,  $(\mathbf{f}_u^* \mathbf{f}_u^T) (\mathbf{f}_d^* \mathbf{f}_d^T)$  and  $(\mathbf{f}_d^* \mathbf{f}_d^T) (\mathbf{f}_u^* \mathbf{f}_u^T)$ , *etc.* A similar analysis shows that,

$$\mathbf{a}_u = \mathbf{f}_u \left[ A_{u0} \mathbf{1} + \alpha_{u1} \mathbf{f}_u^\dagger \mathbf{f}_u + \beta_{u1} \mathbf{f}_d^\dagger \mathbf{f}_d + \dots \right] , \quad (63)$$

where the ellipses denote higher powers of  $\mathbf{f}_{u,d}^\dagger \mathbf{f}_{u,d}$ . A similar formula applies for  $\mathbf{a}_d$ . MFV also enters the slepton sector in an analogous manner.

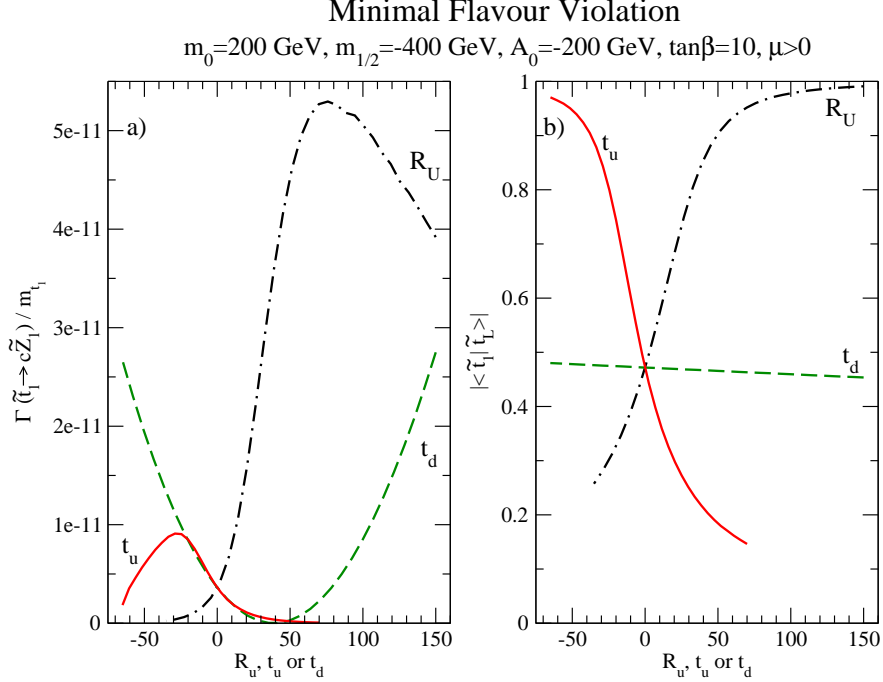


FIG. 12: *a*) Variation of  $\Gamma(\tilde{t}_1 \rightarrow c\tilde{Z}_1)/m_{\tilde{t}_1}$  with MFV parameters  $R_U$  (dot-dashed),  $t_u$  (solid) and  $t_d$  (dashed) that determine the form of the squark mass matrices as described in the text. We introduce flavour-violation into the mSUGRA model with our canonical choice of parameters shown on the figure. For each curve, only the one MFV parameter labelling that curve has a non-zero value. *b*) The variation of  $|\langle \tilde{t}_1 | \tilde{t}_L \rangle|$ , the  $\tilde{t}_L$  content in the lightest top squark, which would equal to  $|\cos \theta_t|$  in the absence of any inter-generational mixing.

It is interesting to examine how  $\Gamma(\tilde{t}_1 \rightarrow c\tilde{Z}_1)$  is affected if instead of choosing *ad hoc* values of  $\mathbf{T}_{U,D,Q}$  as we did above, we choose these according to the MFV ansatz. Toward this end, we once again start with our canonical mSUGRA point, and study how this width varies as we switch on non-vanishing values for the MFV parameters. Since our purpose is only to illustrate this variation, we restrict ourselves to varying only the parameters that enter the squark mass matrices, and leave  $\mathbf{a}_\bullet$ -matrices at their mSUGRA values. The variation of  $\Gamma(\tilde{t}_1 \rightarrow c\tilde{Z}_1)/m_{\tilde{t}_1}$  with  $R_u$ ,  $t_u$  and  $t_d$  is shown in Fig. 12*a*. The reader may be surprised by the large variation of the ratio (which removes the trivial growth of the width with  $m_{\tilde{t}_1}$ ) from the variation in  $R_U$  since we have emphasized that the SSB parameters *do not introduce any flavour violation in this case*. To understand this, we have shown the top-squark “mixing angle”  $|\langle \tilde{t}_1 | \tilde{t}_L \rangle|$  in frame *b*). Since inter-generation mixing is very small,  $\tilde{t}_1$  is dominantly  $\tilde{t}_L$  and  $\tilde{t}_R$ , with tiny admixtures of other squarks. We see that the partial width roughly tracks

this mixing angle which is a reflection of the fact that for these parameters, the  $\tilde{t}_L - \tilde{c}_L$  mixing term is considerably larger than the  $\tilde{c}_L - \tilde{t}_R$  mixing term (see the discussion near (61)). The fall-off in the width toward the right end of the dot-dashed curve is because the splitting between  $m_{\tilde{t}_1}^2$  and the (2,2) element of  $\mathcal{M}_{LL}^2$  increases, leading to a suppression of  $\epsilon$ .

Flavour violation truly enters via the SSB parameters for non-zero values of  $t_u$  and  $t_d$ . For the  $t_u \neq 0$  case, the flavour-violating effects in the up-squark/quark sector will be small because the up quark Yukawa coupling matrix  $\mathbf{f}_u$  is not-very-off diagonal (since its off-diagonal entries arise only from the evolution to the GUT scale) and so is approximately aligned with the  $\mathbf{m}_Q^2$  matrix at  $Q = M_{\text{GUT}}$ .<sup>22</sup> The variation of the branching fraction in the solid curve with  $t_u$  largely tracks the intra-generation  $t$ -squark mixing, just as in the  $R_U$  case discussed in the last paragraph. The solid curve in the left frame turns over because the GUT scale value of  $(\mathbf{m}_U^2)_{33}$ , and hence  $m_{\tilde{t}_1}^2$ , reduces so as to suppress  $\epsilon$ .

We have argued that the variation of the partial width for the  $\tilde{t} \rightarrow c\tilde{Z}_1$  decay for the dot-dashed and solid curves in the figure mostly tracks intra-generation  $t$ -squark mixing and does not derive from large flavour violation of the SSB parameters. This is sharply different from the result for the  $t_d \neq 0$  case, shown by the dashed curve in the figure, where  $\mathbf{m}_Q^2$  receives relatively large off-diagonal contributions from the term involving the down Yukawa coupling matrix (which is *not diagonal* even at  $Q = m_t$ ) in (62). Unlike the other two cases where the large top Yukawa coupling significantly affects the (3,3) entry of either  $\mathcal{M}_{RR}$  or  $\mathcal{M}_{LL}$ , in this case the  $\tilde{t}_1$  mass and the intra-generational mixing are both essentially constant for the entire range of  $t_d$  in the figure, and the variation of the width is truly the effect of the additional flavour-violation. This is why the width continues to grow for very large values of  $|t_d|$ . The reason for the drop in the width for intermediate positive values of  $t_d$  is an accidental cancellation between the two contributions to  $\epsilon$  in (61).

Before closing this section, we remark that the width for flavour-violating decay of  $\tilde{t}_1$  is very sensitive to the parameters  $R_U$ ,  $t_u$  and  $t_d$ . Even for values of these parameters  $\sim 1 - 10$ , the change in the width from its mSUGRA value is  $\mathcal{O}(10-100)\%$ , and much larger if these parameters take on large values (though this may be constrained by low energy data). This

---

<sup>22</sup> We would, however, expect larger flavour-violation in the down type sector, since the down-type Yukawa matrix is not similarly aligned, and because the top Yukawa coupling is larger.

is a reflection of the sensitivity of flavour physics predictions to small changes in the model which would have little impact on the usually studied collider signals for supersymmetry. The flip side of this is that we must view any restriction of parameter regions from low energy constraints from flavour physics in proper perspective, since these will almost surely be sensitive to the underlying flavour structure that has a negligible effect on direct searches for SUSY, either at colliders or via dark matter detection experiments.

## VII. SUMMARY

Renormalization group methods allow us to extract predictions from theories with simple physical principles operating at energy scales many orders of magnitude larger than the highest energies accessible in experiments. Due to effects arising from renormalization, these same simple principles lead to a complex pattern of predictions at experimentally accessible energies. RGEs have played a central role in the analysis of many supersymmetric models, generally assumed to reduce to the MSSM (quite likely augmented by right-handed neutrino superfields, and perhaps also additional Higgs singlets) at energy scales in between the weak scale and the GUT or Planck scales, where almost certainly additional new physics would be anticipated.

This is the second and last of a series of two papers where we have reexamined the RGEs for the MSSM including threshold corrections to the one-loop RGEs (which are comparable to or larger than the usually included two-loop effects) along with flavour effects that arise below the scale of supersymmetry breaking. In Paper I [14], where we studied the scale-dependence of the dimensionless couplings of the MSSM, we showed that we have to extend the system of RGEs to include, in addition to the usually studied RGEs for gauge couplings and Yukawa coupling matrices, RGEs for the couplings of gauginos and higgsinos to matter fermions and their superpartners. Not only do these couplings evolve independently of their supersymmetric analogues below the scale of the highest SUSY threshold where SUSY-breaking effects come into play, the gaugino-fermion-sfermion coupling is also no longer flavour-independent (since it is no longer protected from feeling flavour-breaking effects below the scale of SUSY breaking) and so develops into a matrix in flavour-space. In this paper, we complete this program by extending the analysis of Paper I to the RGEs for the dimensionful parameters of the MSSM.

Toward this end, we have first adapted the RGEs for the dimensionful parameters of a general (*i.e.* non-supersymmetric) gauge field theory [22] that includes interactions of two-component spinor and real scalar fields with one another and with gauge fields, and written these in a form suitable for the derivation of the RGEs for the parameters of the theory with four-component Dirac and Majorana spinors, together with real or complex scalar fields that we find more convenient for our analysis. We use non-supersymmetric methods because we want to include threshold corrections which, of course, break supersymmetry. The details of our method (including some minor corrections to the RGEs in the literature) along with our results for the RGEs for the dimensionful parameters for a non-supersymmetric (albeit not completely general) field theory are found in Sec II. Our procedure for decoupling heavy particles, which is essentially the same as in Paper I, is described in Sec. III with particular attention to some complications that arise when decoupling Higgs bosons, and especially squarks. In Sec. IV, we use these general equations to derive the RGEs for the dimensionful parameters of the MSSM. The complete set of RGEs is listed in Appendix B.

In Sec. V we discuss examples of numerical solutions to the MSSM RGEs for  $\mu$  and the dimensionful SSB parameters, focussing on flavour-violation and threshold correction effects, including a discussion of new technical complications that arise in the treatment of radiative EWSB. We have also presented the most general parametrization of high scale SSB parameters valid assuming that the physics of SUSY breaking is flavour-blind. Unlike in Paper I, where SUSY model-dependence of the dimensionless couplings arises only via the location of the sparticle thresholds, the dimensionful parameters show considerable dependence on the underlying model. For instance, even if the gaugino mass parameters all originate in a common parameter  $m_{1/2}$ , as is the case in all SUSY GUT models where the SUSY-breaking VEV does not also break the GUT symmetry, the resulting gaugino unification condition,

$$\frac{M_2}{M_1} = \frac{\alpha_2}{\alpha_1},$$

receives threshold corrections  $\sim 10\%$  if the scale of SUSY scalars is around  $10^7$  GeV, with gaugino and higgsino masses at the TeV scale. In Fig. 5 – Fig. 9, we show illustrative examples of the scale dependence of trilinear scalar coupling and SSB squark mass matrices, both for mSUGRA as well as for non-universal models where high scale SSB parameters *do not include* a new source of flavour-violation, while in Fig. 10 we show the elements of the singlet squark matrices  $\mathbf{m}_U^2$  and  $\mathbf{m}_D^2$  for a scenario where a large — indeed phenomenologically

unrealistic — flavour-violation is introduced via GUT scale squark mass matrices.

In Sec. VI we apply the results that we have obtained in this paper to the examination of flavour-violating decays of squarks. Since flavour-conserving couplings of squarks to neutralinos are presumably much larger than the corresponding flavour-violating couplings, the branching fraction for flavour-violating squark decays is likely to be small, unless the two body decays of squarks to neutralinos (or charginos) and quarks of the same generation are all kinematically forbidden. With this in mind, we re-visit the decay  $\tilde{t}_1 \rightarrow c\tilde{Z}_1$  that has received the most attention in the literature. In this connection, we find that within the mSUGRA model (where this decay has been most extensively studied) the commonly-used “single-step” approximation to obtain the flavour-violating  $\tilde{t}_1\tilde{Z}_1c$  coupling typically over-estimates the decay rate by a factor of 10-25, and could lead to a qualitatively wrong picture for event-topologies from top-squark pair production for  $m_{\tilde{t}_1} \sim 100 - 300$  GeV. We have also examined the rate for this decay in a number of non-universal scenarios for SSB parameters, with and without flavour-violation. We then saw that the decay rate is sensitive to the individual matrices  $\mathbf{V}_{L,R}(u, d)$  that enter via the diagonalization of the Yukawa coupling matrices, and not just to the KM matrix. Indeed, this dependence of physics on the separate matrices is the generic situation, while the dependence of physics on just the KM combination of these that we have become used to from studies within the SM or the mSUGRA frameworks, is true only in very special situations: see Table III.<sup>23</sup> We have also examined this decay rate in models with non-universal SSB parameters but no new source of flavour-violation, or where flavour violation is introduced in a controlled way via the so-called “minimal flavour violation” ansatz. Interestingly, as shown in Fig. 12, the decay rate changes by a qualitatively similar magnitude as we vary the model parameters, in both classes of models. The reason for this is that the variation of the width due to changes in the (flavour-conserving)  $\tilde{t}_L - \tilde{t}_R$  mixing is comparable to the true flavour-violating contributions to this decay rate in MFV scenarios. A determination of the left-right mixing in the  $t$ -squark sector (which will be difficult at the LHC [46] but possible at an  $e^+e^-$  collider with sufficient centre-of-mass energy [47]) should allow us to readily distinguish between the scenarios.

To sum up, in this series of two papers, we have presented the RGEs for the, in gen-

---

<sup>23</sup> Although this is well-known to many authors, we stress this here because there has been occasional confusion about this issue. For a different example, see p. 215 of Ref. [4].

eral, complex parameters of the MSSM including one-loop threshold effects (necessary for two-loop accuracy) as well as flavour-mixing effects. The complete set of RGEs is listed in the Appendices of these two papers, and will facilitate the examination of the flavour phenomenology in SUSY models with arbitrary ansätze for flavour violation via the Yukawa coupling matrices, as well as via the SSB sector.

### Acknowledgments

We are grateful to H. Baer, D. Castaño, V. Cirigliano, A. Dedes, S. Martin, K. Melnikov, A. Mustafayev and M. Vaughn for clarifying communications and discussions. We thank A. Mustafayev for his comments on the manuscript. This research was supported in part by a grant from the United States Department of Energy.

## Appendix A: Numerical Instabilities Associated with Matrix Diagonalization

### 1. The problem

We have emphasized that in order to properly implement particle decoupling into the RGEs, we have to be in the mass basis of the particles being decoupled. Our procedure for decoupling squarks, therefore, requires us to evaluate the unitary transformation from the given current basis to a new current basis that coincides with the squark mass basis (approximated, as discussed in the main text, to be the basis in which the SSB squark mass squared matrices are diagonal). Below the scale  $Q$  where at least one squark has decoupled, we not only have the rotations  $\mathbf{V}_{L,R}(u, d)$  (unitary matrices by construction) which connect the current basis with the basis in which the Yukawas are diagonal at  $m_t$ , but also the squark rotations  $\mathbf{R}_\bullet$  which connect the current basis to the “squark mass basis” that are obtained by numerically diagonalizing the SSB matrices  $\mathbf{m}_\bullet^2$ .  $\mathbf{R}_\bullet$  is of course the matrix of the orthogonal eigenvectors of  $\mathbf{m}_\bullet^2$ . If there is a degeneracy of eigenvalues, the orthogonal eigenvectors are not uniquely defined. This leads to a practical problem when we *numerically* solve for the eigenvectors in the case that two eigenvalues of any SSB squark mass matrix with large off-diagonal components are degenerate to within  $\sim 1\%$ . In this case, the corresponding eigenvectors, because of (system-dependent) numerical errors are not exactly orthogonal,

and the corresponding matrix  $\mathbf{R}_\bullet$  is not precisely unitary.<sup>24</sup>

The deviation from unitarity is very small, a part in  $10^{10}$  in our case, but is nonetheless orders of magnitude larger than what we can tolerate when calculating the smallest off-diagonal elements of  $\mathbf{m}_\bullet^2$ . To understand why our calculation is sensitive to this seemingly tiny level of noise, let us imagine what would happen if we attempted to evolve the off-diagonal elements of  $\mathbf{m}_U^2$  from  $Q = M_{\text{GUT}}$  in a basis where the Yukawa coupling matrices all have large off-diagonal elements at the GUT scale. (This is not what we actually do, but we could imagine doing so since we know that we are well above all SUSY and Higgs field thresholds where the choice of basis should be irrelevant.) In the mSUGRA framework, the squark mass matrices are all given by  $\mathbf{m}_\bullet^2 = m_0^2 \mathbf{1}$  at  $Q = M_{\text{GUT}}$  in any basis. Then, from (B17) we see that these would develop off-diagonal components  $\sim \text{few} \times f^2 \times m_0^2 \simeq f^2 \times 4 \times 10^4$  for the case shown in Fig. 7, where  $f^2$  denotes the size of the off-diagonal element of  $\mathbf{f}_u^T \mathbf{f}_u^*$ . In this rough estimate we have assumed that the loop factor  $1/(16\pi^2)$  is compensated for by the large logarithm. In the general current basis where  $\mathbf{f}_u$  has comparable off-diagonal and diagonal elements,  $f^2 \sim 1$ , and the magnitude of the off-diagonal elements of  $\mathbf{m}_U^2$  are  $\mathcal{O}(10^4)$  GeV<sup>2</sup>. Rotating to our standard current basis should yield the result in Fig. 7. In particular, we should obtain  $|\mathbf{m}_U^2|_{12} \sim 10^{-9}$  GeV<sup>2</sup> because there would be large cancellations arising from the unitarity of  $\mathbf{R}_U$  that would suppress this matrix element. If instead the unitarity of  $\mathbf{R}$  holds only to a part in  $10^{10}$  because of numerical errors in obtaining the eigenvectors, we will find that because the cancellations are not perfect all off-diagonal elements of  $\mathbf{m}_U^2$  will have a magnitude that is at least  $\text{few} \times 100^2 \times 10^{-10} \sim \text{few} \times 10^{-6}$  GeV<sup>2</sup>, much larger than the magnitude of the (1,2) element in Fig. 7. We note here that the noise that leads to the non-unitarity of  $\mathbf{V}_{L,R}(u, d)$  matrices at the  $10^{-18}$  level is completely irrelevant.

---

<sup>24</sup> Using the g77 FORTRAN compiler with Macintosh Intel Macbook, together with the subroutine CG in the EISPACK collection of subroutines, we found that  $\mathbf{R}_\bullet^\dagger \mathbf{R}_\bullet$  deviated from  $\mathbf{1}$  to about one part in  $10^{10}$  compared to a part in  $10^{18}$  for  $\mathbf{V}_{L,R}(u, d)^\dagger \mathbf{V}_{L,R}(u, d)$  for  $\mathbf{V}_{L,R}(u, d)$  of the form (50). We obtain a similar size deviation from identity using the subroutine ZGEEV in the LAPACK collection of subroutines



## 2. The solution

The non-unitarity of  $\mathbf{R}_\bullet$  is only an issue when the off-diagonal entries of the squark mass matrix, in the basis where the Yukawas are diagonal at  $m_t$ , are small compared to the diagonal entries. Since we, therefore, only need to consider matrices that are already approximately diagonal, we can associate the eigenvectors,  $(\mathbf{e}_1, \mathbf{e}_2, \mathbf{e}_3)$ , with the approximate eigenvalues  $((\mathbf{m}_\bullet^2)_{11}, (\mathbf{m}_\bullet^2)_{22}, (\mathbf{m}_\bullet^2)_{33})$ , respectively. As an illustration, let us take a case where the  $(\mathbf{m}_\bullet^2)_{23}$  entry is the off-diagonal entry with the largest magnitude, and  $(\mathbf{m}_\bullet^2)_{12}$  the one with the smallest. We know the ordering quite unambiguously because above all squark thresholds we do not need to rotate by the matrices  $\mathbf{R}_\bullet$  that potentially are the origin of the noise. We need to ensure that the  $(\mathbf{m}_\bullet^2)_{12}$  entry does not suffer from any numerical noise due to the diagonalisation. This leads us to fix  $\mathbf{e}_1 \cdot \mathbf{e}_2 = 0$  and move any non-orthogonality of the eigenvectors into  $\mathbf{e}_2 \cdot \mathbf{e}_3$  so that the noise moves to  $(\mathbf{m}_\bullet^2)_{23}$ , the off-diagonal element with the largest magnitude. To accomplish this, we slightly modify (by parts in  $10^{10}$ , the limit of accuracy of the diagonalization routines) *only* the eigenvector  $\mathbf{e}_2$  from its value as given by the diagonalization routines, thereby leaving  $\mathbf{e}_1 \cdot \mathbf{e}_3$  unaffected.

To completely clarify what we have just described, although (as we have already stated) we do not need to rotate to the squark mass basis until we reach the highest squark threshold, we plot, in Fig. 13, the result for  $|\mathbf{m}_U^2|_{12}$  obtained by the two different methods mentioned above, in the basis where the up-type Yukawas are diagonal at  $m_t$ , over the whole range  $M_Z < Q < M_{\text{GUT}}$ . The dashed (black) line shows the result where we have no rotation by  $\mathbf{R}_U$  from  $Q = M_{\text{GUT}}$  until the highest squark threshold, beyond which we implement our method for ensuring that the error from the non-orthogonality of the eigenvectors of  $\mathbf{m}_U^2$  only shows up in the (2,3) element. Indeed we see that this curve is smooth over its entire range of  $Q$ . The solid (red) line shows the result of carrying out the squark rotation without our fix of the eigenvectors over the entire range of  $Q$ . Note that there is significant noise all the way down to the low  $Q$  region where only some of the squarks have decoupled. This noise is largest at  $Q = M_{\text{GUT}}$  where the eigenvalues of  $\mathbf{m}_U^2$  are degenerate, and settles down to  $10^{-5} \text{ GeV}^2$ , not far from our estimate above. The important thing is that the frozen value of this element is significantly different in the two cases, as a result of this noise, just before squark decoupling. It is for this range of  $Q$  (where the mass matrices that enter flavour-changing processes involving squarks will be evaluated) that we must

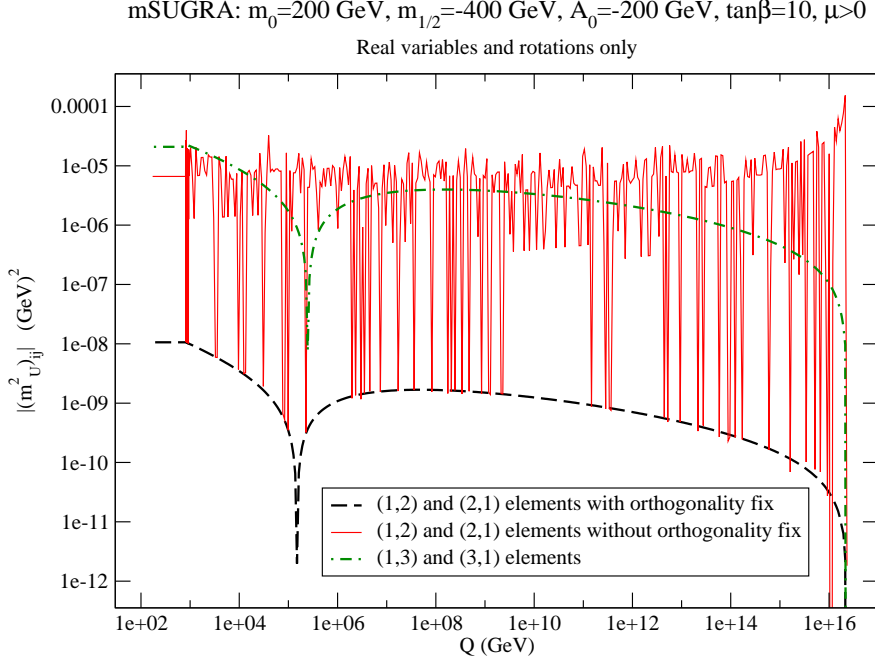


FIG. 13: The scale-dependence of the (1,2) element of the Hermitian  $\mathbf{m}_U^2$  matrix for our sample mSUGRA point (in the basis specified by (51)) calculated using two different procedures discussed in the text. The dashed (black) line shows the magnitude of the smallest element, *i.e.*  $|(\mathbf{m}_U^2)_{12}| = |(\mathbf{m}_U^2)_{21}|$ , when we have used our procedure to ensure that the corresponding eigenvectors are orthogonal. The solid (red) line shows the same element when we do not pay attention to the orthogonality of the eigenvectors of  $\mathbf{m}_U^2$ . The lighter dot-dashed (green) line shows the magnitude of the (1,3) element, and provides a scale for the size of the numerical noise discussed in the text. The noise in this curve is too small to be visible. All elements are zero at the GUT scale.

reduce the numerical error as far as possible. The magnitude of the (1,3) element of  $\mathbf{m}_U^2$  is shown for comparison by the dot-dashed (green) curve. It has no visible noise because the corresponding eigenvalues are sufficiently split, and the corresponding eigenvectors are orthogonal to a very high accuracy.

The reader will be struck by the fact that the random downward fluctuations in the solid curve are roughly bounded by the dashed (black) curve which shows the correct magnitude of the matrix element. The reason for this is that the *fluctuations* whose typical magnitude is  $\sim 10^{-5}$  GeV<sup>2</sup> need to *randomly* fluctuate down by four orders of magnitude to even reach the dashed (black) line, and even more to go below, the chance for which is very small. Indeed it is because we have shown results for the case where the SSB squark mass matrices

mSUGRA:  $m_0=200$  GeV,  $m_{1/2}=-400$  GeV,  $A_0=-200$  GeV,  $\tan\beta=10$ ,  $\mu>0$

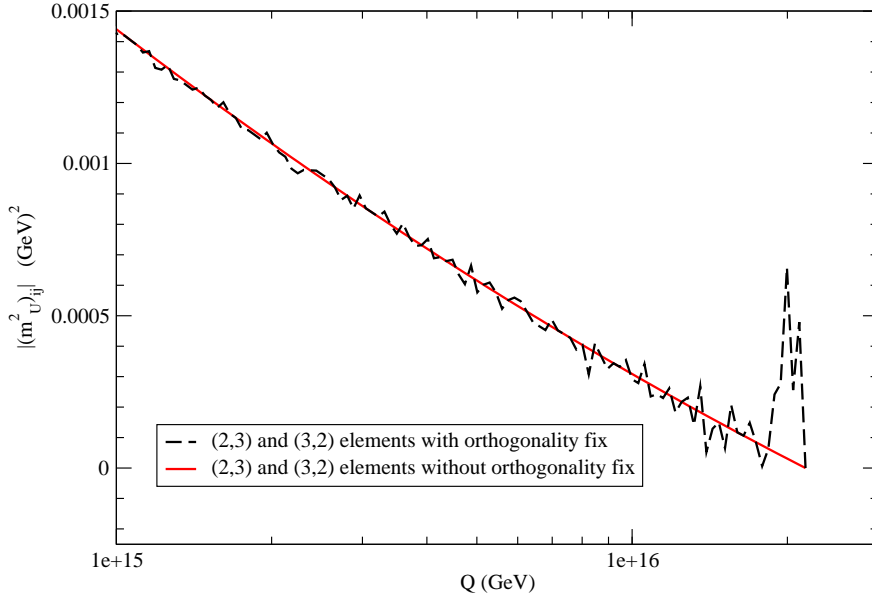


FIG. 14: Scale dependence of the magnitude of the  $(2,3)$  entry of  $\mathbf{m}_U^2$  for the same mSUGRA point as Fig. 13. We focus on the running at the extreme high scale, and compare the noise in the magnitude of just this element, both before and after fixing the orthogonality of the eigenvectors as described in the text. As in Fig. 13, the solid (red) line shows the result before the orthogonality fix while the dashed (black) line shows the result after this fix when this error has been moved to the  $(2,3)$  element which now randomly fluctuates close to  $M_{\text{GUT}}$  where the eigenvalues of  $\mathbf{m}_U^2$  are roughly degenerate.

are real that we see these fluctuations go down to even the level of the dashed (black) line. For the more general case the chance for both the real and the imaginary part of any matrix element to *simultaneously* fluctuate downward by this large magnitude is very small, so that the calculated magnitude (not shown here) is always larger than  $10^{-6}$   $\text{GeV}^2$ .

After our fix of the eigenvectors, any error from the non-unitarity of  $\mathbf{R}_U$  is shifted to the largest off-diagonal element, and the only residue of the resulting noise that remains is in the magnitude of this element for scales close to  $M_{\text{GUT}}$  — where the eigenvalues are closest — as seen in Fig. 14. At lower scales, the eigenvalues split, and the noise level (whose magnitude remains the same as in Fig. 13) becomes insignificant. Again, the solid (red) line shows the evolution of the magnitude of the  $(2,3)$  element before fixing the eigenvectors, while the dashed black line shows the same thing after the orthogonality fix. We see that

the numerical noise has indeed moved to the (2, 3) element which now shows fluctuations, but only close to  $M_{\text{GUT}}$  where the eigenvalues of  $\mathbf{m}_U^2$  are roughly degenerate.

## Appendix B: Renormalization Group Equations of Dimensionful Parameters

This appendix contains the RGEs with full thresholds for the dimensionful couplings of the MSSM with  $R$ -parity conservation. Note that we write these RGEs in the current basis in which the SSB sfermion mass matrices, but not the quark Yukawa matrices, are diagonal. In any other basis they must be modified to account for the rotation from this basis to the sfermion mass basis so that the sfermions can be properly decoupled. In this case the squark  $\theta_{\tilde{q}_k}$ 's become matrices  $\Theta_{q_k}$  as discussed in Sec III B, where further details may be found. The RGEs for the superpotential parameter  $\mu$  and the gaugino SSB mass parameters are,

$$\begin{aligned}
(4\pi)^2 \frac{d\mu}{dt} = & \frac{1}{2} \mu \theta_{\tilde{h}} \left[ 3\theta_{\tilde{u}_k} (\tilde{\mathbf{f}}_u^{uR})_{kl}^\dagger (\tilde{\mathbf{f}}_u^{uR})_{lk} + 3\theta_{\tilde{d}_k} (\tilde{\mathbf{f}}_d^{dR})_{kl}^\dagger (\tilde{\mathbf{f}}_d^{dR})_{lk} + \theta_{\tilde{e}_k} (\tilde{\mathbf{f}}_e^{eR})_{kl}^\dagger (\tilde{\mathbf{f}}_e^{eR})_{lk} \right. \\
& \left. + 3\theta_{\tilde{Q}_k} (\tilde{\mathbf{f}}_u^Q)_{kl} (\tilde{\mathbf{f}}_u^Q)_{lk}^\dagger + 3\theta_{\tilde{Q}_k} (\tilde{\mathbf{f}}_d^Q)_{kl} (\tilde{\mathbf{f}}_d^Q)_{lk}^\dagger + \theta_{\tilde{L}_k} (\tilde{\mathbf{f}}_e^L)_{kl} (\tilde{\mathbf{f}}_e^L)_{lk}^\dagger \right] \\
& + \frac{1}{4} \mu \theta_{\tilde{h}} \left[ \left( 3\theta_{\tilde{W}} |\tilde{g}^{hu}|^2 + \theta_{\tilde{B}} |\tilde{g}^{hu}|^2 \right) (s^2\theta_h + c^2\theta_H) \right. \\
& \left. + \left( 3\theta_{\tilde{W}} |\tilde{g}^{hd}|^2 + \theta_{\tilde{B}} |\tilde{g}^{hd}|^2 \right) (c^2\theta_h + s^2\theta_H) \right] \\
& + sc(-\theta_h + \theta_H) \left[ 3\theta_{\tilde{W}} \tilde{g}^{hu} (M_2 + iM_2') \tilde{g}^{hd} + \theta_{\tilde{B}} \tilde{g}^{hu} (M_1 + iM_1') \tilde{g}^{hd} \right] \\
& - \mu \theta_{\tilde{h}} \left( \frac{3}{2} g'^2 + \frac{9}{2} g_2^2 \right) , \tag{B1}
\end{aligned}$$

$$\begin{aligned}
(4\pi)^2 \frac{dM_1}{dt} = & M_1 \theta_{\tilde{B}} \left[ \frac{1}{3} \theta_{\tilde{Q}_k} (\tilde{\mathbf{g}}'^Q)_{kl} (\tilde{\mathbf{g}}'^Q)_{lk}^\dagger + \theta_{\tilde{L}_k} (\tilde{\mathbf{g}}'^L)_{kl} (\tilde{\mathbf{g}}'^L)_{lk}^\dagger + \frac{8}{3} \theta_{\tilde{u}_k} (\tilde{\mathbf{g}}'^{uR})_{kl}^\dagger (\tilde{\mathbf{g}}'^{uR})_{lk} \right. \\
& \left. + \frac{2}{3} \theta_{\tilde{d}_k} (\tilde{\mathbf{g}}'^{dR})_{kl}^\dagger (\tilde{\mathbf{g}}'^{dR})_{lk} + 2\theta_{\tilde{e}_k} (\tilde{\mathbf{g}}'^{eR})_{kl}^\dagger (\tilde{\mathbf{g}}'^{eR})_{lk} \right. \\
& \left. + \theta_{\tilde{h}} |\tilde{g}^{hu}|^2 (s^2\theta_h + c^2\theta_H) + \theta_{\tilde{h}} |\tilde{g}^{hd}|^2 (c^2\theta_h + s^2\theta_H) \right] \\
& + 2sc(-\theta_h + \theta_H) \theta_{\tilde{h}} \left[ \tilde{g}^{hd} \mu^* \tilde{g}^{hu} + (\tilde{g}^{hd})^* \mu (\tilde{g}^{hu})^* \right] , \tag{B2}
\end{aligned}$$

$$\begin{aligned}
(4\pi)^2 \frac{dM_1'}{dt} = & M_1' \theta_{\tilde{B}} \left[ \frac{1}{3} \theta_{\tilde{Q}_k} (\tilde{\mathbf{g}}'^Q)_{kl} (\tilde{\mathbf{g}}'^Q)_{lk}^\dagger + \theta_{\tilde{L}_k} (\tilde{\mathbf{g}}'^L)_{kl} (\tilde{\mathbf{g}}'^L)_{lk}^\dagger + \frac{8}{3} \theta_{\tilde{u}_k} (\tilde{\mathbf{g}}'^{uR})_{kl}^\dagger (\tilde{\mathbf{g}}'^{uR})_{lk} \right. \\
& \left. + \frac{2}{3} \theta_{\tilde{d}_k} (\tilde{\mathbf{g}}'^{dR})_{kl}^\dagger (\tilde{\mathbf{g}}'^{dR})_{lk} + 2\theta_{\tilde{e}_k} (\tilde{\mathbf{g}}'^{eR})_{kl}^\dagger (\tilde{\mathbf{g}}'^{eR})_{lk} \right. \\
& \left. + \theta_{\tilde{h}} |\tilde{g}^{hu}|^2 (s^2\theta_h + c^2\theta_H) + \theta_{\tilde{h}} |\tilde{g}^{hd}|^2 (c^2\theta_h + s^2\theta_H) \right] \\
& + 2isc(-\theta_h + \theta_H) \theta_{\tilde{h}} \left[ \tilde{g}^{hd} \mu^* \tilde{g}^{hu} - (\tilde{g}^{hd})^* \mu (\tilde{g}^{hu})^* \right] , \tag{B3}
\end{aligned}$$

$$(4\pi)^2 \frac{dM_2}{dt} = M_2 \theta_{\tilde{W}} \left[ 3\theta_{\tilde{Q}_k} (\tilde{\mathbf{g}}^Q)_{kl} (\tilde{\mathbf{g}}^Q)_{lk}^\dagger + \theta_{\tilde{L}_k} (\tilde{\mathbf{g}}^L)_{kl} (\tilde{\mathbf{g}}^L)_{lk}^\dagger + \theta_{\tilde{h}} |\tilde{g}^{hu}|^2 (s^2\theta_h + c^2\theta_H) + \theta_{\tilde{h}} |\tilde{g}^{hd}|^2 (c^2\theta_h + s^2\theta_H) \right] \quad (\text{B4})$$

$$+ 2sc(-\theta_h + \theta_H) \theta_{\tilde{h}} [\tilde{g}^{hd} \mu^* \tilde{g}^{hu} + (\tilde{g}^{hd})^* \mu (\tilde{g}^{hu})^*] - 12\theta_{\tilde{W}} M_2 g_2^2,$$

$$(4\pi)^2 \frac{dM'_2}{dt} = M'_2 \theta_{\tilde{W}} \left[ 3\theta_{\tilde{Q}_k} (\tilde{\mathbf{g}}^Q)_{kl} (\tilde{\mathbf{g}}^Q)_{lk}^\dagger + \theta_{\tilde{L}_k} (\tilde{\mathbf{g}}^L)_{kl} (\tilde{\mathbf{g}}^L)_{lk}^\dagger + \theta_{\tilde{h}} |\tilde{g}^{hu}|^2 (s^2\theta_h + c^2\theta_H) + \theta_{\tilde{h}} |\tilde{g}^{hd}|^2 (c^2\theta_h + s^2\theta_H) \right] \quad (\text{B5})$$

$$+ 2isc(-\theta_h + \theta_H) \theta_{\tilde{h}} [\tilde{g}^{hd} \mu^* \tilde{g}^{hu} - (\tilde{g}^{hd})^* \mu (\tilde{g}^{hu})^*] - 12\theta_{\tilde{W}} M'_2 g_2^2,$$

$$(4\pi)^2 \frac{dM_3}{dt} = M_3 \theta_{\tilde{g}} \left[ 2\theta_{\tilde{Q}_k} (\tilde{\mathbf{g}}_s^Q)_{kl} (\tilde{\mathbf{g}}_s^Q)_{lk}^\dagger + \theta_{\tilde{u}_k} (\tilde{\mathbf{g}}_s^{uR})_{kl}^\dagger (\tilde{\mathbf{g}}_s^{uR})_{lk} + \theta_{\tilde{d}_k} (\tilde{\mathbf{g}}_s^{dR})_{kl}^\dagger (\tilde{\mathbf{g}}_s^{dR})_{lk} - 18g_2^2 \right], \quad (\text{B6})$$

$$(4\pi)^2 \frac{dM'_3}{dt} = M'_3 \theta_{\tilde{g}} \left[ 2\theta_{\tilde{Q}_k} (\tilde{\mathbf{g}}_s^Q)_{kl} (\tilde{\mathbf{g}}_s^Q)_{lk}^\dagger + \theta_{\tilde{u}_k} (\tilde{\mathbf{g}}_s^{uR})_{kl}^\dagger (\tilde{\mathbf{g}}_s^{uR})_{lk} + \theta_{\tilde{d}_k} (\tilde{\mathbf{g}}_s^{dR})_{kl}^\dagger (\tilde{\mathbf{g}}_s^{dR})_{lk} - 18g_2^2 \right]. \quad (\text{B7})$$

The following RGEs are only valid above  $Q = m_H$ , where  $\theta_h = \theta_H = 1$ . We separate the two regimes of different Higgs boson content to simplify the resulting formulae, and to make explicit the parameters which remain in the theory below the heavy Higgs decoupling scale,  $Q = m_H$ .

$$\begin{aligned}
(4\pi)^2 \frac{d(\mathbf{a}_u)_{ij}}{dt} = & \theta_{\tilde{u}_k} (\mathbf{a}_u)_{ik} \left[ -\frac{2g'^2}{3} \delta_{kj} + 2 [(\mathbf{f}_u)^\dagger (\mathbf{f}_u)]_{kj} \right] \\
& + \theta_{\tilde{u}_l} \theta_{\tilde{Q}_k} \left[ -2 \left( \frac{g'^2}{9} + \frac{4g_3^2}{3} \right) \delta_{ik} \delta_{lj} + 6 (\mathbf{f}_u)_{ij} (\mathbf{f}_u)_{lk}^\dagger \right] (\mathbf{a}_u)_{kl} \\
& + \theta_{\tilde{Q}_k} \left[ \left( \frac{g'^2}{6} - \frac{3g_2^2}{2} \right) \delta_{ik} + 4 [(\mathbf{f}_u) (\mathbf{f}_u)^\dagger]_{ik} \right] (\mathbf{a}_u)_{kj} \\
& + 2\theta_{\tilde{d}_k} (\mathbf{a}_d)_{ik} [(\mathbf{f}_d)^\dagger (\mathbf{f}_u)]_{kj} \\
& + \frac{2}{3} \theta_{\tilde{B}} (M_1 - iM'_1) \left( \theta_{\tilde{h}} (\tilde{g}^{h_u})^* (\tilde{\mathbf{g}}'^Q)_{ik}^* (\tilde{\mathbf{f}}_u^{u_R})_{kj} - \frac{4}{3} (\tilde{\mathbf{g}}'^Q)_{ik}^* (\mathbf{f}_u)_{kl} (\tilde{\mathbf{g}}'^{u_R})_{kj}^* \right. \\
& \quad \left. - 4\theta_{\tilde{h}} (\tilde{\mathbf{f}}_u^Q)_{ik} (\tilde{\mathbf{g}}'^{u_R})_{kj}^* (\tilde{g}^{h_u})^* \right) \\
& - 6\theta_{\tilde{W}} \theta_{\tilde{h}} (M_2 - iM'_2) (\tilde{g}^{h_u})^* (\tilde{\mathbf{g}}^Q)_{ik}^* (\tilde{\mathbf{f}}_u^{u_R})_{kj} \\
& - \frac{32}{3} \theta_{\tilde{g}} (M_3 - iM'_3) (\tilde{\mathbf{g}}_s^Q)_{ik}^* (\mathbf{f}_u)_{kl} (\tilde{\mathbf{g}}_s^{u_R})_{kj}^* \\
& + \theta_{\tilde{u}_k} (\mathbf{a}_u)_{ik} \left[ \frac{8}{9} \theta_{\tilde{B}} (\tilde{\mathbf{g}}'^{u_R})_{kl}^T (\tilde{\mathbf{g}}'^{u_R})_{lj}^* + \frac{8}{3} \theta_{\tilde{g}} (\tilde{\mathbf{g}}_s^{u_R})_{kl}^T (\tilde{\mathbf{g}}_s^{u_R})_{lj}^* + 2\theta_{\tilde{h}} (\tilde{\mathbf{f}}_u^{u_R})_{kl}^\dagger (\tilde{\mathbf{f}}_u^{u_R})_{lj} \right] \\
& + \left[ 3(\mathbf{f}_u^\dagger)_{kl} (\mathbf{f}_u)_{lk} + \frac{1}{2} \theta_{\tilde{h}} \theta_{\tilde{B}} |\tilde{g}^{h_u}|^2 + \frac{3}{2} \theta_{\tilde{h}} \theta_{\tilde{W}} |\tilde{g}^{h_u}|^2 \right] (\mathbf{a}_u)_{ij} \\
& + \theta_{\tilde{Q}_l} \left[ \theta_{\tilde{h}} (\tilde{\mathbf{f}}_u^Q)_{ik} (\tilde{\mathbf{f}}_u^Q)_{kl}^\dagger + \theta_{\tilde{h}} (\tilde{\mathbf{f}}_d^Q)_{ik} (\tilde{\mathbf{f}}_d^Q)_{kl}^\dagger + \frac{1}{18} \theta_{\tilde{B}} (\tilde{\mathbf{g}}'^Q)_{ik}^* (\tilde{\mathbf{g}}'^Q)_{kl}^T \right. \\
& \quad \left. + \frac{3}{2} \theta_{\tilde{W}} (\tilde{\mathbf{g}}^Q)_{ik}^* (\tilde{\mathbf{g}}^Q)_{kl}^T + \frac{8}{3} \theta_{\tilde{g}} (\tilde{\mathbf{g}}_s^Q)_{ik}^* (\tilde{\mathbf{g}}_s^Q)_{kl}^T \right] (\mathbf{a}_u)_{lj} \\
& - 3 \left\{ \left( \frac{1}{36} \theta_{\tilde{Q}_i} + \frac{4}{9} \theta_{\tilde{u}_j} + \frac{1}{4} \right) g'^2 + \frac{3}{4} (\theta_{\tilde{Q}_i} + 1) g_2^2 + \frac{4}{3} (\theta_{\tilde{Q}_i} + \theta_{\tilde{u}_j}) g_3^2 \right\} (\mathbf{a}_u)_{ij} ,
\end{aligned} \tag{B8}$$

$$\begin{aligned}
(4\pi)^2 \frac{d(\tilde{\mu}^* \mathbf{f}_u^{h_u})_{ij}}{dt} &= \frac{2g'^2}{3} \theta_{\tilde{u}_k} \delta_{kj} (\tilde{\mu}^* \mathbf{f}_u^{h_u})_{ik} \\
&+ \theta_{\tilde{u}_l} \theta_{\tilde{Q}_k} \left[ -2 \left( \frac{g'^2}{9} + \frac{4g_3^2}{3} \right) \delta_{ik} \delta_{lj} + 6(\mathbf{f}_u)_{ij} (\mathbf{f}_u)_{lk}^\dagger \right] (\tilde{\mu}^* \mathbf{f}_u^{h_u})_{kl} \\
&- \theta_{\tilde{Q}_k} \left[ \left( \frac{g'^2}{6} - \frac{3g_2^2}{2} \right) \delta_{ik} + 2 [(\mathbf{f}_d)(\mathbf{f}_d)^\dagger]_{ik} \right] (\tilde{\mu}^* \mathbf{f}_u^{h_u})_{kj} \\
&- 2\theta_{\tilde{d}_k} (\tilde{\mu}^* \mathbf{f}_d^{h_d})_{ik} [(\mathbf{f}_d)^\dagger (\mathbf{f}_u)]_{kj} \\
&- \frac{2}{3} \theta_{\tilde{B}} \theta_{\tilde{h}} \mu^* \tilde{g}^{h_d} \left( 4(\tilde{\mathbf{f}}_u^Q)_{ik} (\tilde{\mathbf{g}}'^{u_R})_{kj}^* - (\tilde{\mathbf{g}}'^Q)_{ik}^* (\tilde{\mathbf{f}}_u^{u_R})_{kj} \right) \\
&- 6\theta_{\tilde{h}} \theta_{\tilde{W}} \mu^* \tilde{g}^{h_d} (\tilde{\mathbf{g}}^Q)_{ik}^* (\tilde{\mathbf{f}}_u^{u_R})_{kj} + 4\theta_{\tilde{h}} \mu^* (\tilde{\mathbf{f}}_d^Q)_{ik} (\mathbf{f}_d^\dagger)_{kl} (\tilde{\mathbf{f}}_u^{u_R})_{lj} \\
&+ \theta_{\tilde{u}_k} (\tilde{\mu}^* \mathbf{f}_u^{h_u})_{ik} \left[ \frac{8}{9} \theta_{\tilde{B}} (\tilde{\mathbf{g}}'^{u_R})_{kl}^T (\tilde{\mathbf{g}}'^{u_R})_{lj}^* + \frac{8}{3} \theta_{\tilde{g}} (\tilde{\mathbf{g}}_s^{u_R})_{kl}^T (\tilde{\mathbf{g}}_s^{u_R})_{lj}^* \right. \\
&\quad \left. + 2\theta_{\tilde{h}} (\tilde{\mathbf{f}}_u^{u_R})_{kl}^\dagger (\tilde{\mathbf{f}}_u^{u_R})_{lj} \right] \\
&+ \left[ 3(\mathbf{f}_d^\dagger)_{kl} (\mathbf{f}_d)_{lk} + (\mathbf{f}_e^\dagger)_{kl} (\mathbf{f}_e)_{lk} + \frac{1}{2} \theta_{\tilde{B}} \theta_{\tilde{h}} |\tilde{g}^{h_d}|^2 + \frac{3}{2} \theta_{\tilde{W}} \theta_{\tilde{h}} |\tilde{g}^{h_d}|^2 \right] (\tilde{\mu}^* \mathbf{f}_u^{h_u})_{ij} \\
&+ \theta_{\tilde{Q}_i} \left[ \theta_{\tilde{h}} (\tilde{\mathbf{f}}_u^Q)_{ik} (\tilde{\mathbf{f}}_u^Q)_{kl}^\dagger + \theta_{\tilde{h}} (\tilde{\mathbf{f}}_d^Q)_{ik} (\tilde{\mathbf{f}}_d^Q)_{kl}^\dagger + \frac{1}{18} \theta_{\tilde{B}} (\tilde{\mathbf{g}}'^Q)_{ik}^* (\tilde{\mathbf{g}}'^Q)_{kl}^T \right. \\
&\quad \left. + \frac{3}{2} \theta_{\tilde{W}} (\tilde{\mathbf{g}}^Q)_{ik}^* (\tilde{\mathbf{g}}^Q)_{kl}^T + \frac{8}{3} \theta_{\tilde{g}} (\tilde{\mathbf{g}}_s^Q)_{ik}^* (\tilde{\mathbf{g}}_s^Q)_{kl}^T \right] (\tilde{\mu}^* \mathbf{f}_u^{h_u})_{lj} \\
&- 3 \left\{ \left( \frac{1}{36} \theta_{\tilde{Q}_i} + \frac{4}{9} \theta_{\tilde{u}_j} + \frac{1}{4} \right) g'^2 + \frac{3}{4} (\theta_{\tilde{Q}_i} + 1) g_2^2 \right. \\
&\quad \left. + \frac{4}{3} (\theta_{\tilde{Q}_i} + \theta_{\tilde{u}_j}) g_3^2 \right\} (\tilde{\mu}^* \mathbf{f}_u^{h_u})_{ij} ,
\end{aligned} \tag{B9}$$

$$\begin{aligned}
(4\pi)^2 \frac{d(\mathbf{a}_d)_{ij}}{dt} = & \theta_{\tilde{Q}_k} \left[ - \left( \frac{g'^2}{6} + \frac{3g_2^2}{2} \right) \delta_{ik} + 4 [(\mathbf{f}_d)(\mathbf{f}_d)^\dagger]_{ik} \right] (\mathbf{a}_d)_{kj} \\
& + \theta_{\tilde{d}_i} \theta_{\tilde{Q}_k} \left[ 2 \left( \frac{g'^2}{18} - \frac{4g_3^2}{3} \right) \delta_{ik} \delta_{lj} + 6(\mathbf{f}_d)_{ij} (\mathbf{f}_d)_{lk}^\dagger \right] (\mathbf{a}_d)_{kl} \\
& + 2\theta_{\tilde{e}_i} \theta_{\tilde{L}_k} (\mathbf{f}_d)_{ij} (\mathbf{f}_e)_{lk}^\dagger (\mathbf{a}_e)_{kl} \\
& + \theta_{\tilde{d}_k} (\mathbf{a}_d)_{ik} \left[ -\frac{g'^2}{3} \delta_{kj} + 2 [(\mathbf{f}_d)^\dagger (\mathbf{f}_d)]_{kj} \right] + 2\theta_{\tilde{u}_k} (\mathbf{a}_u)_{ik} [(\mathbf{f}_u)^\dagger (\mathbf{f}_d)]_{kj} \\
& + \frac{2}{3} \theta_{\tilde{B}} (M_1 - iM'_1) \left( -\theta_{\tilde{h}} (\tilde{g}^{hd})^* (\tilde{\mathbf{g}}'^Q)_{ik}^* (\tilde{\mathbf{f}}_d^{dR})_{kj} + \frac{2}{3} (\tilde{\mathbf{g}}'^Q)_{ik}^* (\mathbf{f}_d)_{kl} (\tilde{\mathbf{g}}'^{dR})_{lj}^* \right. \\
& \quad \left. - 2\theta_{\tilde{h}} (\tilde{\mathbf{f}}_d^Q)_{ik} (\tilde{\mathbf{g}}'^{dR})_{kj}^* (\tilde{g}^{hd})^* \right) \\
& - 6\theta_{\tilde{W}} \theta_{\tilde{h}} (M_2 - iM'_2) (\tilde{g}^{hd})^* (\tilde{\mathbf{g}}^Q)_{ik}^* (\tilde{\mathbf{f}}_d^{dR})_{kj} \\
& - \frac{32}{3} \theta_{\tilde{g}} (M_3 - iM'_3) (\tilde{\mathbf{g}}_s^Q)_{ik}^* (\mathbf{f}_d)_{kl} (\tilde{\mathbf{g}}_s^{dR})_{lj}^* \\
& + \theta_{\tilde{Q}_i} \left[ \theta_{\tilde{h}} (\tilde{\mathbf{f}}_u^Q)_{ik} (\tilde{\mathbf{f}}_u^Q)_{kl}^\dagger + \theta_{\tilde{h}} (\tilde{\mathbf{f}}_d^Q)_{ik} (\tilde{\mathbf{f}}_d^Q)_{kl}^\dagger + \frac{1}{18} \theta_{\tilde{B}} (\tilde{\mathbf{g}}'^Q)_{ik}^* (\tilde{\mathbf{g}}'^Q)_{kl}^T \right. \\
& \quad \left. + \frac{3}{2} \theta_{\tilde{W}} (\tilde{\mathbf{g}}^Q)_{ik}^* (\tilde{\mathbf{g}}^Q)_{kl}^T + \frac{8}{3} \theta_{\tilde{g}} (\tilde{\mathbf{g}}_s^Q)_{ik}^* (\tilde{\mathbf{g}}_s^Q)_{kl}^T \right] (\mathbf{a}_d)_{lj} \\
& + \left[ 3(\mathbf{f}_d)_{kl} (\mathbf{f}_d^\dagger)_{lk} + (\mathbf{f}_e)_{kl} (\mathbf{f}_e^\dagger)_{lk} + \frac{1}{2} \theta_{\tilde{B}} \theta_{\tilde{h}} |\tilde{g}^{hd}|^2 + \frac{3}{2} \theta_{\tilde{W}} \theta_{\tilde{h}} |\tilde{g}^{hd}|^2 \right] (\mathbf{a}_d)_{ij} \\
& + \theta_{\tilde{d}_k} (\mathbf{a}_d)_{ik} \left[ \frac{2}{9} \theta_{\tilde{B}} (\tilde{\mathbf{g}}'^{dR})_{kl}^T (\tilde{\mathbf{g}}'^{dR})_{lj}^* + \frac{8}{3} \theta_{\tilde{g}} (\tilde{\mathbf{g}}_s^{dR})_{kl}^T (\tilde{\mathbf{g}}_s^{dR})_{lj}^* + 2\theta_{\tilde{h}} (\tilde{\mathbf{f}}_d^{dR})_{kl}^\dagger (\tilde{\mathbf{f}}_d^{dR})_{lj} \right] \\
& - 3 \left\{ \left( \frac{1}{36} \theta_{\tilde{Q}_i} + \frac{1}{9} \theta_{\tilde{d}_j} + \frac{1}{4} \right) g'^2 + \frac{3}{4} (\theta_{\tilde{Q}_i} + 1) g_2^2 + \frac{4}{3} (\theta_{\tilde{Q}_i} + \theta_{\tilde{d}_j}) g_3^2 \right\} (\mathbf{a}_d)_{ij} ,
\end{aligned} \tag{B10}$$



$$\begin{aligned}
(4\pi)^2 \frac{d\left(\tilde{\mu}^* \mathbf{f}_d^{h_d}\right)_{ij}}{dt} = & \frac{g'^2}{3} \theta_{\tilde{d}_k} \delta_{kj} \left(\tilde{\mu}^* \mathbf{f}_d^{h_d}\right)_{ik} \\
& + \theta_{\tilde{d}_i} \theta_{\tilde{Q}_k} \left[ 2 \left( \frac{g'^2}{18} - \frac{4g_3^2}{3} \right) \delta_{ik} \delta_{lj} + 6(\mathbf{f}_d)_{ij} (\mathbf{f}_d)_{lk}^\dagger \right] \left(\tilde{\mu}^* \mathbf{f}_d^{h_d}\right)_{kl} \\
& + 2\theta_{\tilde{e}_i} \theta_{\tilde{L}_k} (\mathbf{f}_d)_{ij} (\mathbf{f}_e)_{lk}^\dagger \left(\tilde{\mu}^* \mathbf{f}_e^{h_d}\right)_{kl} \\
& + \theta_{\tilde{Q}_k} \left[ \left( \frac{g'^2}{6} + \frac{3g_2^2}{2} \right) \delta_{ik} - 2 [(\mathbf{f}_u) (\mathbf{f}_u)^\dagger]_{ik} \right] \left(\tilde{\mu}^* \mathbf{f}_d^{h_d}\right)_{kj} \\
& - 2\theta_{\tilde{u}_k} \left(\tilde{\mu}^* \mathbf{f}_u^{h_u}\right)_{ik} [(\mathbf{f}_u)^\dagger (\mathbf{f}_d)]_{kj} \\
& - \frac{2}{3} \theta_{\tilde{B}} \theta_{\tilde{h}} \mu^* \tilde{g}^{h_u} \left( 2(\tilde{\mathbf{f}}_d^Q)_{ik} (\tilde{\mathbf{g}}'^{d_R})_{kj}^* + (\tilde{\mathbf{g}}'^Q)_{ik}^* (\tilde{\mathbf{f}}_d^{d_R})_{kj} \right) \\
& - 6\theta_{\tilde{h}} \theta_{\tilde{W}} \mu^* \tilde{g}^{h_u} (\tilde{\mathbf{g}}^Q)_{ik}^* (\tilde{\mathbf{f}}_d^{d_R})_{kj} + 4\theta_{\tilde{h}} \mu^* (\tilde{\mathbf{f}}_u^Q)_{ik} (\mathbf{f}_u^\dagger)_{kl} (\tilde{\mathbf{f}}_d^{d_R})_{lj} \\
& + \theta_{\tilde{d}_k} \left(\tilde{\mu}^* \mathbf{f}_d^{h_d}\right)_{ik} \left[ \frac{2}{9} \theta_{\tilde{B}} (\tilde{\mathbf{g}}'^{d_R})_{kl}^T (\tilde{\mathbf{g}}'^{d_R})_{lj}^* + \frac{8}{3} \theta_{\tilde{g}} (\tilde{\mathbf{g}}_s^{d_R})_{kl}^T (\tilde{\mathbf{g}}_s^{d_R})_{lj}^* \right. \\
& \quad \left. + 2\theta_{\tilde{h}} (\tilde{\mathbf{f}}_d^{d_R})_{kl}^\dagger (\tilde{\mathbf{f}}_d^{d_R})_{lj} \right] \\
& + \left[ 3(\mathbf{f}_u)_{kl} (\mathbf{f}_u^\dagger)_{lk} + \frac{1}{2} \theta_{\tilde{B}} \theta_{\tilde{h}} |\tilde{g}^{h_u}|^2 + \frac{3}{2} \theta_{\tilde{W}} \theta_{\tilde{h}} |\tilde{g}^{h_u}|^2 \right] \left(\tilde{\mu}^* \mathbf{f}_d^{h_d}\right)_{ij} \\
& + \theta_{\tilde{Q}_i} \left[ \theta_{\tilde{h}} (\tilde{\mathbf{f}}_u^Q)_{ik} (\tilde{\mathbf{f}}_u^\dagger)_{kl} + \theta_{\tilde{h}} (\tilde{\mathbf{f}}_d^Q)_{ik} (\tilde{\mathbf{f}}_d^\dagger)_{kl} + \frac{1}{18} \theta_{\tilde{B}} (\tilde{\mathbf{g}}'^Q)_{ik}^* (\tilde{\mathbf{g}}'^Q)_{kl}^T \right. \\
& \quad \left. + \frac{3}{2} \theta_{\tilde{W}} (\tilde{\mathbf{g}}^Q)_{ik}^* (\tilde{\mathbf{g}}^Q)_{kl}^T + \frac{8}{3} \theta_{\tilde{g}} (\tilde{\mathbf{g}}_s^Q)_{ik}^* (\tilde{\mathbf{g}}_s^Q)_{kl}^T \right] \left(\tilde{\mu}^* \mathbf{f}_d^{h_d}\right)_{lj} \\
& - 3 \left\{ \left( \frac{1}{36} \theta_{\tilde{Q}_i} + \frac{1}{9} \theta_{\tilde{d}_j} + \frac{1}{4} \right) g'^2 + \frac{3}{4} (\theta_{\tilde{Q}_i} + 1) g_2^2 \right. \\
& \quad \left. + \frac{4}{3} (\theta_{\tilde{Q}_i} + \theta_{\tilde{d}_j}) g_3^2 \right\} \left(\tilde{\mu}^* \mathbf{f}_d^{h_d}\right)_{ij} ,
\end{aligned} \tag{B11}$$

$$\begin{aligned}
(4\pi)^2 \frac{d(\mathbf{a}_e)_{ij}}{dt} = & \theta_{\tilde{L}_k} \left[ \left( \frac{g'^2}{2} - \frac{3g_2^2}{2} \right) \delta_{ik} + 4 [(\mathbf{f}_e)(\mathbf{f}_e)^\dagger]_{ik} \right] (\mathbf{a}_e)_{kj} \\
& + \theta_{\tilde{e}_l} \theta_{\tilde{L}_k} \left[ -g'^2 \delta_{ik} \delta_{lj} + 2(\mathbf{f}_e)_{ij} (\mathbf{f}_e)_{lk}^\dagger \right] (\mathbf{a}_e)_{kl} + 6\theta_{\tilde{d}_l} \theta_{\tilde{Q}_k} (\mathbf{f}_e)_{ij} (\mathbf{f}_d)_{lk}^\dagger (\mathbf{a}_d)_{kl} \\
& + \theta_{\tilde{e}_k} (\mathbf{a}_e)_{ik} \left[ -g'^2 \delta_{kj} + 2 [(\mathbf{f}_e)^\dagger (\mathbf{f}_e)]_{kj} \right] \\
& + 2\theta_{\tilde{B}} (M_1 - iM'_1) \left( \theta_{\tilde{h}} (\tilde{g}^{hd})^* (\tilde{\mathbf{g}}'^L)_{ik}^* (\tilde{\mathbf{f}}_e^{eR})_{kj} - 2(\tilde{\mathbf{g}}'^L)_{ik}^* (\mathbf{f}_e)_{kl} (\tilde{\mathbf{g}}'^{eR})_{lj}^* \right. \\
& \quad \left. - 2\theta_{\tilde{h}} (\tilde{\mathbf{f}}_e^L)_{ik} (\tilde{\mathbf{g}}'^{eR})_{kj}^* (\tilde{g}^{hd})^* \right) \\
& - 6\theta_{\tilde{W}} \theta_{\tilde{h}} (M_2 - iM'_2) (\tilde{g}^{hd})^* (\tilde{\mathbf{g}}^L)_{ik}^* (\tilde{\mathbf{f}}_e^{eR})_{kj} \\
& + \theta_{\tilde{L}_i} \left[ \theta_{\tilde{h}} (\tilde{\mathbf{f}}_e^L)_{ik} (\tilde{\mathbf{f}}_e^L)_{kl}^\dagger + \frac{1}{2} \theta_{\tilde{B}} (\tilde{\mathbf{g}}'^L)_{ik}^* (\tilde{\mathbf{g}}'^L)_{kl}^T + \frac{3}{2} \theta_{\tilde{W}} (\tilde{\mathbf{g}}^L)_{ik}^* (\tilde{\mathbf{g}}^L)_{kl}^T \right] (\mathbf{a}_e)_{lj} \\
& + \left[ 3(\mathbf{f}_d)_{kl} (\mathbf{f}_d)_{lk}^\dagger + (\mathbf{f}_e)_{kl} (\mathbf{f}_e)_{lk}^\dagger + \frac{1}{2} \theta_{\tilde{B}} \theta_{\tilde{h}} |\tilde{g}^{hd}|^2 + \frac{3}{2} \theta_{\tilde{W}} \theta_{\tilde{h}} |\tilde{g}^{hd}|^2 \right] (\mathbf{a}_e)_{ij} \\
& + \theta_{\tilde{e}_k} (\mathbf{a}_e)_{ik} \left[ 2\theta_{\tilde{B}} (\tilde{\mathbf{g}}'^{eR})_{kl}^T (\tilde{\mathbf{g}}'^{eR})_{lj}^* + 2\theta_{\tilde{h}} (\tilde{\mathbf{f}}_e^{eR})_{kl}^\dagger (\tilde{\mathbf{f}}_e^{eR})_{lj} \right] \\
& - 3 \left\{ \left( \frac{1}{4} \theta_{\tilde{L}_i} + \theta_{\tilde{e}_j} + \frac{1}{4} \right) g'^2 + \frac{3}{4} (\theta_{\tilde{L}_i} + 1) g_2^2 \right\} (\mathbf{a}_e)_{ij} ,
\end{aligned} \tag{B12}$$

$$\begin{aligned}
(4\pi)^2 \frac{d(\tilde{\mu}^* \mathbf{f}_e^{hd})_{ij}}{dt} = & g'^2 \theta_{\tilde{e}_k} \delta_{kj} (\tilde{\mu}^* \mathbf{f}_e^{hd})_{ik} \\
& + \theta_{\tilde{e}_l} \theta_{\tilde{L}_k} \left[ -g'^2 \delta_{ik} \delta_{lj} + 2(\mathbf{f}_e)_{ij} (\mathbf{f}_e)_{lk}^\dagger \right] (\tilde{\mu}^* \mathbf{f}_e^{hd})_{kl} \\
& + 6\theta_{\tilde{d}_l} \theta_{\tilde{Q}_k} (\mathbf{f}_e)_{ij} (\mathbf{f}_d)_{lk}^\dagger (\tilde{\mu}^* \mathbf{f}_d^{hd})_{kl} \\
& - \theta_{\tilde{L}_k} \left[ \left( \frac{g'^2}{2} - \frac{3g_2^2}{2} \right) \delta_{ik} \right] (\tilde{\mu}^* \mathbf{f}_e^{hd})_{kj} \\
& - 2\theta_{\tilde{B}} \theta_{\tilde{h}} \mu^* \tilde{g}^{hu} \left( 2(\tilde{\mathbf{f}}_e^L)_{ik} (\tilde{\mathbf{g}}'^{eR})_{kj}^* - (\tilde{\mathbf{g}}'^L)_{ik}^* (\tilde{\mathbf{f}}_e^{eR})_{kj} \right) \\
& - 6\theta_{\tilde{h}} \theta_{\tilde{W}} \mu^* \tilde{g}^{hu} (\tilde{\mathbf{g}}^L)_{ik}^* (\tilde{\mathbf{f}}_e^{eR})_{kj} \\
& + \theta_{\tilde{e}_k} (\tilde{\mu}^* \mathbf{f}_e^{hd})_{ik} \left[ 2\theta_{\tilde{B}} (\tilde{\mathbf{g}}'^{eR})_{kl}^T (\tilde{\mathbf{g}}'^{eR})_{lj}^* + 2\theta_{\tilde{h}} (\tilde{\mathbf{f}}_e^{eR})_{kl}^\dagger (\tilde{\mathbf{f}}_e^{eR})_{lj} \right] \\
& + \left[ 3(\mathbf{f}_u)_{kl} (\mathbf{f}_u)_{lk}^\dagger + \frac{1}{2} \theta_{\tilde{B}} \theta_{\tilde{h}} |\tilde{g}^{hu}|^2 + \frac{3}{2} \theta_{\tilde{W}} \theta_{\tilde{h}} |\tilde{g}^{hu}|^2 \right] (\tilde{\mu}^* \mathbf{f}_e^{hd})_{ij} \\
& + \theta_{\tilde{L}_i} \left[ \theta_{\tilde{h}} (\tilde{\mathbf{f}}_e^L)_{ik} (\tilde{\mathbf{f}}_e^L)_{kl}^\dagger + \frac{1}{2} \theta_{\tilde{B}} (\tilde{\mathbf{g}}'^L)_{ik}^* (\tilde{\mathbf{g}}'^L)_{kl}^T + \frac{3}{2} \theta_{\tilde{W}} (\tilde{\mathbf{g}}^L)_{ik}^* (\tilde{\mathbf{g}}^L)_{kl}^T \right] (\tilde{\mu}^* \mathbf{f}_e^{hd})_{lj} \\
& - 3 \left\{ \left( \frac{1}{4} \theta_{\tilde{L}_i} + \theta_{\tilde{e}_j} + \frac{1}{4} \right) g'^2 + \frac{3}{4} (\theta_{\tilde{L}_i} + 1) g_2^2 \right\} (\tilde{\mu}^* \mathbf{f}_e^{hd})_{ij} ,
\end{aligned} \tag{B13}$$

$$\begin{aligned}
(4\pi)^2 \frac{d(m_{H_u}^2 + |\tilde{\mu}|^2)}{dt} &= \frac{3}{2} [g'^2 + g_2^2] (m_{H_u}^2 + |\tilde{\mu}|^2) - g'^2 (m_{H_d}^2 + |\tilde{\mu}|^2) \\
&+ \theta_{\tilde{u}_k} \theta_{\tilde{u}_l} [-2g'^2 \delta_{lk} + 6 [(\mathbf{f}_u)^T (\mathbf{f}_u)^*]_{lk}] (\mathbf{m}_U^2)_{kl} \\
&+ \theta_{\tilde{Q}_k} \theta_{\tilde{Q}_l} [g'^2 \delta_{lk} + 6 [(\mathbf{f}_u)^* (\mathbf{f}_u)^T]_{lk}] (\mathbf{m}_Q^2)_{kl} \\
&+ \theta_{\tilde{d}_k} \theta_{\tilde{d}_l} g'^2 \delta_{lk} (\mathbf{m}_D^2)_{kl} - \theta_{\tilde{L}_k} \theta_{\tilde{L}_l} g'^2 \delta_{lk} (\mathbf{m}_L^2)_{kl} \\
&+ \theta_{\tilde{e}_k} \theta_{\tilde{e}_l} g'^2 \delta_{lk} (\mathbf{m}_E^2)_{kl} + 6\theta_{\tilde{u}_k} \theta_{\tilde{Q}_l} (\mathbf{a}_u)^*_{lk} (\mathbf{a}_u)^T_{kl} \\
&+ 6\theta_{\tilde{Q}_l} \theta_{\tilde{d}_k} (\tilde{\mu}^* \mathbf{f}_d^{h_d})^*_{lk} (\tilde{\mu}^* \mathbf{f}_d^{h_d})^T_{kl} + 2\theta_{\tilde{L}_l} \theta_{\tilde{e}_k} (\tilde{\mu}^* \mathbf{f}_e^{h_d})^*_{lk} (\tilde{\mu}^* \mathbf{f}_e^{h_d})^T_{kl} \\
&- 2\theta_{\tilde{h}} |\mu|^2 \left\{ \theta_{\tilde{B}} |\tilde{g}^{h_u}|^2 + 3\theta_{\tilde{W}} |\tilde{g}^{h_u}|^2 \right\} \\
&- 2\theta_{\tilde{h}} \left\{ \theta_{\tilde{B}} (M_1^2 + M_1'^2) |\tilde{g}^{h_u}|^2 + 3\theta_{\tilde{W}} (M_2^2 + M_2'^2) |\tilde{g}^{h_u}|^2 \right\} \\
&- \left( \frac{3g'^2}{2} + \frac{9g_2^2}{2} \right) (m_{H_u}^2 + |\tilde{\mu}|^2) \\
&+ \left\{ [6\mathbf{f}_u^* \mathbf{f}_u^T]_{kk} + \theta_{\tilde{B}} \theta_{\tilde{h}} |\tilde{g}^{h_u}|^2 + 3\theta_{\tilde{W}} \theta_{\tilde{h}} |\tilde{g}^{h_u}|^2 \right\} (m_{H_u}^2 + |\tilde{\mu}|^2) ,
\end{aligned} \tag{B14}$$

$$\begin{aligned}
(4\pi)^2 \frac{d(m_{H_d}^2 + |\tilde{\mu}|^2)}{dt} &= -g'^2 (m_{H_u}^2 + |\tilde{\mu}|^2) + \frac{3}{2} [g'^2 + g_2^2] (m_{H_d}^2 + |\tilde{\mu}|^2) \\
&+ 2\theta_{\tilde{u}_k} \theta_{\tilde{u}_l} g'^2 \delta_{lk} (\mathbf{m}_U^2)_{kl} \\
&+ \theta_{\tilde{Q}_k} \theta_{\tilde{Q}_l} [-g'^2 \delta_{lk} + 6 [(\mathbf{f}_d)^* (\mathbf{f}_d)^T]_{lk}] (\mathbf{m}_Q^2)_{kl} \\
&+ \theta_{\tilde{d}_k} \theta_{\tilde{d}_l} [-g'^2 \delta_{lk} + 6 [(\mathbf{f}_d)^T (\mathbf{f}_d)^*]_{lk}] (\mathbf{m}_D^2)_{kl} \\
&+ \theta_{\tilde{L}_k} \theta_{\tilde{L}_l} [g'^2 \delta_{lk} + 2 [(\mathbf{f}_e)^* (\mathbf{f}_e)^T]_{lk}] (\mathbf{m}_L^2)_{kl} \\
&+ \theta_{\tilde{e}_k} \theta_{\tilde{e}_l} [-g'^2 \delta_{lk} + 2 [(\mathbf{f}_e)^T (\mathbf{f}_e)^*]_{lk}] (\mathbf{m}_E^2)_{kl} \\
&+ 6\theta_{\tilde{u}_k} \theta_{\tilde{Q}_l} (\tilde{\mu}^* \mathbf{f}_u^{h_u})^*_{lk} (\tilde{\mu}^* \mathbf{f}_u^{h_u})^T_{kl} + 6\theta_{\tilde{Q}_l} \theta_{\tilde{d}_k} (\mathbf{a}_d)^*_{lk} (\mathbf{a}_d)^T_{kl} \\
&+ 2\theta_{\tilde{L}_l} \theta_{\tilde{e}_k} (\mathbf{a}_e)^*_{lk} (\mathbf{a}_e)^T_{kl} \\
&- 2\theta_{\tilde{h}} |\mu|^2 \left\{ \theta_{\tilde{B}} |\tilde{g}^{h_d}|^2 + 3\theta_{\tilde{W}} |\tilde{g}^{h_d}|^2 \right\} \\
&- 2\theta_{\tilde{h}} \left\{ \theta_{\tilde{B}} (M_1^2 + M_1'^2) |\tilde{g}^{h_d}|^2 + 3\theta_{\tilde{W}} (M_2^2 + M_2'^2) |\tilde{g}^{h_d}|^2 \right\} \\
&- \left( \frac{3g'^2}{2} + \frac{9g_2^2}{2} \right) (m_{H_d}^2 + |\tilde{\mu}|^2) \\
&+ \left\{ [6\mathbf{f}_d^* \mathbf{f}_d^T + 2\mathbf{f}_e^* \mathbf{f}_e^T]_{kk} + \theta_{\tilde{B}} \theta_{\tilde{h}} |\tilde{g}^{h_d}|^2 + 3\theta_{\tilde{W}} \theta_{\tilde{h}} |\tilde{g}^{h_d}|^2 \right\} (m_{H_d}^2 + |\tilde{\mu}|^2) ,
\end{aligned} \tag{B15}$$

$$\begin{aligned}
(4\pi)^2 \frac{d(\mathbf{m}_Q^2)_{ij}}{dt} = & \left\{ \frac{1}{3} g'^2 \delta_{ij} + 2 [(\mathbf{f}_u)^* (\mathbf{f}_u)^T]_{ij} \right\} (m_{H_u}^2 + |\tilde{\mu}|^2) \\
& + \left\{ -\frac{1}{3} g'^2 \delta_{ij} + 2 [(\mathbf{f}_d)^* (\mathbf{f}_d)^T]_{ij} \right\} (m_{H_d}^2 + |\tilde{\mu}|^2) \\
& - \frac{2}{3} \theta_{\tilde{u}_k} g'^2 \delta_{ij} (\mathbf{m}_U^2)_{kk} + \frac{1}{3} \theta_{\tilde{Q}_k} g'^2 \delta_{ij} (\mathbf{m}_Q^2)_{kk} \\
& + \theta_{\tilde{Q}_k} \theta_{\tilde{Q}_l} \left( \frac{g'^2}{18} + \frac{3g_2^2}{2} + \frac{8g_3^2}{3} \right) \delta_{ik} \delta_{lj} (\mathbf{m}_Q^2)_{kl} \\
& + \frac{1}{3} \theta_{\tilde{d}_k} g'^2 \delta_{ij} (\mathbf{m}_D^2)_{kk} - \frac{1}{3} \theta_{\tilde{L}_k} g'^2 \delta_{ij} (\mathbf{m}_L^2)_{kk} + \frac{1}{3} \theta_{\tilde{e}_k} g'^2 \delta_{ij} (\mathbf{m}_E^2)_{kk} \\
& + 2\theta_{\tilde{u}_k} \theta_{\tilde{u}_l} (\mathbf{f}_u)^*_{ik} (\mathbf{m}_U^2)_{kl} (\mathbf{f}_u)^T_{lj} + 2\theta_{\tilde{d}_k} \theta_{\tilde{d}_l} (\mathbf{f}_d)^*_{ik} (\mathbf{m}_D^2)_{kl} (\mathbf{f}_d)^T_{lj} \\
& + 2\theta_{\tilde{u}_k} (\mathbf{a}_u)^*_{ik} (\mathbf{a}_u)^T_{kj} + 2\theta_{\tilde{u}_k} (\tilde{\mu}^* \mathbf{f}_u^{h_u})^*_{ik} (\tilde{\mu}^* \mathbf{f}_u^{h_u})^T_{kj} \\
& + 2\theta_{\tilde{d}_k} (\mathbf{a}_d)^*_{ik} (\mathbf{a}_d)^T_{kj} + 2\theta_{\tilde{d}_k} (\tilde{\mu}^* \mathbf{f}_d^{h_d})^*_{ik} (\tilde{\mu}^* \mathbf{f}_d^{h_d})^T_{kj} \\
& - \frac{2}{9} \theta_{\tilde{B}} (M_1^2 + M_1'^2) (\tilde{\mathbf{g}}'^Q)_{ik} (\tilde{\mathbf{g}}'^Q)^\dagger_{kj} - 6\theta_{\tilde{W}} (M_2^2 + M_2'^2) (\tilde{\mathbf{g}}^Q)_{ik} (\tilde{\mathbf{g}}^Q)^\dagger_{kj} \\
& - \frac{32}{3} \theta_{\tilde{g}} (M_3^2 + M_3'^2) (\tilde{\mathbf{g}}_s^Q)_{ik} (\tilde{\mathbf{g}}_s^Q)^\dagger_{kj} \\
& - 4\theta_{\tilde{h}} |\mu|^2 \left[ (\tilde{\mathbf{f}}_u^Q)^*_{ik} (\tilde{\mathbf{f}}_u^Q)^T_{kj} + (\tilde{\mathbf{f}}_d^Q)^*_{ik} (\tilde{\mathbf{f}}_d^Q)^T_{kj} \right] \\
& - 3 \left( \theta_{\tilde{Q}_i} + \theta_{\tilde{Q}_j} \right) \left( \frac{1}{36} g'^2 + \frac{3}{4} g_2^2 + \frac{4}{3} g_3^2 \right) (\mathbf{m}_Q^2)_{ij} \\
& + \theta_{\tilde{Q}_l} \left[ \frac{1}{18} \theta_{\tilde{B}} (\tilde{\mathbf{g}}'^Q)_{ik} (\tilde{\mathbf{g}}'^Q)^\dagger_{kl} + \frac{3}{2} \theta_{\tilde{W}} (\tilde{\mathbf{g}}^Q)_{ik} (\tilde{\mathbf{g}}^Q)^\dagger_{kl} + \frac{8}{3} \theta_{\tilde{g}} (\tilde{\mathbf{g}}_s^Q)_{ik} (\tilde{\mathbf{g}}_s^Q)^\dagger_{kl} \right. \\
& \quad \left. + \theta_{\tilde{h}} (\tilde{\mathbf{f}}_u^Q)^*_{ik} (\tilde{\mathbf{f}}_u^Q)^T_{kl} + \theta_{\tilde{h}} (\tilde{\mathbf{f}}_d^Q)^*_{ik} (\tilde{\mathbf{f}}_d^Q)^T_{kl} \right] (\mathbf{m}_Q^2)_{lj} \\
& + \theta_{\tilde{Q}_k} (\mathbf{m}_Q^2)_{ik} \left[ \frac{1}{18} \theta_{\tilde{B}} (\tilde{\mathbf{g}}'^Q)_{kl} (\tilde{\mathbf{g}}'^Q)^\dagger_{lj} + \frac{3}{2} \theta_{\tilde{W}} (\tilde{\mathbf{g}}^Q)_{kl} (\tilde{\mathbf{g}}^Q)^\dagger_{lj} + \frac{8}{3} \theta_{\tilde{g}} (\tilde{\mathbf{g}}_s^Q)_{kl} (\tilde{\mathbf{g}}_s^Q)^\dagger_{lj} \right. \\
& \quad \left. + \theta_{\tilde{h}} (\tilde{\mathbf{f}}_u^Q)^*_{kl} (\tilde{\mathbf{f}}_u^Q)^T_{lj} + \theta_{\tilde{h}} (\tilde{\mathbf{f}}_d^Q)^*_{kl} (\tilde{\mathbf{f}}_d^Q)^T_{lj} \right] ,
\end{aligned} \tag{B16}$$

$$\begin{aligned}
(4\pi)^2 \frac{d(\mathbf{m}_U^2)_{ij}}{dt} = & \left\{ -\frac{4}{3}g'^2\delta_{ij} + 4 [(\mathbf{f}_u)^T(\mathbf{f}_u)^*]_{ij} \right\} (m_{H_u}^2 + |\tilde{\mu}|^2) + \frac{4}{3}g'^2\delta_{ij} (m_{H_d}^2 + |\tilde{\mu}|^2) \\
& + \frac{8}{3}\theta_{\tilde{u}_k}g'^2\delta_{ij} (\mathbf{m}_U^2)_{kk} + \frac{8}{3}\theta_{\tilde{u}_k}\theta_{\tilde{u}_l} \left[ \frac{1}{3}g'^2 + g_3^2 \right] \delta_{ik}\delta_{lj} (\mathbf{m}_U^2)_{kl} \\
& - \frac{4}{3}\theta_{\tilde{Q}_k}g'^2\delta_{ij} (\mathbf{m}_Q^2)_{kk} - \frac{4}{3}\theta_{\tilde{d}_k}g'^2\delta_{ij} (\mathbf{m}_D^2)_{kk} + \frac{4}{3}\theta_{\tilde{L}_k}g'^2\delta_{ij} (\mathbf{m}_L^2)_{kk} \\
& - \frac{4}{3}\theta_{\tilde{e}_k}g'^2\delta_{ij} (\mathbf{m}_E^2)_{kk} + 4\theta_{\tilde{Q}_k}\theta_{\tilde{Q}_l}(\mathbf{f}_u)_{ik}^T(\mathbf{f}_u)_{lj}^* (\mathbf{m}_Q^2)_{kl} \\
& + 4\theta_{\tilde{Q}_k}(\mathbf{a}_u)_{ik}^T(\mathbf{a}_u)_{kj}^* + 4\theta_{\tilde{Q}_k}(\tilde{\mu}^*\mathbf{f}_u^{h_u})_{ik}^T(\tilde{\mu}^*\mathbf{f}_u^{h_u})_{kj}^* \\
& - \frac{32}{9}\theta_{\tilde{B}}(M_1^2 + M_1'^2) (\tilde{\mathbf{g}}'^{uR})_{ik}^\dagger(\tilde{\mathbf{g}}'^{uR})_{kj} - \frac{32}{3}\theta_{\tilde{g}}(M_3^2 + M_3'^2) (\tilde{\mathbf{g}}_s^{uR})_{ik}^\dagger(\tilde{\mathbf{g}}_s^{uR})_{kj} \\
& - 8\theta_{\tilde{h}}|\mu|^2 (\tilde{\mathbf{f}}_u^{uR})_{ik}^T(\tilde{\mathbf{f}}_u^{uR})_{kj}^* - 3(\theta_{\tilde{u}_i} + \theta_{\tilde{u}_j}) \left( \frac{4}{9}g'^2 + \frac{4}{3}g_3^2 \right) (\mathbf{m}_U^2)_{ij} \\
& + \theta_{\tilde{u}_l} \left[ \frac{8}{9}\theta_{\tilde{B}}(\tilde{\mathbf{g}}'^{uR})_{ik}^\dagger(\tilde{\mathbf{g}}'^{uR})_{kl} + \frac{8}{3}\theta_{\tilde{g}}(\tilde{\mathbf{g}}_s^{uR})_{ik}^\dagger(\tilde{\mathbf{g}}_s^{uR})_{kl} + 2\theta_{\tilde{h}}(\tilde{\mathbf{f}}_u^{uR})_{ik}^T(\tilde{\mathbf{f}}_u^{uR})_{kl}^* \right] (\mathbf{m}_U^2)_{lj} \\
& + \theta_{\tilde{u}_k} (\mathbf{m}_U^2)_{ik} \left[ \frac{8}{9}\theta_{\tilde{B}}(\tilde{\mathbf{g}}'^{uR})_{kl}^\dagger(\tilde{\mathbf{g}}'^{uR})_{lj} + \frac{8}{3}\theta_{\tilde{g}}(\tilde{\mathbf{g}}_s^{uR})_{kl}^\dagger(\tilde{\mathbf{g}}_s^{uR})_{lj} + 2\theta_{\tilde{h}}(\tilde{\mathbf{f}}_u^{uR})_{kl}^T(\tilde{\mathbf{f}}_u^{uR})_{lj}^* \right], 
\end{aligned} \tag{B17}$$

$$\begin{aligned}
(4\pi)^2 \frac{d(\mathbf{m}_D^2)_{ij}}{dt} = & \frac{2}{3}g'^2\delta_{ij} (m_{H_u}^2 + |\tilde{\mu}|^2) + \left\{ -\frac{2}{3}g'^2\delta_{ij} + 4 [(\mathbf{f}_d)^T(\mathbf{f}_d)^*]_{ij} \right\} (m_{H_d}^2 + |\tilde{\mu}|^2) \\
& - \frac{4}{3}\theta_{\tilde{u}_k}g'^2\delta_{ij} (\mathbf{m}_U^2)_{kk} + \frac{2}{3}\theta_{\tilde{Q}_k}g'^2\delta_{ij} (\mathbf{m}_Q^2)_{kk} + \frac{2}{3}\theta_{\tilde{d}_k}g'^2\delta_{ij} (\mathbf{m}_D^2)_{kk} \\
& + \frac{2}{3}\theta_{\tilde{d}_k}\theta_{\tilde{d}_l} \left[ \frac{1}{3}g'^2 + 4g_3^2 \right] \delta_{ik}\delta_{lj} (\mathbf{m}_D^2)_{kl} - \frac{2}{3}\theta_{\tilde{L}_k}g'^2\delta_{ij} (\mathbf{m}_L^2)_{kk} \\
& + \frac{2}{3}\theta_{\tilde{e}_k}g'^2\delta_{ij} (\mathbf{m}_E^2)_{kk} + 4\theta_{\tilde{Q}_k}\theta_{\tilde{Q}_l}(\mathbf{f}_d)_{ik}^T(\mathbf{f}_d)_{lj}^* (\mathbf{m}_Q^2)_{kl} \\
& + 4\theta_{\tilde{Q}_k}(\mathbf{a}_d)_{ik}^T(\mathbf{a}_d)_{kj}^* + 4\theta_{\tilde{Q}_k}(\tilde{\mu}^*\mathbf{f}_d^{h_d})_{ik}^T(\tilde{\mu}^*\mathbf{f}_d^{h_d})_{kj}^* \\
& - \frac{8}{9}\theta_{\tilde{B}}(M_1^2 + M_1'^2) (\tilde{\mathbf{g}}'^{dR})_{ik}^\dagger(\tilde{\mathbf{g}}'^{dR})_{kj} - \frac{32}{3}\theta_{\tilde{g}}(M_3^2 + M_3'^2) (\tilde{\mathbf{g}}_s^{dR})_{ik}^\dagger(\tilde{\mathbf{g}}_s^{dR})_{kj} \\
& - 8\theta_{\tilde{h}}|\mu|^2 (\tilde{\mathbf{f}}_d^{dR})_{ik}^T(\tilde{\mathbf{f}}_d^{dR})_{kj}^* - 3(\theta_{\tilde{d}_i} + \theta_{\tilde{d}_j}) \left( \frac{1}{9}g'^2 + \frac{4}{3}g_3^2 \right) (\mathbf{m}_D^2)_{ij} \\
& + \theta_{\tilde{d}_l} \left[ \frac{2}{9}\theta_{\tilde{B}}(\tilde{\mathbf{g}}'^{dR})_{ik}^\dagger(\tilde{\mathbf{g}}'^{dR})_{kl} + \frac{8}{3}\theta_{\tilde{g}}(\tilde{\mathbf{g}}_s^{dR})_{ik}^\dagger(\tilde{\mathbf{g}}_s^{dR})_{kl} + 2\theta_{\tilde{h}}(\tilde{\mathbf{f}}_d^{dR})_{ik}^T(\tilde{\mathbf{f}}_d^{dR})_{kl}^* \right] (\mathbf{m}_D^2)_{lj} \\
& + \theta_{\tilde{d}_k} (\mathbf{m}_D^2)_{ik} \left[ \frac{2}{9}\theta_{\tilde{B}}(\tilde{\mathbf{g}}'^{dR})_{kl}^\dagger(\tilde{\mathbf{g}}'^{dR})_{lj} + \frac{8}{3}\theta_{\tilde{g}}(\tilde{\mathbf{g}}_s^{dR})_{kl}^\dagger(\tilde{\mathbf{g}}_s^{dR})_{lj} + 2\theta_{\tilde{h}}(\tilde{\mathbf{f}}_d^{dR})_{kl}^T(\tilde{\mathbf{f}}_d^{dR})_{lj}^* \right], 
\end{aligned} \tag{B18}$$

$$\begin{aligned}
(4\pi)^2 \frac{d(\mathbf{m}_L^2)_{ij}}{dt} = & -g'^2 \delta_{ij} (m_{H_u}^2 + |\tilde{\mu}|^2) + \left\{ g'^2 \delta_{ij} + 2 [(\mathbf{f}_e)^* (\mathbf{f}_e)^T]_{ij} \right\} (m_{H_d}^2 + |\tilde{\mu}|^2) \\
& + 2\theta_{\tilde{u}_k} g'^2 \delta_{ij} (\mathbf{m}_U^2)_{kk} - \theta_{\tilde{Q}_k} g'^2 \delta_{ij} (\mathbf{m}_Q^2)_{kk} - \theta_{\tilde{d}_k} g'^2 \delta_{ij} (\mathbf{m}_D^2)_{kk} \\
& + \theta_{\tilde{L}_k} g'^2 \delta_{ij} (\mathbf{m}_L^2)_{kk} + \theta_{\tilde{L}_k} \theta_{\tilde{L}_l} \left( \frac{g'^2}{2} + \frac{3g_2^2}{2} \right) \delta_{ik} \delta_{lj} (\mathbf{m}_L^2)_{kl} \\
& - \theta_{\tilde{e}_k} g'^2 \delta_{ij} (\mathbf{m}_E^2)_{kk} + 2\theta_{\tilde{e}_k} \theta_{\tilde{e}_l} (\mathbf{f}_e)_{ik}^* (\mathbf{m}_E^2)_{kl} (\mathbf{f}_e)_{lj}^T \\
& + 2\theta_{\tilde{e}_k} (\mathbf{a}_e)_{ik}^* (\mathbf{a}_e)_{kj}^T + 2\theta_{\tilde{e}_k} (\tilde{\mu}^* \mathbf{f}_e^{hd})_{ik}^* (\tilde{\mu}^* \mathbf{f}_e^{hd})_{kj}^T \\
& - 2\theta_{\tilde{B}} (M_1^2 + M_1'^2) (\tilde{\mathbf{g}}'^L)_{ik} (\tilde{\mathbf{g}}'^L)_{kj}^\dagger - 6\theta_{\tilde{W}} (M_2^2 + M_2'^2) (\tilde{\mathbf{g}}^L)_{ik} (\tilde{\mathbf{g}}^L)_{kj}^\dagger \\
& - 4\theta_{\tilde{h}} |\mu|^2 (\tilde{\mathbf{f}}_e^L)_{ik}^* (\tilde{\mathbf{f}}_e^L)_{kj}^T - 3 \left( \theta_{\tilde{L}_i} + \theta_{\tilde{L}_j} \right) \left( \frac{1}{4} g'^2 + \frac{3}{4} g_2^2 \right) (\mathbf{m}_L^2)_{ij} \\
& + \theta_{\tilde{L}_l} \left[ \frac{1}{2} (\tilde{\mathbf{g}}'^L)_{ik} (\tilde{\mathbf{g}}'^L)_{kl}^\dagger \theta_{\tilde{B}} + \frac{3}{2} (\tilde{\mathbf{g}}^L)_{ik} (\tilde{\mathbf{g}}^L)_{kl}^\dagger \theta_{\tilde{W}} + (\tilde{\mathbf{f}}_e^L)_{ik}^* (\tilde{\mathbf{f}}_e^L)_{kl}^T \theta_{\tilde{h}} \right] (\mathbf{m}_L^2)_{lj} \\
& + \theta_{\tilde{L}_k} (\mathbf{m}_L^2)_{ik} \left[ \frac{1}{2} (\tilde{\mathbf{g}}'^L)_{kl} (\tilde{\mathbf{g}}'^L)_{lj}^\dagger \theta_{\tilde{B}} + \frac{3}{2} (\tilde{\mathbf{g}}^L)_{kl} (\tilde{\mathbf{g}}^L)_{lj}^\dagger \theta_{\tilde{W}} + (\tilde{\mathbf{f}}_e^L)_{kl}^* (\tilde{\mathbf{f}}_e^L)_{lj}^T \theta_{\tilde{h}} \right],
\end{aligned} \tag{B19}$$

$$\begin{aligned}
(4\pi)^2 \frac{d(\mathbf{m}_E^2)_{ij}}{dt} = & 2g'^2 \delta_{ij} (m_{H_u}^2 + |\tilde{\mu}|^2) + \left\{ -2g'^2 \delta_{ij} + 4 [(\mathbf{f}_e)^T (\mathbf{f}_e)^*]_{ij} \right\} (m_{H_d}^2 + |\tilde{\mu}|^2) \\
& - 4\theta_{\tilde{u}_k} g'^2 \delta_{ij} (\mathbf{m}_U^2)_{kk} + 2\theta_{\tilde{Q}_k} g'^2 \delta_{ij} (\mathbf{m}_Q^2)_{kk} + 2\theta_{\tilde{d}_k} g'^2 \delta_{ij} (\mathbf{m}_D^2)_{kk} \\
& - 2\theta_{\tilde{L}_k} g'^2 \delta_{ij} (\mathbf{m}_L^2)_{kk} + 2\theta_{\tilde{e}_k} g'^2 \delta_{ij} (\mathbf{m}_E^2)_{kk} \\
& + 2\theta_{\tilde{e}_k} \theta_{\tilde{e}_l} g'^2 \delta_{lj} \delta_{ik} (\mathbf{m}_E^2)_{kl} + 4\theta_{\tilde{L}_k} \theta_{\tilde{L}_l} (\mathbf{f}_e)_{ik}^T (\mathbf{m}_L^2)_{kl} (\mathbf{f}_e)_{lj}^* \\
& + 4\theta_{\tilde{L}_k} (\mathbf{a}_e)_{ik}^T (\mathbf{a}_e)_{kj}^* + 4\theta_{\tilde{L}_k} (\tilde{\mu}^* \mathbf{f}_e^{hd})_{ik}^T (\tilde{\mu}^* \mathbf{f}_e^{hd})_{kj}^* \\
& - 8\theta_{\tilde{B}} (M_1^2 + M_1'^2) (\tilde{\mathbf{g}}'^{eR})_{ik}^\dagger (\tilde{\mathbf{g}}'^{eR})_{kj} - 8\theta_{\tilde{h}} |\mu|^2 (\tilde{\mathbf{f}}_e^{eR})_{ik}^T (\tilde{\mathbf{f}}_e^{eR})_{kj}^* \\
& - 3 (\theta_{\tilde{e}_i} + \theta_{\tilde{e}_j}) g'^2 (\mathbf{m}_E^2)_{ij} \\
& + \theta_{\tilde{e}_l} \left[ 2(\tilde{\mathbf{g}}'^{eR})_{ik}^\dagger (\tilde{\mathbf{g}}'^{eR})_{kl} \theta_{\tilde{B}} + 2(\tilde{\mathbf{f}}_e^{eR})_{ik}^T (\tilde{\mathbf{f}}_e^{eR})_{kl}^* \theta_{\tilde{h}} \right] (\mathbf{m}_E^2)_{lj} \\
& + \theta_{\tilde{e}_k} (\mathbf{m}_E^2)_{ik} \left[ 2(\tilde{\mathbf{g}}'^{eR})_{kl}^\dagger (\tilde{\mathbf{g}}'^{eR})_{lj} \theta_{\tilde{B}} + 2(\tilde{\mathbf{f}}_e^{eR})_{kl}^T (\tilde{\mathbf{f}}_e^{eR})_{lj}^* \theta_{\tilde{h}} \right].
\end{aligned} \tag{B20}$$

Below the scale  $Q = m_H$ , as discussed in Sec. IV B, the trilinear couplings to the doublet  $\mathbf{h}$ , and the mass parameter  $m_h^2$  remain in the theory, with RGEs given by,

$$\begin{aligned}
& (4\pi)^2 \frac{d[s(\mathbf{a}_u)_{ij} - c(\tilde{\mu}^* \mathbf{f}_u^{h_u})_{ij}]}{dt} \\
&= \theta_h \theta_{\tilde{u}_k} [s(\mathbf{a}_u)_{ik} - c(\tilde{\mu}^* \mathbf{f}_u^{h_u})_{ik}] \left[ \frac{2g'^2}{3} (c^2 - s^2) \delta_{kj} + 2s^2 [(\mathbf{f}_u)^\dagger (\mathbf{f}_u)]_{kj} \right] \\
&+ \theta_{\tilde{u}_l} \theta_{\tilde{Q}_k} \left[ -2 \left( \frac{g'^2}{9} + \frac{4g_3^2}{3} \right) \delta_{ik} \delta_{lj} + 6(\mathbf{f}_u)_{ij} (\mathbf{f}_u)_{lk}^\dagger \right] [s(\mathbf{a}_u)_{kl} - c(\tilde{\mu}^* \mathbf{f}_u^{h_u})_{kl}] \\
&+ 2\theta_h \theta_{\tilde{Q}_k} \left[ \left( \frac{g'^2}{12} - \frac{3g_2^2}{4} \right) (s^2 - c^2) \delta_{ik} + 2s^2 [(\mathbf{f}_u) (\mathbf{f}_u)^\dagger]_{ik} - c^2 [(\mathbf{f}_d) (\mathbf{f}_d)^\dagger]_{ik} \right] \\
&\hspace{15em} \times [s(\mathbf{a}_u)_{kj} - c(\tilde{\mu}^* \mathbf{f}_u^{h_u})_{kj}] \\
&+ \frac{2}{3} \theta_{\tilde{B}} s (M_1 - iM'_1) \\
&\quad \times \left( \theta_{\tilde{h}} (\tilde{g}^{h_u})^* (\tilde{\mathbf{g}}'^Q)_{ik}^* (\tilde{\mathbf{f}}_u^{u_R})_{kj} - \frac{4}{3} (\tilde{\mathbf{g}}'^Q)_{ik}^* (\mathbf{f}_u)_{kl} (\tilde{\mathbf{g}}'^{u_R})_{kj}^* - 4\theta_{\tilde{h}} (\tilde{\mathbf{f}}_u^Q)_{ik} (\tilde{\mathbf{g}}'^{u_R})_{kj}^* (\tilde{g}^{h_u})^* \right) \\
&- \frac{32}{3} \theta_{\tilde{g}} s (M_3 - iM'_3) (\tilde{\mathbf{g}}_s^Q)_{ik}^* (\mathbf{f}_u)_{kl} (\tilde{\mathbf{g}}_s^{u_R})_{lj}^* - 6\theta_{\tilde{W}} \theta_{\tilde{h}} s (M_2 - iM'_2) (\tilde{g}^{h_u})^* (\tilde{\mathbf{g}}_s^Q)_{ik}^* (\tilde{\mathbf{f}}_u^{u_R})_{kj} \\
&+ \frac{2}{3} \theta_{\tilde{B}} \theta_{\tilde{h}} c \mu^* \tilde{g}^{h_d} \left( 4(\tilde{\mathbf{f}}_u^Q)_{ik} (\tilde{\mathbf{g}}'^{u_R})_{kj}^* - (\tilde{\mathbf{g}}'^Q)_{ik}^* (\tilde{\mathbf{f}}_u^{u_R})_{kj} \right) + 6\theta_{\tilde{h}} \theta_{\tilde{W}} c \mu^* \tilde{g}^{h_d} (\tilde{\mathbf{g}}_s^Q)_{ik}^* (\tilde{\mathbf{f}}_u^{u_R})_{kj} \\
&- 4\theta_{\tilde{h}} c \mu^* (\tilde{\mathbf{f}}_d^Q)_{ik} (\mathbf{f}_d^\dagger)_{kl} (\tilde{\mathbf{f}}_u^{u_R})_{lj} \\
&+ \theta_{\tilde{u}_k} [s(\mathbf{a}_u)_{ik} - c(\tilde{\mu}^* \mathbf{f}_u^{h_u})_{ik}] \left[ \frac{8}{9} \theta_{\tilde{B}} (\tilde{\mathbf{g}}'^{u_R})_{kl}^T (\tilde{\mathbf{g}}'^{u_R})_{lj}^* + \frac{8}{3} \theta_{\tilde{g}} (\tilde{\mathbf{g}}_s^{u_R})_{kl}^T (\tilde{\mathbf{g}}_s^{u_R})_{lj}^* + 2\theta_{\tilde{h}} (\tilde{\mathbf{f}}_u^{u_R})_{kl}^\dagger (\tilde{\mathbf{f}}_u^{u_R})_{lj} \right] \\
&+ \theta_h \left[ 3s^2 (\mathbf{f}_u^\dagger)_{kl} (\mathbf{f}_u)_{lk} + c^2 \left\{ 3(\mathbf{f}_d^\dagger)_{kl} (\mathbf{f}_d)_{lk} + (\mathbf{f}_e^\dagger)_{kl} (\mathbf{f}_e)_{lk} \right\} \right] [s(\mathbf{a}_u)_{ij} - c(\tilde{\mu}^* \mathbf{f}_u^{h_u})_{ij}] \\
&+ \frac{1}{2} \theta_h \theta_{\tilde{h}} \left[ c^2 \left\{ \theta_{\tilde{B}} |\tilde{g}^{h_d}|^2 + 3\theta_{\tilde{W}} |\tilde{g}^{h_d}|^2 \right\} + s^2 \left\{ \theta_{\tilde{B}} |\tilde{g}^{h_u}|^2 + 3\theta_{\tilde{W}} |\tilde{g}^{h_u}|^2 \right\} \right] \\
&\hspace{15em} \times [s(\mathbf{a}_u)_{ij} - c(\tilde{\mu}^* \mathbf{f}_u^{h_u})_{ij}] \\
&+ \theta_{\tilde{Q}_l} \left[ \theta_{\tilde{h}} (\tilde{\mathbf{f}}_u^Q)_{ik} (\tilde{\mathbf{f}}_u^Q)_{kl}^\dagger + \theta_{\tilde{h}} (\tilde{\mathbf{f}}_d^Q)_{ik} (\tilde{\mathbf{f}}_d^Q)_{kl}^\dagger + \frac{1}{18} \theta_{\tilde{B}} (\tilde{\mathbf{g}}'^Q)_{ik}^* (\tilde{\mathbf{g}}'^Q)_{kl}^T + \frac{3}{2} \theta_{\tilde{W}} (\tilde{\mathbf{g}}^Q)_{ik}^* (\tilde{\mathbf{g}}^Q)_{kl}^T \right. \\
&\quad \left. + \frac{8}{3} \theta_{\tilde{g}} (\tilde{\mathbf{g}}_s^Q)_{ik}^* (\tilde{\mathbf{g}}_s^Q)_{kl}^T \right] [s(\mathbf{a}_u)_{lj} - c(\tilde{\mu}^* \mathbf{f}_u^{h_u})_{lj}] \\
&- 3 \left\{ \left( \frac{1}{36} \theta_{\tilde{Q}_i} + \frac{4}{9} \theta_{\tilde{u}_j} + \frac{1}{4} \theta_h \right) g'^2 + \frac{3}{4} (\theta_{\tilde{Q}_i} + \theta_h) g_2^2 + \frac{4}{3} (\theta_{\tilde{Q}_i} + \theta_{\tilde{u}_j}) g_3^2 \right\} \\
&\hspace{15em} \times [s(\mathbf{a}_u) - c(\tilde{\mu}^* \mathbf{f}_u^{h_u})]_{ij} ,
\end{aligned} \tag{B21}$$

$$\begin{aligned}
& (4\pi)^2 \frac{d \left[ c(\mathbf{a}_d)_{ij} - s \left( \tilde{\mu}^* \mathbf{f}_d^{hd} \right)_{ij} \right]}{dt} \\
&= 2\theta_h \theta_{\tilde{Q}_k} \left[ - \left( \frac{g'^2}{12} + \frac{3g_2^2}{4} \right) (c^2 - s^2) \delta_{ik} - s^2 [(\mathbf{f}_u)(\mathbf{f}_u)^\dagger]_{ik} + 2c^2 [(\mathbf{f}_d)(\mathbf{f}_d)^\dagger]_{ik} \right] \\
&\quad \times \left[ c(\mathbf{a}_d)_{kj} - s \left( \tilde{\mu}^* \mathbf{f}_d^{hd} \right)_{kj} \right] \\
&+ \theta_{\tilde{d}_i} \theta_{\tilde{Q}_k} \left[ 2 \left( \frac{g'^2}{18} - \frac{4g_3^2}{3} \right) \delta_{ik} \delta_{lj} + 6(\mathbf{f}_d)_{lk}^\dagger (\mathbf{f}_d)_{ij} \right] \left[ c(\mathbf{a}_d)_{kl} - s \left( \tilde{\mu}^* \mathbf{f}_d^{hd} \right)_{kl} \right] \\
&+ 2\theta_{\tilde{e}_i} \theta_{\tilde{L}_k} (\mathbf{f}_d)_{ij} (\mathbf{f}_e)_{lk}^\dagger \left[ c(\mathbf{a}_e)_{kl} - s \left( \tilde{\mu}^* \mathbf{f}_e^{hd} \right)_{kl} \right] \\
&+ \theta_h \theta_{\tilde{d}_k} \left[ c(\mathbf{a}_d)_{ik} - s \left( \tilde{\mu}^* \mathbf{f}_d^{hd} \right)_{ik} \right] \left[ -\frac{g'^2}{3} (c^2 - s^2) \delta_{kj} + 2c^2 [(\mathbf{f}_d)^\dagger (\mathbf{f}_d)]_{kj} \right] \\
&- 4\theta_{\tilde{h}} s \mu^* (\tilde{\mathbf{f}}_u^Q)_{ik} (\mathbf{f}_u^\dagger)_{kl} (\tilde{\mathbf{f}}_d^{dR})_{lj} + \frac{2}{3} \theta_{\tilde{B}} \theta_{\tilde{h}} s \mu^* \tilde{g}^{hu} \left( 2(\tilde{\mathbf{f}}_d^Q)_{ik} (\tilde{\mathbf{g}}'^{dR})_{kj}^* + (\tilde{\mathbf{g}}'^Q)_{ik}^* (\tilde{\mathbf{f}}_d^{dR})_{kj} \right) \\
&+ 6\theta_{\tilde{h}} \theta_{\tilde{W}} s \mu^* \tilde{g}^{hu} (\tilde{\mathbf{g}}^Q)_{ik}^* (\tilde{\mathbf{f}}_d^{dR})_{kj} \\
&+ \frac{2}{3} \theta_{\tilde{B}} c (M_1 - iM'_1) \\
&\quad \times \left( -\theta_{\tilde{h}} (\tilde{g}^{hd})^* (\tilde{\mathbf{g}}'^Q)_{ik}^* (\tilde{\mathbf{f}}_d^{dR})_{kj} + \frac{2}{3} (\tilde{\mathbf{g}}'^Q)_{ik}^* (\mathbf{f}_d)_{kl} (\tilde{\mathbf{g}}'^{dR})_{lj}^* - 2\theta_{\tilde{h}} (\tilde{\mathbf{f}}_d^Q)_{ik} (\tilde{\mathbf{g}}'^{dR})_{kj}^* (\tilde{g}^{hd})^* \right) \\
&- \frac{32}{3} \theta_{\tilde{g}} c (M_3 - iM'_3) (\tilde{\mathbf{g}}_s^Q)_{ik}^* (\mathbf{f}_d)_{kl} (\tilde{\mathbf{g}}_s^{dR})_{lj}^* - 6\theta_{\tilde{W}} \theta_{\tilde{h}} c (M_2 - iM'_2) (\tilde{g}^{hd})^* (\tilde{\mathbf{g}}^Q)_{ik}^* (\tilde{\mathbf{f}}_d^{dR})_{kj} \\
&+ \theta_{\tilde{Q}_l} \left[ \theta_{\tilde{h}} (\tilde{\mathbf{f}}_u^Q)_{ik} (\tilde{\mathbf{f}}_u^\dagger)_{kl} + \theta_{\tilde{h}} (\tilde{\mathbf{f}}_d^Q)_{ik} (\tilde{\mathbf{f}}_d^\dagger)_{kl} + \frac{1}{18} \theta_{\tilde{B}} (\tilde{\mathbf{g}}'^Q)_{ik} (\tilde{\mathbf{g}}'^Q)_{kl}^T + \frac{3}{2} \theta_{\tilde{W}} (\tilde{\mathbf{g}}^Q)_{ik} (\tilde{\mathbf{g}}^Q)_{kl}^T \right. \\
&\quad \left. + \frac{8}{3} \theta_{\tilde{g}} (\tilde{\mathbf{g}}_s^Q)_{ik}^* (\tilde{\mathbf{g}}_s^Q)_{kl}^T \right] \left[ c(\mathbf{a}_d)_{lj} - s \left( \tilde{\mu}^* \mathbf{f}_d^{hd} \right)_{lj} \right] \\
&+ \theta_h \left[ 3s^2 (\mathbf{f}_u)_{kl} (\mathbf{f}_u^\dagger)_{lk} + c^2 \left\{ 3(\mathbf{f}_d)_{kl} (\mathbf{f}_d^\dagger)_{lk} + (\mathbf{f}_e)_{kl} (\mathbf{f}_e^\dagger)_{lk} \right\} \right] \left[ c(\mathbf{a}_d)_{ij} - s \left( \tilde{\mu}^* \mathbf{f}_d^{hd} \right)_{ij} \right] \\
&+ \frac{1}{2} \theta_h \theta_{\tilde{h}} \left[ c^2 \left\{ \theta_{\tilde{B}} |\tilde{g}^{hd}|^2 + 3\theta_{\tilde{W}} |\tilde{g}^{hd}|^2 \right\} + s^2 \left\{ \theta_{\tilde{B}} |\tilde{g}^{hu}|^2 + 3\theta_{\tilde{W}} |\tilde{g}^{hu}|^2 \right\} \right] \\
&\quad \times \left[ c(\mathbf{a}_d)_{ij} - s \left( \tilde{\mu}^* \mathbf{f}_d^{hd} \right)_{ij} \right] \\
&+ \theta_{\tilde{d}_k} \left[ c(\mathbf{a}_d)_{ik} - s \left( \tilde{\mu}^* \mathbf{f}_d^{hd} \right)_{ik} \right] \left[ \frac{2}{9} \theta_{\tilde{B}} (\tilde{\mathbf{g}}'^{dR})_{kl}^T (\tilde{\mathbf{g}}'^{dR})_{lj}^* + \frac{8}{3} \theta_{\tilde{g}} (\tilde{\mathbf{g}}_s^{dR})_{kl}^T (\tilde{\mathbf{g}}_s^{dR})_{lj}^* + 2\theta_{\tilde{h}} (\tilde{\mathbf{f}}_d^{dR})_{kl}^\dagger (\tilde{\mathbf{f}}_d^{dR})_{lj} \right] \\
&- 3 \left\{ \left( \frac{1}{36} \theta_{\tilde{Q}_i} + \frac{1}{9} \theta_{\tilde{d}_j} + \frac{1}{4} \theta_h \right) g'^2 + \frac{3}{4} (\theta_{\tilde{Q}_i} + \theta_h) g_2^2 + \frac{4}{3} (\theta_{\tilde{Q}_i} + \theta_{\tilde{d}_j}) g_3^2 \right\} \\
&\quad \times \left[ c(\mathbf{a}_d) - s \left( \tilde{\mu}^* \mathbf{f}_d^{hd} \right) \right]_{ij}, \tag{B22}
\end{aligned}$$



$$\begin{aligned}
& (4\pi)^2 \frac{d}{dt} \left[ c(\mathbf{a}_e)_{ij} - s(\tilde{\mu}^* \mathbf{f}_e^{hd})_{ij} \right] \\
&= 2\theta_h \theta_{\tilde{L}_k} \left[ \left( \frac{g'^2}{4} - \frac{3g_2^2}{4} \right) (c^2 - s^2) \delta_{ik} + 2c^2 [(\mathbf{f}_e)(\mathbf{f}_e)^\dagger]_{ik} \right] \left[ c(\mathbf{a}_e)_{kj} - s(\tilde{\mu}^* \mathbf{f}_e^{hd})_{kj} \right] \\
&\quad + \theta_{\tilde{e}_i} \theta_{\tilde{L}_k} \left[ -g'^2 \delta_{ik} \delta_{lj} + 2(\mathbf{f}_e)_{lk}^\dagger (\mathbf{f}_e)_{ij} \right] \left[ c(\mathbf{a}_e)_{kl} - s(\tilde{\mu}^* \mathbf{f}_e^{hd})_{kl} \right] \\
&\quad + 6\theta_{\tilde{d}_i} \theta_{\tilde{Q}_k} (\mathbf{f}_e)_{ij} (\mathbf{f}_d)_{lk}^\dagger \left[ c(\mathbf{a}_d)_{kl} - s(\tilde{\mu}^* \mathbf{f}_d^{hd})_{kl} \right] \\
&\quad + \theta_h \theta_{\tilde{e}_k} \left[ c(\mathbf{a}_e)_{ik} - s(\tilde{\mu}^* \mathbf{f}_e^{hd})_{ik} \right] \left[ -g'^2 (c^2 - s^2) \delta_{kj} + 2c^2 [(\mathbf{f}_e)^\dagger (\mathbf{f}_e)]_{kj} \right] \\
&\quad + 2\theta_{\tilde{B}} \theta_{\tilde{h}} s \mu^* \tilde{g}^{hu} \left( 2(\tilde{\mathbf{f}}_e^L)_{ik} (\tilde{\mathbf{g}}'^{eR})_{kj}^* - (\tilde{\mathbf{g}}'^L)_{ik}^* (\tilde{\mathbf{f}}_e^{eR})_{kj} \right) + 6\theta_{\tilde{h}} \theta_{\tilde{W}} s \mu^* \tilde{g}^{hu} (\tilde{\mathbf{g}}^L)_{ik}^* (\tilde{\mathbf{f}}_e^{eR})_{kj} \\
&\quad + 2\theta_{\tilde{B}} c (M_1 - iM'_1) \\
&\quad \quad \times \left( \theta_{\tilde{h}} (\tilde{g}^{hd})^* (\tilde{\mathbf{g}}'^L)_{ik}^* (\tilde{\mathbf{f}}_e^{eR})_{kj} - 2(\tilde{\mathbf{g}}'^L)_{ik}^* (\mathbf{f}_e)_{kl} (\tilde{\mathbf{g}}'^{eR})_{lj}^* - 2\theta_{\tilde{h}} (\tilde{\mathbf{f}}_e^L)_{ik} (\tilde{\mathbf{g}}'^{eR})_{kj}^* (\tilde{g}^{hd})^* \right) \\
&\quad - 6\theta_{\tilde{W}} \theta_{\tilde{h}} c (M_2 - iM'_2) (\tilde{g}^{hd})^* (\tilde{\mathbf{g}}^L)_{ik}^* (\tilde{\mathbf{f}}_e^{eR})_{kj} \\
&\quad + \theta_{\tilde{L}_i} \left[ \theta_{\tilde{h}} (\tilde{\mathbf{f}}_e^L)_{ik} (\tilde{\mathbf{f}}_e^L)_{kl}^\dagger + \frac{1}{2} \theta_{\tilde{B}} (\tilde{\mathbf{g}}'^L)_{ik}^* (\tilde{\mathbf{g}}'^L)_{kl}^T + \frac{3}{2} \theta_{\tilde{W}} (\tilde{\mathbf{g}}^L)_{ik}^* (\tilde{\mathbf{g}}^L)_{kl}^T \right] \left[ c(\mathbf{a}_e)_{lj} - s(\tilde{\mu}^* \mathbf{f}_e^{hd})_{lj} \right] \\
&\quad + \theta_h \left[ 3s^2 (\mathbf{f}_u)_{kl} (\mathbf{f}_u^\dagger)_{lk} + c^2 \left\{ 3(\mathbf{f}_d)_{kl} (\mathbf{f}_d^\dagger)_{lk} + (\mathbf{f}_e)_{kl} (\mathbf{f}_e^\dagger)_{lk} \right\} \right] \left[ c(\mathbf{a}_e)_{ij} - s(\tilde{\mu}^* \mathbf{f}_e^{hd})_{ij} \right] \\
&\quad + \frac{1}{2} \theta_h \theta_{\tilde{h}} \left[ c^2 \left\{ \theta_{\tilde{B}} |\tilde{g}^{hd}|^2 + 3\theta_{\tilde{W}} |\tilde{g}^{hd}|^2 \right\} + s^2 \left\{ \theta_{\tilde{B}} |\tilde{g}^{hu}|^2 + 3\theta_{\tilde{W}} |\tilde{g}^{hu}|^2 \right\} \right] \\
&\quad \quad \quad \times \left[ c(\mathbf{a}_e)_{ij} - s(\tilde{\mu}^* \mathbf{f}_e^{hd})_{ij} \right] \\
&\quad + \theta_{\tilde{e}_k} \left[ c(\mathbf{a}_e)_{ik} - s(\tilde{\mu}^* \mathbf{f}_e^{hd})_{ik} \right] \left[ 2\theta_{\tilde{B}} (\tilde{\mathbf{g}}'^{eR})_{kl}^T (\tilde{\mathbf{g}}'^{eR})_{lj}^* + 2\theta_{\tilde{h}} (\tilde{\mathbf{f}}_e^{eR})_{kl}^\dagger (\tilde{\mathbf{f}}_e^{eR})_{lj} \right] \\
&\quad - 3 \left\{ \left( \frac{1}{4} \theta_{\tilde{L}_i} + \theta_{\tilde{e}_j} + \frac{1}{4} \theta_h \right) g'^2 + \frac{3}{4} (\theta_{\tilde{L}_i} + \theta_h) g_2^2 \right\} \left[ c(\mathbf{a}_e) - s(\tilde{\mu}^* \mathbf{f}_e^{hd}) \right]_{ij} ,
\end{aligned} \tag{B23}$$

$$\begin{aligned}
& (4\pi)^2 \frac{d \left[ s^2 (m_{H_u}^2 + |\tilde{\mu}|^2) + c^2 (m_{H_d}^2 + |\tilde{\mu}|^2) - sc(b+b^*) \right]}{dt} \\
&= \frac{3}{2} \theta_h \left[ g'^2 + g_2^2 \right] (c^2 - s^2)^2 \left[ s^2 (m_{H_u}^2 + |\tilde{\mu}|^2) + c^2 (m_{H_d}^2 + |\tilde{\mu}|^2) - sc(b+b^*) \right] \\
&\quad + \theta_{\tilde{u}_k} \theta_{\tilde{u}_l} \left[ -2g'^2 (s^2 - c^2) \delta_{lk} + 6s^2 [(\mathbf{f}_u)^T (\mathbf{f}_u)^*]_{lk} \right] (\mathbf{m}_U^2)_{kl} \\
&\quad + \theta_{\tilde{Q}_k} \theta_{\tilde{Q}_l} \left[ g'^2 (s^2 - c^2) \delta_{lk} + 6s^2 [(\mathbf{f}_u)^* (\mathbf{f}_u)^T]_{lk} + 6c^2 [(\mathbf{f}_d)^* (\mathbf{f}_d)^T]_{lk} \right] (\mathbf{m}_Q^2)_{kl} \\
&\quad + \theta_{\tilde{d}_k} \theta_{\tilde{d}_l} \left[ g'^2 (s^2 - c^2) \delta_{lk} + 6c^2 [(\mathbf{f}_d)^T (\mathbf{f}_d)^*]_{lk} \right] (\mathbf{m}_D^2)_{kl} \\
&\quad + \theta_{\tilde{L}_k} \theta_{\tilde{L}_l} \left[ -g'^2 (s^2 - c^2) \delta_{lk} + 2c^2 [(\mathbf{f}_e)^* (\mathbf{f}_e)^T]_{lk} \right] (\mathbf{m}_L^2)_{kl} \\
&\quad + \theta_{\tilde{e}_k} \theta_{\tilde{e}_l} \left[ g'^2 (s^2 - c^2) \delta_{lk} + 2c^2 [(\mathbf{f}_e)^T (\mathbf{f}_e)^*]_{lk} \right] (\mathbf{m}_E^2)_{kl} \\
&\quad + 6\theta_{\tilde{u}_k} \theta_{\tilde{Q}_l} \left[ s(\mathbf{a}_u)_{lk} - c(\tilde{\mu}^* \mathbf{f}_u^{h_u})_{lk} \right] \left[ s(\mathbf{a}_u)_{kl}^\dagger - c(\tilde{\mu}^* \mathbf{f}_u^{h_u})_{kl}^\dagger \right] \\
&\quad + 6\theta_{\tilde{Q}_l} \theta_{\tilde{d}_k} \left[ c(\mathbf{a}_d)_{lk} - s(\tilde{\mu}^* \mathbf{f}_d^{h_d})_{lk} \right] \left[ c(\mathbf{a}_d)_{kl}^\dagger - s(\tilde{\mu}^* \mathbf{f}_d^{h_d})_{kl}^\dagger \right] \\
&\quad + 2\theta_{\tilde{L}_l} \theta_{\tilde{e}_k} \left[ c(\mathbf{a}_e)_{lk} - s(\tilde{\mu}^* \mathbf{f}_e^{h_e})_{lk} \right] \left[ c(\mathbf{a}_e)_{kl}^\dagger - s(\tilde{\mu}^* \mathbf{f}_e^{h_e})_{kl}^\dagger \right] \\
&\quad - 2\theta_{\tilde{h}} |\mu|^2 \left\{ \theta_{\tilde{B}} \left[ s^2 |\tilde{g}^{h_u}|^2 + c^2 |\tilde{g}^{h_d}|^2 \right] + 3\theta_{\tilde{W}} \left[ s^2 |\tilde{g}^{h_u}|^2 + c^2 |\tilde{g}^{h_d}|^2 \right] \right\} \\
&\quad - 2\theta_{\tilde{h}} \left\{ \theta_{\tilde{B}} (M_1^2 + M_1'^2) \left[ s^2 |\tilde{g}^{h_u}|^2 + c^2 |\tilde{g}^{h_d}|^2 \right] + 3\theta_{\tilde{W}} (M_2^2 + M_2'^2) \left[ s^2 |\tilde{g}^{h_u}|^2 + c^2 |\tilde{g}^{h_d}|^2 \right] \right\} \\
&\quad - \frac{1}{2} \left\{ -4\theta_{\tilde{h}} \theta_{\tilde{B}} sc \mu^* \tilde{g}^{h_u} \tilde{g}^{h_d} (M_1 + iM_1') - 12\theta_{\tilde{h}} \theta_{\tilde{W}} sc \mu^* \tilde{g}^{h_u} \tilde{g}^{h_d} (M_2 + iM_2') \right\} \\
&\quad - \frac{1}{2} \left\{ -4\theta_{\tilde{h}} \theta_{\tilde{B}} sc \mu (\tilde{g}^{h_u})^* (\tilde{g}^{h_d})^* (M_1 - iM_1') - 12\theta_{\tilde{h}} \theta_{\tilde{W}} sc \mu (\tilde{g}^{h_u})^* (\tilde{g}^{h_d})^* (M_2 - iM_2') \right\} \\
&\quad - \theta_h \left( \frac{3g'^2}{2} + \frac{9g_2^2}{2} \right) \left[ s^2 (m_{H_u}^2 + |\tilde{\mu}|^2) + c^2 (m_{H_d}^2 + |\tilde{\mu}|^2) - sc(b+b^*) \right] \\
&\quad + \theta_h \left[ s^2 \left\{ [6\mathbf{f}_u^* \mathbf{f}_u^T]_{kk} + \theta_{\tilde{B}} \theta_{\tilde{h}} |\tilde{g}^{h_u}|^2 + 3\theta_{\tilde{W}} \theta_{\tilde{h}} |\tilde{g}^{h_u}|^2 \right\} \right. \\
&\quad \quad \left. + c^2 \left\{ [6\mathbf{f}_d^* \mathbf{f}_d^T + 2\mathbf{f}_e^* \mathbf{f}_e^T]_{kk} + \theta_{\tilde{B}} \theta_{\tilde{h}} |\tilde{g}^{h_d}|^2 + 3\theta_{\tilde{W}} \theta_{\tilde{h}} |\tilde{g}^{h_d}|^2 \right\} \right] \\
&\quad \quad \times \left[ s^2 (m_{H_u}^2 + |\tilde{\mu}|^2) + c^2 (m_{H_d}^2 + |\tilde{\mu}|^2) - sc(b+b^*) \right] .
\end{aligned} \tag{B24}$$

With  $\theta_H = 0$ , RGEs for the remaining SSB scalar mass parameters take the form,

$$\begin{aligned}
(4\pi)^2 \frac{d(\mathbf{m}_Q^2)_{ij}}{dt} = & \theta_h \left\{ -\frac{1}{3} (c^2 - s^2) g'^2 \delta_{ij} + 2s^2 [(\mathbf{f}_u)^* (\mathbf{f}_u)^T]_{ij} + 2c^2 [(\mathbf{f}_d)^* (\mathbf{f}_d)^T]_{ij} \right\} \\
& \times [s^2 (m_{H_u}^2 + |\tilde{\mu}|^2) + c^2 (m_{H_d}^2 + |\tilde{\mu}|^2) - sc(b + b^*)] \\
& - \frac{2}{3} \theta_{\tilde{u}_k} g'^2 \delta_{ij} (\mathbf{m}_U^2)_{kk} + \frac{1}{3} \theta_{\tilde{Q}_k} g'^2 \delta_{ij} (\mathbf{m}_Q^2)_{kk} \\
& + \theta_{\tilde{Q}_k} \theta_{\tilde{Q}_l} \left( \frac{g'^2}{18} + \frac{3g_2^2}{2} + \frac{8g_3^2}{3} \right) \delta_{ik} \delta_{lj} (\mathbf{m}_Q^2)_{kl} \\
& + \frac{1}{3} \theta_{\tilde{d}_k} g'^2 \delta_{ij} (\mathbf{m}_D^2)_{kk} - \frac{1}{3} \theta_{\tilde{L}_k} g'^2 \delta_{ij} (\mathbf{m}_L^2)_{kk} + \frac{1}{3} \theta_{\tilde{e}_k} g'^2 \delta_{ij} (\mathbf{m}_E^2)_{kk} \\
& + 2\theta_{\tilde{u}_k} \theta_{\tilde{u}_l} (\mathbf{f}_u)^*_{ik} (\mathbf{m}_U^2)_{kl} (\mathbf{f}_u)^T_{lj} + 2\theta_{\tilde{d}_k} \theta_{\tilde{d}_l} (\mathbf{f}_d)^*_{ik} (\mathbf{m}_D^2)_{kl} (\mathbf{f}_d)^T_{lj} \\
& + 2\theta_{\tilde{u}_k} \theta_h \left[ s(\mathbf{a}_u)^*_{ik} - c(\tilde{\mu}^* \mathbf{f}_u^{h_u})^*_{ik} \right] \left[ s(\mathbf{a}_u)^T_{kj} - c(\tilde{\mu}^* \mathbf{f}_u^{h_u})^T_{kj} \right] \\
& + 2\theta_{\tilde{d}_k} \theta_h \left[ c(\mathbf{a}_d)^*_{ik} - s(\tilde{\mu}^* \mathbf{f}_d^{h_d})^*_{ik} \right] \left[ c(\mathbf{a}_d)^T_{kj} - s(\tilde{\mu}^* \mathbf{f}_d^{h_d})^T_{kj} \right] \\
& - \frac{2}{9} \theta_{\tilde{B}} (M_1^2 + M_1'^2) (\tilde{\mathbf{g}}'^Q)_{ik} (\tilde{\mathbf{g}}'^Q)^\dagger_{kj} - 6\theta_{\tilde{W}} (M_2^2 + M_2'^2) (\tilde{\mathbf{g}}^Q)_{ik} (\tilde{\mathbf{g}}^Q)^\dagger_{kj} \\
& - \frac{32}{3} \theta_{\tilde{g}} (M_3^2 + M_3'^2) (\tilde{\mathbf{g}}_s^Q)_{ik} (\tilde{\mathbf{g}}_s^Q)^\dagger_{kj} \\
& - 4\theta_{\tilde{h}} |\mu|^2 \left[ (\tilde{\mathbf{f}}_u^Q)^*_{ik} (\tilde{\mathbf{f}}_u^Q)^T_{kj} + (\tilde{\mathbf{f}}_d^Q)^*_{ik} (\tilde{\mathbf{f}}_d^Q)^T_{kj} \right] \\
& - 3 \left( \theta_{\tilde{Q}_i} + \theta_{\tilde{Q}_j} \right) \left( \frac{1}{36} g'^2 + \frac{3}{4} g_2^2 + \frac{4}{3} g_3^2 \right) (\mathbf{m}_Q^2)_{ij} \\
& + \theta_{\tilde{Q}_l} \left[ \frac{1}{18} \theta_{\tilde{B}} (\tilde{\mathbf{g}}'^Q)_{ik} (\tilde{\mathbf{g}}'^Q)^\dagger_{kl} + \frac{3}{2} \theta_{\tilde{W}} (\tilde{\mathbf{g}}^Q)_{ik} (\tilde{\mathbf{g}}^Q)^\dagger_{kl} + \frac{8}{3} \theta_{\tilde{g}} (\tilde{\mathbf{g}}_s^Q)_{ik} (\tilde{\mathbf{g}}_s^Q)^\dagger_{kl} \right. \\
& \quad \left. + \theta_{\tilde{h}} (\tilde{\mathbf{f}}_u^Q)^*_{ik} (\tilde{\mathbf{f}}_u^Q)^T_{kl} + \theta_{\tilde{h}} (\tilde{\mathbf{f}}_d^Q)^*_{ik} (\tilde{\mathbf{f}}_d^Q)^T_{kl} \right] (\mathbf{m}_Q^2)_{lj} \\
& + \theta_{\tilde{Q}_k} (\mathbf{m}_Q^2)_{ik} \left[ \frac{1}{18} \theta_{\tilde{B}} (\tilde{\mathbf{g}}'^Q)_{kl} (\tilde{\mathbf{g}}'^Q)^\dagger_{lj} + \frac{3}{2} \theta_{\tilde{W}} (\tilde{\mathbf{g}}^Q)_{kl} (\tilde{\mathbf{g}}^Q)^\dagger_{lj} + \frac{8}{3} \theta_{\tilde{g}} (\tilde{\mathbf{g}}_s^Q)_{kl} (\tilde{\mathbf{g}}_s^Q)^\dagger_{lj} \right. \\
& \quad \left. + \theta_{\tilde{h}} (\tilde{\mathbf{f}}_u^Q)^*_{kl} (\tilde{\mathbf{f}}_u^Q)^T_{lj} + \theta_{\tilde{h}} (\tilde{\mathbf{f}}_d^Q)^*_{kl} (\tilde{\mathbf{f}}_d^Q)^T_{lj} \right] ,
\end{aligned} \tag{B25}$$

$$\begin{aligned}
(4\pi)^2 \frac{d(\mathbf{m}_U^2)_{ij}}{dt} = & \theta_h \left\{ \frac{4}{3} (c^2 - s^2) g'^2 \delta_{ij} + 4s^2 [(\mathbf{f}_u)^T (\mathbf{f}_u)^*]_{ij} \right\} \\
& \times [s^2 (m_{H_u}^2 + |\tilde{\mu}|^2) + c^2 (m_{H_d}^2 + |\tilde{\mu}|^2) - sc (b + b^*)] \\
& + \frac{8}{3} \theta_{\tilde{u}_k} g'^2 \delta_{ij} (\mathbf{m}_U^2)_{kk} + \frac{8}{3} \theta_{\tilde{u}_k} \theta_{\tilde{u}_l} \left[ \frac{1}{3} g'^2 + g_3^2 \right] \delta_{ik} \delta_{lj} (\mathbf{m}_U^2)_{kl} \\
& - \frac{4}{3} \theta_{\tilde{Q}_k} g'^2 \delta_{ij} (\mathbf{m}_Q^2)_{kk} - \frac{4}{3} \theta_{\tilde{d}_k} g'^2 \delta_{ij} (\mathbf{m}_D^2)_{kk} + \frac{4}{3} \theta_{\tilde{L}_k} g'^2 \delta_{ij} (\mathbf{m}_L^2)_{kk} \\
& - \frac{4}{3} \theta_{\tilde{e}_k} g'^2 \delta_{ij} (\mathbf{m}_E^2)_{kk} + 4\theta_{\tilde{Q}_k} \theta_{\tilde{Q}_l} (\mathbf{f}_u)^T_{ik} (\mathbf{f}_u)^*_{lj} (\mathbf{m}_Q^2)_{kl} \\
& + 4\theta_{\tilde{Q}_k} \theta_h \left[ s(\mathbf{a}_u)^T_{ik} - c(\tilde{\mu}^* \mathbf{f}_u^{hu})^T_{ik} \right] \left[ s(\mathbf{a}_u)^*_{kj} - c(\tilde{\mu}^* \mathbf{f}_u^{hu})^*_{kj} \right] \\
& - \frac{32}{9} \theta_{\tilde{B}} (M_1^2 + M_1'^2) (\tilde{\mathbf{g}}'^{uR})^\dagger_{ik} (\tilde{\mathbf{g}}'^{uR})_{kj} - \frac{32}{3} \theta_{\tilde{g}} (M_3^2 + M_3'^2) (\tilde{\mathbf{g}}_s^{uR})^\dagger_{ik} (\tilde{\mathbf{g}}_s^{uR})_{kj} \\
& - 8\theta_{\tilde{h}} |\mu|^2 (\tilde{\mathbf{f}}_u^{uR})^T_{ik} (\tilde{\mathbf{f}}_u^{uR})^*_{kj} - 3(\theta_{\tilde{u}_i} + \theta_{\tilde{u}_j}) \left( \frac{4}{9} g'^2 + \frac{4}{3} g_3^2 \right) (\mathbf{m}_U^2)_{ij} \\
& + \theta_{\tilde{u}_l} \left[ \frac{8}{9} \theta_{\tilde{B}} (\tilde{\mathbf{g}}'^{uR})^\dagger_{ik} (\tilde{\mathbf{g}}'^{uR})_{kl} + \frac{8}{3} \theta_{\tilde{g}} (\tilde{\mathbf{g}}_s^{uR})^\dagger_{ik} (\tilde{\mathbf{g}}_s^{uR})_{kl} + 2\theta_{\tilde{h}} (\tilde{\mathbf{f}}_u^{uR})^T_{ik} (\tilde{\mathbf{f}}_u^{uR})^*_{kl} \right] (\mathbf{m}_U^2)_{lj} \\
& + \theta_{\tilde{u}_k} (\mathbf{m}_U^2)_{ik} \left[ \frac{8}{9} \theta_{\tilde{B}} (\tilde{\mathbf{g}}'^{uR})^\dagger_{kl} (\tilde{\mathbf{g}}'^{uR})_{lj} + \frac{8}{3} \theta_{\tilde{g}} (\tilde{\mathbf{g}}_s^{uR})^\dagger_{kl} (\tilde{\mathbf{g}}_s^{uR})_{lj} + 2\theta_{\tilde{h}} (\tilde{\mathbf{f}}_u^{uR})^T_{kl} (\tilde{\mathbf{f}}_u^{uR})^*_{lj} \right], \tag{B26}
\end{aligned}$$

$$\begin{aligned}
(4\pi)^2 \frac{d(\mathbf{m}_D^2)_{ij}}{dt} = & \theta_h \left\{ -\frac{2}{3} (c^2 - s^2) g'^2 \delta_{ij} + 4c^2 [(\mathbf{f}_d)^T (\mathbf{f}_d)^*]_{ij} \right\} \\
& \times [s^2 (m_{H_u}^2 + |\tilde{\mu}|^2) + c^2 (m_{H_d}^2 + |\tilde{\mu}|^2) - sc (b + b^*)] \\
& - \frac{4}{3} \theta_{\tilde{u}_k} g'^2 \delta_{ij} (\mathbf{m}_U^2)_{kk} + \frac{2}{3} \theta_{\tilde{Q}_k} g'^2 \delta_{ij} (\mathbf{m}_Q^2)_{kk} + \frac{2}{3} \theta_{\tilde{d}_k} g'^2 \delta_{ij} (\mathbf{m}_D^2)_{kk} \\
& + \frac{2}{3} \theta_{\tilde{d}_k} \theta_{\tilde{d}_l} \left[ \frac{1}{3} g'^2 + 4g_3^2 \right] \delta_{ik} \delta_{lj} (\mathbf{m}_D^2)_{kl} - \frac{2}{3} \theta_{\tilde{L}_k} g'^2 \delta_{ij} (\mathbf{m}_L^2)_{kk} \\
& + \frac{2}{3} \theta_{\tilde{e}_k} g'^2 \delta_{ij} (\mathbf{m}_E^2)_{kk} + 4\theta_{\tilde{Q}_k} \theta_{\tilde{Q}_l} (\mathbf{f}_d)^T_{ik} (\mathbf{f}_d)^*_{lj} (\mathbf{m}_Q^2)_{kl} \\
& + 4\theta_{\tilde{Q}_k} \theta_h \left[ c(\mathbf{a}_d)^T_{ik} - s(\tilde{\mu}^* \mathbf{f}_d^{hd})^T_{ik} \right] \left[ c(\mathbf{a}_d)^*_{kj} - s(\tilde{\mu}^* \mathbf{f}_d^{hd})^*_{kj} \right] \\
& - \frac{8}{9} \theta_{\tilde{B}} (M_1^2 + M_1'^2) (\tilde{\mathbf{g}}'^{dR})^\dagger_{ik} (\tilde{\mathbf{g}}'^{dR})_{kj} - \frac{32}{3} \theta_{\tilde{g}} (M_3^2 + M_3'^2) (\tilde{\mathbf{g}}_s^{dR})^\dagger_{ik} (\tilde{\mathbf{g}}_s^{dR})_{kj} \\
& - 8\theta_{\tilde{h}} |\mu|^2 (\tilde{\mathbf{f}}_d^{dR})^T_{ik} (\tilde{\mathbf{f}}_d^{dR})^*_{kj} - 3(\theta_{\tilde{d}_i} + \theta_{\tilde{d}_j}) \left( \frac{1}{9} g'^2 + \frac{4}{3} g_3^2 \right) (\mathbf{m}_D^2)_{ij} \\
& + \theta_{\tilde{d}_l} \left[ \frac{2}{9} \theta_{\tilde{B}} (\tilde{\mathbf{g}}'^{dR})^\dagger_{ik} (\tilde{\mathbf{g}}'^{dR})_{kl} + \frac{8}{3} \theta_{\tilde{g}} (\tilde{\mathbf{g}}_s^{dR})^\dagger_{ik} (\tilde{\mathbf{g}}_s^{dR})_{kl} + 2\theta_{\tilde{h}} (\tilde{\mathbf{f}}_d^{dR})^T_{ik} (\tilde{\mathbf{f}}_d^{dR})^*_{kl} \right] (\mathbf{m}_D^2)_{lj} \\
& + \theta_{\tilde{d}_k} (\mathbf{m}_D^2)_{ik} \left[ \frac{2}{9} \theta_{\tilde{B}} (\tilde{\mathbf{g}}'^{dR})^\dagger_{kl} (\tilde{\mathbf{g}}'^{dR})_{lj} + \frac{8}{3} \theta_{\tilde{g}} (\tilde{\mathbf{g}}_s^{dR})^\dagger_{kl} (\tilde{\mathbf{g}}_s^{dR})_{lj} + 2\theta_{\tilde{h}} (\tilde{\mathbf{f}}_d^{dR})^T_{kl} (\tilde{\mathbf{f}}_d^{dR})^*_{lj} \right], \tag{B27}
\end{aligned}$$

$$\begin{aligned}
(4\pi)^2 \frac{d(\mathbf{m}_L^2)_{ij}}{dt} = & \theta_h \left\{ (c^2 - s^2) g'^2 \delta_{ij} + 2c^2 [(\mathbf{f}_e)^* (\mathbf{f}_e)^T]_{ij} \right\} \\
& \times [s^2 (m_{Hu}^2 + |\tilde{\mu}|^2) + c^2 (m_{Hd}^2 + |\tilde{\mu}|^2) - sc(b + b^*)] \\
& + 2\theta_{\tilde{u}_k} g'^2 \delta_{ij} (\mathbf{m}_U^2)_{kk} - \theta_{\tilde{Q}_k} g'^2 \delta_{ij} (\mathbf{m}_Q^2)_{kk} - \theta_{\tilde{d}_k} g'^2 \delta_{ij} (\mathbf{m}_D^2)_{kk} \\
& + \theta_{\tilde{L}_k} g'^2 \delta_{ij} (\mathbf{m}_L^2)_{kk} + \theta_{\tilde{L}_k} \theta_{\tilde{L}_l} \left( \frac{g'^2}{2} + \frac{3g_2^2}{2} \right) \delta_{ik} \delta_{lj} (\mathbf{m}_L^2)_{kl} \\
& - \theta_{\tilde{e}_k} g'^2 \delta_{ij} (\mathbf{m}_E^2)_{kk} + 2\theta_{\tilde{e}_k} \theta_{\tilde{e}_l} (\mathbf{f}_e)_{ik}^* (\mathbf{m}_E^2)_{kl} (\mathbf{f}_e)_{lj}^T \\
& + 2\theta_{\tilde{e}_k} \theta_h \left[ c(\mathbf{a}_e)_{ik}^* - s(\tilde{\mu}^* \mathbf{f}_e^{hd})_{ik}^* \right] \left[ c(\mathbf{a}_e)_{kj}^T - s(\tilde{\mu}^* \mathbf{f}_e^{hd})_{kj}^T \right] \\
& - 2\theta_{\tilde{B}} (M_1^2 + M_1'^2) (\tilde{\mathbf{g}}'^L)_{ik} (\tilde{\mathbf{g}}'^L)_{kj}^\dagger - 6\theta_{\tilde{W}} (M_2^2 + M_2'^2) (\tilde{\mathbf{g}}^L)_{ik} (\tilde{\mathbf{g}}^L)_{kj}^\dagger \\
& - 4\theta_{\tilde{h}} |\mu|^2 (\tilde{\mathbf{f}}_e^L)_{ik}^* (\tilde{\mathbf{f}}_e^L)_{kj}^T - 3(\theta_{\tilde{L}_i} + \theta_{\tilde{L}_j}) \left( \frac{1}{4} g'^2 + \frac{3}{4} g_2^2 \right) (\mathbf{m}_L^2)_{ij} \\
& + \theta_{\tilde{L}_l} \left[ \frac{1}{2} (\tilde{\mathbf{g}}'^L)_{ik} (\tilde{\mathbf{g}}'^L)_{kl}^\dagger \theta_{\tilde{B}} + \frac{3}{2} (\tilde{\mathbf{g}}^L)_{ik} (\tilde{\mathbf{g}}^L)_{kl}^\dagger \theta_{\tilde{W}} + (\tilde{\mathbf{f}}_e^L)_{ik}^* (\tilde{\mathbf{f}}_e^L)_{kl}^T \theta_{\tilde{h}} \right] (\mathbf{m}_L^2)_{lj} \\
& + \theta_{\tilde{L}_k} (\mathbf{m}_L^2)_{ik} \left[ \frac{1}{2} (\tilde{\mathbf{g}}'^L)_{kl} (\tilde{\mathbf{g}}'^L)_{lj}^\dagger \theta_{\tilde{B}} + \frac{3}{2} (\tilde{\mathbf{g}}^L)_{kl} (\tilde{\mathbf{g}}^L)_{lj}^\dagger \theta_{\tilde{W}} + (\tilde{\mathbf{f}}_e^L)_{kl}^* (\tilde{\mathbf{f}}_e^L)_{lj}^T \theta_{\tilde{h}} \right], \\
\end{aligned} \tag{B28}$$

$$\begin{aligned}
(4\pi)^2 \frac{d(\mathbf{m}_E^2)_{ij}}{dt} = & \theta_h \left\{ -2(c^2 - s^2) g'^2 \delta_{ij} + 4c^2 [(\mathbf{f}_e)^T (\mathbf{f}_e)^*]_{ij} \right\} \\
& \times [s^2 (m_{Hu}^2 + |\tilde{\mu}|^2) + c^2 (m_{Hd}^2 + |\tilde{\mu}|^2) - sc(b + b^*)] \\
& - 4\theta_{\tilde{u}_k} g'^2 \delta_{ij} (\mathbf{m}_U^2)_{kk} + 2\theta_{\tilde{Q}_k} g'^2 \delta_{ij} (\mathbf{m}_Q^2)_{kk} + 2\theta_{\tilde{d}_k} g'^2 \delta_{ij} (\mathbf{m}_D^2)_{kk} \\
& - 2\theta_{\tilde{L}_k} g'^2 \delta_{ij} (\mathbf{m}_L^2)_{kk} + 2\theta_{\tilde{e}_k} g'^2 \delta_{ij} (\mathbf{m}_E^2)_{kk} \\
& + 2\theta_{\tilde{e}_k} \theta_{\tilde{e}_l} g'^2 \delta_{lj} \delta_{ik} (\mathbf{m}_E^2)_{kl} + 4\theta_{\tilde{L}_k} \theta_{\tilde{L}_l} (\mathbf{f}_e)_{ik}^T (\mathbf{m}_L^2)_{kl} (\mathbf{f}_e)_{lj}^* \\
& + 4\theta_{\tilde{L}_k} \theta_h \left[ c(\mathbf{a}_e)_{ik}^T - s(\tilde{\mu}^* \mathbf{f}_e^{hd})_{ik}^T \right] \left[ c(\mathbf{a}_e)_{kj}^* - s(\tilde{\mu}^* \mathbf{f}_e^{hd})_{kj}^* \right] \\
& - 8\theta_{\tilde{B}} (M_1^2 + M_1'^2) (\tilde{\mathbf{g}}'^{eR})_{ik}^\dagger (\tilde{\mathbf{g}}'^{eR})_{kj} - 8\theta_{\tilde{h}} |\mu|^2 (\tilde{\mathbf{f}}_e^{eR})_{ik}^T (\tilde{\mathbf{f}}_e^{eR})_{kj}^* \\
& - 3(\theta_{\tilde{e}_i} + \theta_{\tilde{e}_j}) g'^2 (\mathbf{m}_E^2)_{ij} \\
& + \theta_{\tilde{e}_l} \left[ 2(\tilde{\mathbf{g}}'^{eR})_{ik}^\dagger (\tilde{\mathbf{g}}'^{eR})_{kl} \theta_{\tilde{B}} + 2(\tilde{\mathbf{f}}_e^{eR})_{ik}^T (\tilde{\mathbf{f}}_e^{eR})_{kl}^* \theta_{\tilde{h}} \right] (\mathbf{m}_E^2)_{lj} \\
& + \theta_{\tilde{e}_k} (\mathbf{m}_E^2)_{ik} \left[ 2(\tilde{\mathbf{g}}'^{eR})_{kl}^\dagger (\tilde{\mathbf{g}}'^{eR})_{lj} \theta_{\tilde{B}} + 2(\tilde{\mathbf{f}}_e^{eR})_{kl}^T (\tilde{\mathbf{f}}_e^{eR})_{lj}^* \theta_{\tilde{h}} \right]. \\
\end{aligned} \tag{B29}$$

- 
- [1] H. Georgi, H. Quinn and S. Weinberg, Phys. Rev. Lett. **33**, 451 (1974). For other early implications using RGE methods, see A. J. Buras, J. Ellis, M. K. Gaillard and D. V. Nanopoulos, Nucl. Phys. B **135**, 66 (1978); N. Cabibbo, L. Maiani, G. Parisi and R. Petronzio, Nucl. Phys. B **158**, 295 (1979).
- [2] U. Amaldi, W. de Boer and H. Fürstenau, Phys. Lett. B **260**, 447 (1991); P. Langacker and N. Polonsky, Phys. Rev. D **47**, 4028 (1993).
- [3] S. Dimopoulos and H. Georgi, Nucl. Phys. B **193**, 150 (1981); N. Sakai, Z. Phys. C **11**, 153 (1981); R. Kaul, Phys. Lett. B **109**, 19 (1982).
- [4] H. Baer and X. Tata, *Weak Scale Supersymmetry*, Cambridge University Press (2006).
- [5] M. Drees, R.M. Godbole and P. Roy, *Theory and Phenomenology of Sparticles*, World Scientific (2004)
- [6] P. Binétruy, *Supersymmetry*, Oxford University Press (2006)
- [7] S.P. Martin, *A Supersymmetry Primer*, arXiv:hep-ph/9709356 (1997).
- [8] L. Girardello, M. Grisaru, Nucl. Phys. B **194**, 65 (1982).
- [9] Gravity-mediated SUSY breaking: A. Chamseddine, R. Arnowitt and P. Nath, Phys. Rev. Lett. **49**, 970 (1982); R. Barbieri, S. Ferrara and C. Savoy, Phys. Lett. B **119**, 343 (1982); N. Ohta, Prog. Theor. Phys. **70**, 542 (1983); L. Hall, J. Lykken and S. Weinberg, Phys. Rev. D **27**, 2359 (1983). For reviews see P. Nath, arXiv:hep-ph/0307123, and H.P. Nilles, Phys. Rept. **110**, 1 (1984).
- [10] Gauge-mediated SUSY breaking: M. Dine and A. Nelson, Phys. Rev. D **48**, 1277 (1993); M. Dine, A. Nelson, Y. Nir and Y. Shirman, Phys. Rev. D **53**, 2658 (1996). See G.F. Giudice and R. Rattazzi Phys. Rep. **322**, 419 (1999) for a review of gauge-mediated SUSY breaking models.
- [11] Anomaly-mediated SUSY breaking: L. Randall and R. Sundrum, Nucl. Phys. B **557**, 79 (1999); G. Giudice, *et al.*, JHEP **12**, 027 (1998).
- [12] Gaugino-mediated SUSY breaking: D.E. Kaplan, G.D. Kribs and M. Schmaltz, Phys. Rev. D **62**, 035010 (2000); Z. Chacko, *et al.*, JHEP **01**, 003 (2000); M. Schmaltz and W. Skiba, Phys. Rev. D **62**, 095004 (2000) and Phys. Rev. D **62**, 095005 (2000).
- [13] K. Inoue, A. Kakuto, H. Komatsu and S. Takeshita, Prog. Theor. Phys. **68**, 927 (1982); **71**,

- 314 (1984); **71**, 413 (1984); L. Alvarez-Gaume, J. Polchinski and M. Wise, Nucl. Phys. B **221**, 495 (1983); L. Ibañez and C. Lopez, Nucl. Phys. B **233**, 511 (1984). One-loop  $\beta$ -functions for a general supersymmetric theory were worked out by N. Falck, Z. Phys. C **30**, 247 (1986).
- [14] A.D. Box, X. Tata, Phys. Rev. D **77**, 055007 (2008).
- [15] M.E. Machacek and M.T. Vaughn, Nucl. Phys. B **222**, 83 (1983); Nucl. Phys. B **236**, 221 (1984); Nucl. Phys. B **249**, 70 (1985).
- [16] D.J. Castaño, E.J. Piard and P. Ramond, Phys. Rev. D **49**, 4882 (1994) and erratum (private communication).
- [17] A. Dedes, A.B. Lahanas and K. Tamvakis, Phys. Rev. D **53**, 3793 (1996).
- [18] S. Martin and M.T. Vaughn, Phys. Rev. D **50**, 2282 (1994).
- [19] V. Barger, M. Berger and P. Ohmann, Phys. Rev. D. **47**, 1093 (1993)
- [20] Y. Yamada, Phys. Lett. B **316**, 109 (1993); Phys. Rev. Lett., **72**, 25 (1994); Phys. Rev. D **50**, 3537 (1994).
- [21] D.R.T. Jones and I. Jack, Phys. Lett. B **333**, 372 (1994).
- [22] M. Luo, H. Wang and Y. Xiao, Phys. Rev. D **67**, 065019 (2003).
- [23] M.J. Duncan, Nucl. Phys. B **221**, 285 (1983).
- [24] L. Hall and L. Randall, Phys. Rev. Lett. **65** (1990) 2939.
- [25] D. Pierce, J.A. Bagger, K.T. Matchev and R. Zhang, Nucl. Phys. B **491**, 3 (1997).
- [26] ISAJET v7.74, by H. Baer, F. Paige, S. Protopopescu and X. Tata, arXiv:hep-ph/0312045.
- [27] M. Luo and Y. Xiao, Phys. Rev. Lett. **90** (2003) 011601.
- [28] M. Kobayashi and T. Maskawa, Prog. Theor. Phys. **49**, 652 (1973).
- [29] C. Amsler et al. (Particle Data Group), Phys. Lett. B **667**, 1 (2008).
- [30] S. Weinberg, Phys. Lett. B **91**, 51 (1980); L. Hall, Nucl. Phys. B **178**, 75 (1981); B. Ovrut and H.J. Schnitzer, Nucl. Phys. B **184**, 109 (1981); K.G. Chetyrkin, B.A. Kniehl, M. Steinhauser, Phys. Rev. Lett. **79**, 2184 (1997). See also, B. Wright, arXiv:hep-ph/9404217 (1994) and H. Baer, J. Ferrandis, S. Kraml and W. Porod, Phys. Rev. D **73**, 015010 (2006) for discussions of this in the SUSY context.
- [31] H. Arason, D.J. Castaño, B. Keszthelyi, S. Mikaelian, E.J. Piard, P. Ramond and B.D. Wright, Phys. Rev. D **46**, 3945 (1992).
- [32] S. Martin and M.T. Vaughn, Phys. Lett. B **318**, 331 (1993).
- [33] H. Fusaoka, Y. Koide, Phys. Rev. D **57**, 3986 (1998).

- [34] H. Baer, J. Ferrandis, K. Melnikov and X. Tata, Phys. Rev. **D66** (2002) 074007.
- [35] J. L. Diaz-Cruz and J. Ferrandis, Phys. Rev. **D72** (2005) 035003.
- [36] L. Hall and L. Randall, Ref.[24]; G. D'Ambrosio, G. Giudice, G. Isidori and A. Strumia, Nucl. Phys. **B645** (2002) 155; P. Paradisi, M. Ratz, R. Schieren and C. Simonetto, Phys.Lett. B **668** (2008) 202; G. Colangelo, E. Nikolidakis and C. Smith, arXiv:0807.0801 [hep-ph]; for a discussion of minimal flavour violation in the lepton sector, see *e.g.* V. Cirigliano, B. Grinstein, G. Isidori and M. Wise, Nucl. Phys. **B728**( 2005) 121.
- [37] J. Feng, K.T. Matchev, T. Moroi, Phys. Rev. D **61**, 075005 (2000); K.L. Chan, U. Chattopadhyay and P. Nath, Phys. Rev. D **58**, 096004 (1998).
- [38] For an overview of neutralino dark matter in supersymmetric theories, see *e.g.* H. Baer, A. Mustafayev, E. Park and X. Tata, JHEP **0805** (2008) 058, and references cited therein.
- [39] D. N. Spergel *et al.* (WMAP Collaboration), Astrophys. J. (Suppl.) **170** (2007) 377.
- [40] N. Arkani-Hamed, S. Dimopoulos, *J. High Energy Phys.* **0506** (073) 2005 and *Nucl. Phys. B* **709** (3) 2005; G. Giudice and A. Romanino, *Nucl. Phys. B* **699** (65) 2004, *ibid Nucl. Phys. B* **706** (65) 2005 (E).
- [41] K. Hikasa and M. Kobayashi, Phys. Rev. D **36**, 724 (1987).
- [42] H. Baer, M. Drees, R. Godbole, J.F. Gunion and X. Tata, Phys. Rev. D **44**, 725 (1991); T. Han, K. Hikasa, J.M. Yang and X. Zhang, Phys. Rev. D **70**, 055001 (2004).
- [43] C. Boehm, A. Djouadi and Y. Mambrini, Phys. Rev. **D61** (2000) 095006.
- [44] W. Porod , T. Wöhrmann, Phys. Rev. D **55**, 2907 (1997).
- [45] S. Martin, Phys. Rev. **D75** (2007) 115005; the phenomenology of this scenario is discussed in H. Baer, A. Box and X. Tata, JHEP **0708** (2007) 060; S. Martin, Phys. Rev. **D76** (2007) 095005, and Phys. Rev. **D78** (2008) 055019.
- [46] For an illustration of how third generation parameters may be extracted in a favourable mSUGRA scenario, see J. Hisano, K. Kawagoe and M. Nojiri, Phys. Rev. **D68** (2003) 035007.
- [47] R. Keranen, A. Sopczak, H. Novak and M. Berggren, Eur. Phys. J. **C7** (2000) 1.